Universität Ulm

Institut für Anatomie und Zellbiologie

Amtierender Direktor: Prof. Dr. med. Tobias M. Böckers

Characterization of the new synaptic protein LAPSER1

Dissertation zur Erlangung des Doktorgrades der Medizin der Medizinischen Fakultät der Universität Ulm

Michael Joachim Schmeißer

aus Kempten (Allgäu)

2009

Amtierender Dekan: Prof. Dr. rer. nat. Thomas Wirth

1. Berichterstatter: Prof. Dr. med. Tobias M. Böckers
2. Berichterstatter: Prof. Dr. med. Hayrettin Tumani

Tag der Promotion: 28.10.2010

Für meine lieben Eltern

und meinen Opa Kurt, der leider 2008 von uns ging.

Table of contents

List of abbreviations **III**

1. Introduction **1**

1.1 Neurons 1

1.2 Synapses 1

1.3 Synaptogenesis 3

1.4 Synaptic plasticity 4

1.5 The presynaptic active zone 5

1.6 The postsynaptic density 6

1.7 Goals of this work 15

2. Materials & Methods **16**

2.1 Materials 16

2.2 Methods of microbiology 27

2.3 Methods of molecular biology 30

2.4 Methods of eukaryotic cell culture 34

2.5 Methods of protein biochemistry 38

2.6 Analysis of mRNA and protein localization 45

2.7 Analysis of protein-protein interactions 50

3. Results **54**

3.1 Genomic and protein structure of LAPSER1 54

3.2 LAPSER1 belongs to the *“Fezzin”* protein family 56

3.3 Localization of LAPSER1 mRNA 57

3.4 Localization of the LAPSER1 protein 58

3.5 Studies of LAPSER1 and its interaction partners 64

4. Discussion **72**

4.1 LAPSER1 and other *"Fezzins"* contain conserved sequences mediating protein-protein interactions 72

4.2 LAPSER1 is a novel PSD protein which shows a wide distribution in rat brain 73

4.3 *"Fezzin"* family members interact with ProSAP molecules of the PSD 74

4.4 The *"Fezzin"* family of PSD proteins serves as binding scaffold for SPARs 75

4.5 LAPSER1 is linked to the Wnt signaling pathway 77

4.6 LAPSER1 and its interaction partner β-Catenin take part in activity-dependent synapse-to-nucleus shuttling 79

4.7 LAPSER1 regulates the nuclear localization of β-Catenin in hippocampal neurons 80

4.8 Conclusion 81

5. Summary **82**

6. List of literature **83**

Figures and tables **100**

Danksagung 101

Lebenslauf 102

List of abbreviations

Amino acids

Amino acid	3-Letters	1-Letter
Alanine	Ala	A
Arginine	Arg	R
Asparagine	Asn	N
Aspartic acid	Asp	D
Cysteine	Cys	C
Glutamic Acid	Glu	E
Glutamine	Gln	Q
Glycine	Gly	G
Histidine	His	H
Isoleucine	Ile	I
Leucine	Leu	L
Lysine	Lys	K
Methionine	Met	M
Phenylalanine	Phe	F
Proline	Pro	P
Serine	Ser	S
Threonine	Thr	T
Tryptophan	Trp	W
Tyrosine	Tyr	Y
Valine	Val	V

aa	amino acid(s)
ABC	avidin-biotin-peroxidase-complex
Abi-1	Abelson interacting protein 1
Abp1	Actin-binding protein 1
ab	antibody
acc. no.	accession number

ad	adult
ag/ab	antigen/antibody
AHS	adenine hemisulfate
amp	ampicillin
AMPA	alpha-amino-3-hydroxy-5-methyl-4-isoxazole propionic acid
AMPAR	AMPA-receptor
Ank	ankyrin repeats
APC	Adenomatous polyposis coli
approx.	approximately
APS	ammonium persulfate
ARC	AMPA-receptor complex
ATP	adenosine triphosphate
AZ	active zone
BCA	bicinchoninic acid
bp	base pairs
Br	brain
BSA	bovine serum albumin
CA1 & 3	Cornu ammonis region(s) 1 & 3
$CaCl_2$	calcium chloride
CAM	cell adhesion molecule
CaMKII	calcium/calmodulin-dependent protein kinase II
CAST	CAZ-associated structural protein
CAZ	cytomatrix at the active zone
CC	coiled-coil domain
Cdc42	cell division cycle 42
cDNA	copy DNA
Ce	cerebellum
ceCo	cerebral cortex
Ch + R	channels + receptors
Chemcomp	chemocompetent
CIRL	calcium-independent receptor for α-latrotoxin
CK1ε	Casein kinase 1 epsilon
CNS	central nervous system
co.	company

CO_2	carbon dioxide
Co-IP	co-immunoprecipitation
CoCa	corpus callosum
CREB	cAMP-response element-binding protein
CSM	complete supplement mixture
Ct	C-term
C-terminal	carboxyterminal
C-terminus	carboxyterminus
DAB	diaminobenzidine hydrochlorid
DAPI	4,6-di-amidino-2-phenylindol
dATP	deoxy-adenosine triphosphate
dCTP	deoxy-cytosine triphosphate
DG	dentate gyrus
DIV	days in vitro
DMEM	Dulbecco's modified eagle medium
DMF	dimethylformamide
DMSO	di-methyl-sulfoxid
DNA	desoxy-ribonucleic-acid
dNTP	deoxy-nucleotide triphosphate(s)
DOB	dropout broth
DOBA	dropout broth agar
DTT	dithiothreitol
DVL	Dishevelled
E-LTP	early long term potentiation
E18	embryonic day 18
E.coli	*Escherichia coli*
EDTA	ethylene diamine tetraacetic acid
EGFP	enhancedGFP
EPSP	excitatory postsynaptic potential
F-actin	filamentous-actin
Fez1	F37/esophageal cancer-related gene coding leucine zipper motif 1
FBS	fetal bovine serum
Fz	Frizzled
g	Earth's gravity

GABA	gamma-aminobutyric acid
GAL4-AD	GAL4-activation domain
GAL4-BD	GAL4-binding domain
GFP	green fluorescent protein
GKAP	guanylate kinase-associated protein
GKBD	guanylate kinase binding domain
GL	granular layer
GluR	glutamate receptor
GSK-3β	Glycogen synthase kinase-3β
GST	Glutathione-s-transferase
GTP	guanosine triphosphate
H_2O_2	hydrogen peroxide
HBSS	Hanks' balanced salt solution
Hc	hippocampus
HCl	hydrochloric acid
He	heart
HEPES	4-(2-hydroxyethyl)-1-piperazineethanesulfonic acid
Ho	brain homogenate
HRP	horseradish peroxidase
IP3R	inositol trisphosphate receptor
IPTG	isopropyl-beta-D-thiogalactopyranoside
IRS	insulin receptor substrate
KAc	potassium acetate
kan	kanamycin
kb	kilobases
KCl	potassium chloride
kDa	kilodalton
KH_2PO_4	potassiumdihydrogenphosphate
Ki	kidney
kV	kilovolts
L-LTP	late long term potentiation
LB	Luria Bertani
Li	liver
LRP-5/6	low density lipoprotein receptor-related proteins 5 and 6

LTD	long term depression
LTP	long term potentiation
Lu	lung
LZ	leucine zipper
LZTS	Leucin Zipper Tumor Suppressor
mab	monoclonal antibody
MAGuK	Membrane-associated guanylate kinase
MAPK	mitogen-activated protein kinase
mGC	mGluR complex
mGluR	metabotropic glutamate receptor
Mi	mitochondrial fraction
µg	microgram(s)
µl	microliter(s)
µmol	micromol
$MnCl_2$	manganese chloride
MOPS	3-morpholinopropane sulfonic acid
mRNA	messenger RNA
ms	millisecond(s)
Mu	skeletal muscle
Munc	mammalian uncoordinated
My	myelin fraction
N4BP3	Nedd4 binding protein 3
NaCl	sodium chloride
Na_2HPO_4	disodiumhydrogenphosphate
NaOH	sodium hydroxide
NCBI	National Center for Biotechnology Information
NES	nuclear export signal
NHS	N-hydroxysuccimide
nm	nanometer
NMDA	N-methyl-D-aspartate
NMDAR	NMDA-receptor
NR1/2	NMDA-receptor subunit 1/2
NRC	NMDA-receptor complex
N-terminal	Aminoterminal

N-terminus	Aminoterminus
OD	optical density
ORF	open reading frame
pab	polyclonal antibody
PAGE	polyacrylamide gel electrophoresis
PBS	phosphate-buffered saline
PCP	planar cell polarity
PCR	polymerase chain reaction
pd	postnatal day
PDZ	PSD-95; DlgA & ZO-1
PFA	paraformaldehyde
PIM	protease inhibitor mix
PKA	protein kinase A
PKC	protein kinase C
pm	posnatal month
ProSAP	Proline-rich synapse-associated protein
ProSAPiP1	ProSAP interacting protein 1
ProSAPiP2	ProSAP interacting protein 2
PSD	postsynaptic density
PSP	ProSAP/Shank platform
PTV	Piccolo-Bassoon transport vesicle
PVDF	polyvinylidene fluoride
Rap	Ras proximate
RapGAP	Rap GTPase activating protein
Rac	Ras-related C3 botulinum toxin substrate
Ras	Rat sarcoma
RbCl	rubidium chloride
RFP	red fluorescent protein
RIM	Rab3-interacting molecule
RIPA	radio-immunoprecipitation assay
Rn	*Rattus norvegicus*
RNA	ribonucleic-acid
RNAi	RNA interference
rpm	rounds per minute

RT	room temperature
RYK	tyrosine kinase-related receptor
S-SCAM	synaptic scaffolding molecule
SA	spine apparatus
SAM	sterile alpha motif
SAPAP	SAP90/PSD-95-associated protein
SD	synthetic dropout
SDS	sodium dodecyl sulfate
SER	smooth endoplasmic reticulum
SH3	Src homology3
Sj	synaptic junctions
SOB	Super Optimal Broth
Sp	spleen
SPAR	Spine-associated RapGap
ss	sodium salt
SSC	standard saline citrate
SSTR	somatostatin receptor
Sy	synaptosomal fraction
SynGAP	Synaptic GTPase activating protein
TAE	Tris-acetate-EDTA
TBS	Tris-buffered saline
TBS-T	Tris-buffered saline + tween 20
Te	testis
TEMED	N-tetramethylethylenediamine
Tris	Tris-hydroxymethyl-aminomethane
tRNA	transfer RNA
U	unit
UNC	uncoordinated
UV	ultraviolet
X-Gal	5-bromo-4-chloro-3-indoyl-β-D-galactopyranoside
YPD	yeast extract/peptone/dextrose
YT	yeast extract tryptone
YTA	yeast extract tryptone with antibiotic
YTH	yeast-two-hybrid

1. Introduction

1.1 Neurons

The human brain contains more than 10^{11} neurons. These primary functional units of the nervous system are mostly amitotic cells processing and transmitting signals. The main part of a neuron is the soma or cell body which includes the nucleus. Further, a large number of processes, the dendrites, extend out from the soma like branches receiving incoming afferent information from other neurons. The axon is a single protrusion differing from the dendrites as being the efferent part of signal transmission (Kandel, 1991).

1.2 Synapses

The term “synapse” was introduced by Sherrington in 1897, who described that this close connection between two nerve cells is simply a contact without the continuity of substance. In fact, synapses are specialized structures where the axon terminal of a neuron impinges upon a dendritic extension or the soma of another neuron, muscle or gland cell leaving a small space in between, the synaptic cleft. There are electrical and chemical synapses of which the latter are the predominant ones in the mammalian central nervous system (CNS) having either excitatory or inhibitory function (Kuno, 1995). Each of the 10^{11} neurons in the human brain is capable of forming approximately 10 000 synaptic contacts, so one can totally count about 10^{14} - 10^{15} synapses. It is believed that this dense network of neuronal communication is the basic cellular prerequisite for learning and memory (Kandel, 1991).

1.2.1 Electrical synapses

Electrical synapses were first described between escape-related giant neurons in crayfish in 1959 (Furshpan & Potter, 1959). Since then, they have been characterized as clusters of channels connecting the interiors of adjacent cells thus mediating electrical coupling and transfer of small molecules (Bennett & Zukin, 2004). As the extracellular space between the adjacent cells appeared reduced to a narrow gap as seen by electron microscopy (Revel & Karnovsky, 1967), electrical synapses are often referred to as gap junctions. The proteins

forming these junctions are called connexins which are encoded by a gene family of at least 20 members in mammals (Willecke et al., 2002). Latest findings indicate the important role of gap junctions in brain where electrical transmission mediates junctional communication between astrocytes and neurons (Alvarez-Maubecin et al., 2000) or the synchronization of interaction between interneurons (Gibson et al., 2005; Hjorth et al., 2009). Furthermore, gap junctions also emerge to play an important role during neurogenesis and neuromigration (Kunze et al., 2009). In comparison to chemical synapses whose synaptic cleft spans a distance up to 30 nm and whose synaptic delay is typically about 2 ms (Hormuzdi et al., 2004), gap junctions between neurons approach within 3,5 nm with a synaptic delay of only 0,2 ms allowing fast and efficient signal transmission (Bennett & Zukin, 2004).

1.2.2 Chemical synapses

Chemical synpases are complex cell-cell contact sites formed by a specialized axon terminal membrane of one neuron containing the presynaptic release apparatus for neurotransmitters, and the postsynaptic membrane of another neuron specialized for receiving the neurotransmitter signals. Depending on the neurotransmitter type and the corresponding postsynaptic receptor apparatus, synapses are either excitatory or inhibitory (Gundelfinger & tom Dieck, 2000). The most common excitatory neurotransmitter of the mammalian CNS is glutamate (Genoux & Montgomery, 2007) whereas gamma-aminobutyric acid (GABA) and glycine are the most common inhibitory ones (Kirsch, 2006). Neurotransmitters are released from presynaptic nerve terminals at the active zone, a restricted area of the cell membrane situated exactly opposite to the postsynaptic neurotransmitter reception apparatus. At the active zone, neurotransmitter-containing synaptic vesicles dock, fuse, release their content and are recycled in a strictly regulated manner (Dresbach et al., 2001). The corresponding postsynaptic receptors are clustered in the postsynaptic density (PSD), an organized structure beneath the postsynaptic membrane which is composed of a dense network of several hundred proteins, creating a macromolecular complex that serves a wide range of functions (Boeckers, 2006). Active zone and postsynaptic density stay counterparts due to a largely uncharacterized matrix of cell-adhesion molecules and extracellular matrix proteins (Craig et al., 2006).

From the morphological point of view, chemical synapses can further be classified as Gray type 1 and Gray type 2 (Gray, 1959). Type 1 synapses, also called asymmetric synapses, are usually excitatory and characterized by a relatively wide synaptic cleft (~ 20 nm), small, round synaptic vesicles within the presynaptic specialization and a pronounced postsynaptic density situated at the tips of dendritic spines. These are small protrusions along the lengths of dendrites within certain brain areas (Yuste & Bonhoeffer, 2001). Type 2 synapses, or symmetric synapses, are usually inhibitory, have a smaller synaptic cleft (~ 12 nm), pleomorphic synaptic vesicles and a less pronounced postsynaptic density (Spires et al., 2005).

1.3 Synaptogenesis

The formation of basic synaptic circuits in the mammalian CNS is a complex process beginning in the embryo extending into early postnatal life. During this period of time, synaptogenesis is tightly coupled to neuronal differentiation. Shortly after neurons begin to differentiate, many of the genes encoding synaptic proteins are turned on, resulting in the formation, accumulation, and directional trafficking of pre- and postsynaptic protein complexes. The specification of correct neuronal connections is determined as axons and dendrites contact each other establishing initial, often transient synapses (Waites et al., 2005). Synaptic cell adhesion molecules like cadherins, neurexins or neuroligins are believed to mediate initial interactions and stabilize connections. Recent studies have shown that cadherins and their cytoplasmic partners, catenins, can modulate axon-spine contacts in a manner that responds to neural activity (Takeichi & Abe, 2005). Additionally, the trans-synaptic extracellular interaction between postsynaptic neuroligins and presynaptic neurexins promotes adhesion between dendrites and axons to form functional synapses (Dean & Dresbach, 2006).

Basically, synaptogenesis can be divided into five steps. The first of these is the formation of an initial contact site which means that one neuronal process recognizes the other as a potential and appropriate target (Garner et al., 2006). Several studies have shown that the filopodia of the dendrite are deterministic for the later stabilization of the established contact (Ziv & Smith, 1996; Fiala et al., 1998; Jontes & Smith, 2000). The second step, an induction of pre- and

postsynaptic differentiation is followed by a 1-2 h lasting third step during which vesicles or synaptic protein complexes accumulate within pre- and postsynaptic specializations (Friedman et al., 2000; Garner et al., 2006). Interestingly, the presynaptic specialization which seems to be the first to be assembled, subsequently induces the formation of the postsynaptic one (Goda & Davis, 2003). The fourth step is a prolonged phase (hours to days) of structural and functional maturation accompanied by molecular changes in the composition of active zones and the postsynaptic density while the fifth and final step involves the maintenance of mature synapses for hours, days, weeks and possibly years (Garner et al., 2006).

1.4 Synaptic plasticity

Psychologist Donald O. Hebb first introduced the term “synaptic plasticity” in 1949. He developed a theory about the molecular processes of learning and memory and proposed the ability of the connection between two neurons to change in strength : *“When an axon of cell A is near enough to excite cell B and repeatedly or persistently takes part in firing it, some growth process or metabolic change takes place in one or both cells such that A's efficiency, as one of the cells firing B, is increased”* (Hebb, 1949). Synaptic contacts can be regulated via this mechanism which is the basis for flexibility as well as stability of the mammalian CNS both during development and in adult life (Schulz, 2006). In 1973, neurophysiologists Tim V. P. Bliss and Terje Lomo could show that repetitive stimulation of perforant path fibres of the hippocampus result in an increase in synaptic transmission efficiency in granular cells of the dentate gyrus which means that subsequent single-pulse stimulation of presynaptic fibres elicits stronger, prolonged excitatory postsynaptic potentials (EPSPs) in the postsynaptic cells (Bliss & Lomo, 1973). Due to its long lasting effect, this phenomenon was called long term potentiation or LTP (Douglas & Goddard, 1975) which has been observed in various neural structures over the years and is thus proposed to occur at all excitatory synapses in the mammalian brain.

LTP is best studied in the hippocampus. The process of long term potentiation can be divided into three phases occuring sequentially: short-term potentiation, early LTP (E-LTP) and late LTP (L-LTP). So far, short-term potentiation has not been

thoroughly investigated, but E- and L-LTP can each be further subdivided into three events: induction, maintenance and expression (Sweatt, 1999). After experimental stimulation, the presynaptic neuron releases glutamate which binds to alpha-amino-3-hydroxy-5-methyl-4-isoxazoleproprionic acid receptors (AMPARs) of the postsynaptic membrane resulting in the influx of sodium ions causing depolarization. Repeated stimuli lead to an EPSP summation that unblocks N-methyl-D-aspartate receptors (NMDAR) which finally allows calcium influx. E-LTP induction emerges when the calcium concentration in the postsynaptic cell exceeds a certain threshold. (Lynch, 2004). While induction leads to transient activation of enzymes like calcium/calmodulin-dependent protein kinase II (CaMKII), protein kinase C (PKC) or mitogen-activated protein kinases (MAPKs), maintenance of E-LTP comes along with the persistent activation of those. The following expression phase is characterized by kinase-dependent phosphorylation and further insertion of AMPARs into the postsynaptic membrane increasing the efficiency and magnitude of future postsynaptic responses (Malinow, 2003). MAPKs are able to cause changes in gene expression and protein synthesis resulting in L-LTP, the natural extension of E-LTP. Proteins synthesized during L-LTP may lead to an increase in dendritic spine number, surface and postsynaptic sensitivity forming the basis for long-term memory (Kelleher RJ 3rd et al., 2004 a & b; Costa-Mattioli M et al., 2005; Wu et al., 2007). The opposite mechanism called long term depression or LTD, is responsible for the weakening of synapses which may play a role in the clearing of old memories - as far as the hippocampus is concerned (Massey & Bashir, 2007).

1.5 The presynaptic active zone

The active zone (AZ) within presynaptic nerve terminals is defined as the site right at the presynaptic membrane that is essential for the regulated exocytosis of synaptic vesicles filled with neurotransmitters. It is tightly associated with an electron-dense matrix called cytomatrix at the active zone (CAZ), a dense meshwork of cytoskeletal filaments responsible for the anchoring and mobilization of synaptic vesicles and the assembly of presynaptic proteins (Dresbach et al., 2003). Within this molecular network, several different protein families can be found involved in synaptic vesicle fusion, cytoskeletal molecules, ion channels, scaffolding proteins and cell adhesion molecules. Interestingly, five protein families

have been identified which are highly enriched in the CAZ: UNC13/Munc13 proteins, Rab3-interacting molecules (RIMs), CAZ-associated proteins (CASTs), liprins, Bassoon and Piccolo. These proteins play important roles in organizing the docking, fusion and recycling of synaptic vesicles (Schoch & Gundelfinger, 2006). UNC13/Munc13 proteins, for example, are essential for the maturation of synaptic vesicles to acquire a fusion competent state (Augustin et al., 1999; Aravamudan et al., 1999; Siksou et al., 2009) while RIMs interact with multiple proteins responsible for presynaptic vesicle priming and fusion (Calakos et al., 2004). CASTs (Ohtsuka et al., 2002) and liprins (Zürner & Schoch, 2009) are the most recently identified molecules involved in the formation and maintenance of AZs while Bassoon (tom Dieck et al., 1998) and Piccolo (Fenster et al., 2000) are two very large, structurally related major scaffolding proteins, both key players in AZ assembly and functioning (Zhai et al., 2000; Fenster et al., 2003). Due to the fact that the delivery of Bassoon and Piccolo to presynaptic nerve terminals during synaptogenesis requires an intact Golgi apparatus (Dresbach et al., 2006), AZ molecules are presumably assembled at the Golgi and transported to nascent synapses as preformed complexes in axonal dense-core vesicles, the so-called Piccolo-Bassoon transport vesicles (PTVs) (Ziv & Garner, 2004; Fejtová & Gundelfinger, 2006). This hypothesis is supported by the fact that functional AZs can be formed within 30-60 min of initial axo-dendritical contact suggesting the deposition of various CAZ molecules in the presynaptic bouton at identical timepoints in synaptogenesis (Bresler et al., 2004). Interestingly, it has been shown that the incorporation of two or three of these PTVs into the presynaptic membrane is sufficient to create new AZs (Shapira et al., 2003). A recent study has revealed that synaptic vesicles are interconnected via a dense meshwork of short filaments while this vesicle network is in turn bound to the AZ by longer filaments for further stabilization within the presynaptic bouton (Siksou et al., 2007).

1.6 The postsynaptic density

Several hundred different proteins underneath the postsynaptic membrane of excitatory synapses within the CNS create a macromolecular complex which appears as an electrondense thickening on a subcellular level and is therefore called postsynaptic density (PSD) (Boeckers, 2006). The PSD of almost every

excitatory synapse (Gray type 1) is a 30-60 nm thick structure with a diameter of 200-500 nm (Spacek & Harris, 1998) and can mainly be found in the dilated tip of a dendritic spine, the “spine head” which is connected to the dendrite through a thin “spine neck”. In contrast, PSDs of inhibitory synapses (Gray type 2) or of excitatory synapses in neurons lacking spines are much smaller and localized directly in the dendritic shaft (Sheng & Hoogenraad, 2007). Dendritic spines are heterogenous, actin-rich structures showing high dynamic motility (Ethell & Pasquale, 2005). This is the reason why different spine shapes like “mushroom”, “thin” or “stubby” seem to reflect different developmental maturation stages. Additionally, spines contain a specialization of the calcium storing smooth endoplasmic reticulum (SER), the spine apparatus (SA), typically located in the spine head approaching the lateral margin of the PSD (Spacek & Harris, 1997). PSD assembly during synaptogenesis has not yet been fully understood. On the one hand, it has been reported that in neurons of late developmental stages, recruitment of major postsynaptic proteins occurs gradually, thus being fundamentally different from presynaptic AZ assembly (Bresler et al., 2004). On the other hand, a more recent study shows that preformed complexes containing the same major postsynaptic proteins are involved in early synapse formation which is totally in concordance with the development of the presynaptic AZ (Gerrow et al., 2006).

Throughout the last ten years, research has focused on the identification of a huge variety of PSD proteins which can currently be subdivided into the following classes due to recent mass spectrometry data: (i) cytoskeletal elements (16%) (ii) kinases, phosphatases and regulators (11%), (iii) GTPases and regulators (8%), (iv) cell adhesion molecules (7%), (v) metabolic proteins (7%), (vi) scaffolds (6%), (vii) receptors and channels (6%), (viii) translation machinery components (6%), (ix) mitochondrial proteins (6%), (x) membrane trafficking molecules (5%), (xi) motor proteins (4%), (xii) chaperones (2%) and others (15%) (Cheng et al., 2006). This large protein network contributes to synaptic plasticity by changing its composition and structure in response to neural activity.

1.6.1 Glutamate receptors

Excitatory synapses contain different glutamate receptors (GluRs) that are specifically clustered at the postsynaptic membrane. The predominant types are ionotropic NMDA and AMPA receptors (NMDAR & AMPAR) as well as the metabotropic glutamate receptor (mGluR) (Hollmann & Heinemann, 1994).

Two NR1 and two NR2 subunits combine to form the tetrameric NMDAR which is mainly concentrated in the middle of the PSD (Racca et al., 2000). The NR2 subunit which contains the binding site for glutamate, controls the electrophysiological properties of the receptor (Stephenson, 2006) and is differentially expressed during brain development (Liu et al., 2004). The most commonly found receptor in the mammalian CNS, the AMPAR, appears to be dense in the periphery of the PSD (Racca et al., 2000). It is composed of 4 types of subunits (GluR1, GluR2, GluR3 and GluR4) that combine to form tetramers (Song & Huganir, 2002). Cation permeability depends on the GluR2 subunit which can prevent calcium influx to guard excitotoxicity (Kim et al., 2001). As already mentioned in 1.4, NMDARs and AMPARs are essential for synaptic plasticity. Interestingly, the total number of NMDARs and AMPARs per PSD is only ~ 20 and ~ 15, respectively (Sheng & Hoogenraad, 2007). The mGluR belongs to the group C family of G-protein coupled receptors. In total, there are 8 different types of mGluRs that can be divided into groups I, II and III. Group I mGluRs that are predominantly found in the postsynaptic membrane can modulate the function of the NMDAR having influence on synaptic plasticity (Skeberdis et al., 2001).

All these receptors belong to individual multiprotein complexes, the AMPA receptor complex (ARC), the NMDA receptor complex (NRC) and the metabotropic glutamate receptor complex (mGC) (Kim & Sheng, 2004, Collins et al., 2005). Furthermore, ARCs, NRCs and mGCs are co-clustered by a dense platform of postsynaptic scaffolding molecules of the ProSAP/Shank family, the ProSAP/Shank platform (PSP) (Boeckers, 2006, Figure 1).

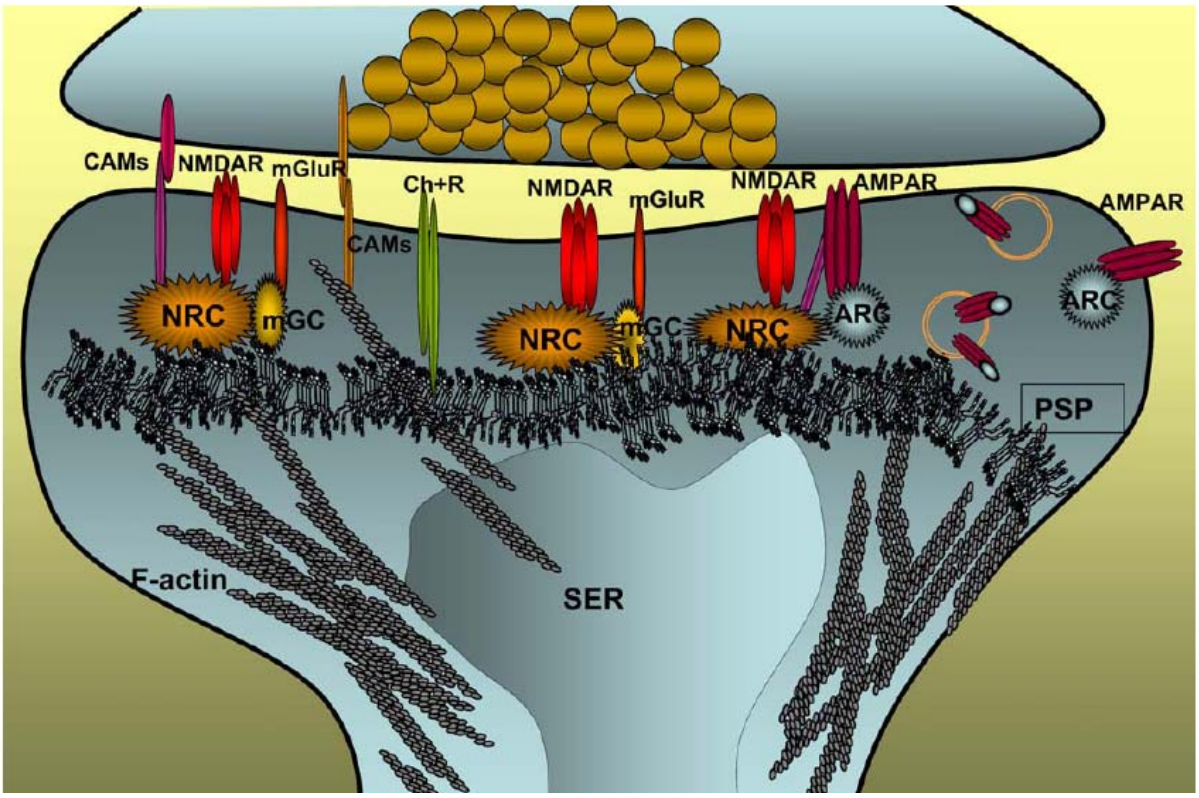

Figure 1 "Scaffolding" within PSDs of glutamatergic synapses of the CNS.
The NMDA receptor and metabotropic glutamate receptor complexes (NRC, marked *light brown* & mGC, marked *yellow*) that are associated with their corresponding receptors (NMDAR, marked *red* & mGluR, marked *orange*) are further co-clustered by the ProSAP/Shank platform (PSP, presented as *horizontal chain of oligomers within the spine head* marked *black*) which is in turn attached to the F-actin based cytoskeleton (presented as *filamentous structures mostly within the spine neck* marked *grey*) and, if present, to the smooth endoplasmic reticulum (SER) of dendritic spines. AMPA receptor complexes (ARC, receptor marked *violet &* complex *light grey*) don't necessarily need the PSP for clustering. Adhesion between the pre- and postsynaptic membrane is promoted by cell adhesion molecules (CAMs, marked *pink* or *ochre-colored*) while there are other channels and receptors (Ch + R, marked *olive green*) directly clustered by the PSP. The presynaptic bouton can be recognized by a group of synaptic vesicles (figure taken & modified from Boeckers, 2006).

1.6.2 The ProSAP/Shank family

The ProSAP/Shank protein family counts 3 members which are highly enriched in the PSD and localized at the interface between membrane receptors and the actin cytoskeleton (Boeckers et al., 1999 a; Naisbitt et al., 1999; Boeckers et al., 2002). These major scaffolding molecules contain multiple conserved domains allowing various protein-protein interactions: N-terminal ankyrin repeats followed by a Src homology3 (SH3) domain, a PSD-95/DLG/ZO-1 (PDZ) domain and a sterile alpha motif (SAM) domain. The name ProSAP (Proline-rich synapse-associated protein)

derives from conserved proline-rich clusters that can be found within all three proteins (Boeckers et al., 1999 a, b & Figure 2) while the term Shank reflects the SH3 domain and multiple ankyrin repeats (Naisbitt et al., 1999 & Figure 2).

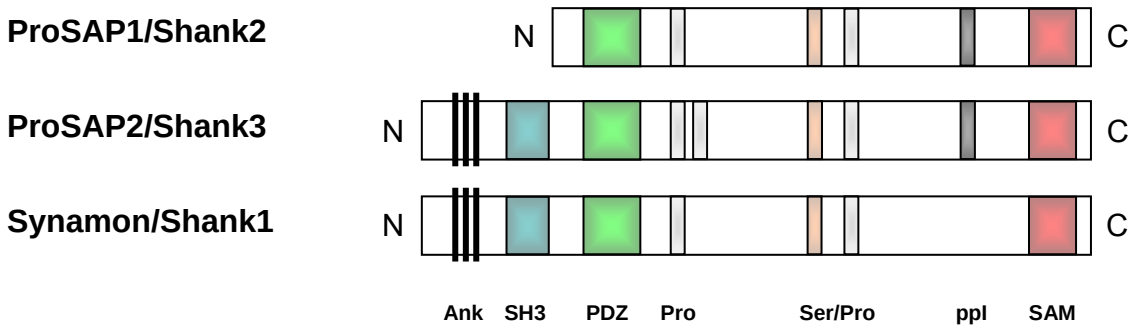

Figure 2 The ProSAP/Shank family of PSD proteins in brain

ProSAP1/Shank2, ProSAP2/Shank3 and Synamon/Shank1 are defined by a pattern of highly conserved protein-protein interaction domains. In brain, N-terminal ankyrin repeats (Ank, marked as *3 consecutive black bars*) and an SH3 domain (SH3, marked *blue*) can only be found in ProSAP2/Shank3 and Synamon/Shank1. All three proteins harbor a PDZ domain (PDZ, marked *green*), proline/serine-rich clusters (Pro, marked *light grey*; Ser, marked *light brown*) and a C-terminal SAM domain (SAM, marked *red*) while the cortactin-interacting ppI motif (Du et al., 1998; marked *dark grey*) can only be found in ProSAP1/Shank2 and ProSAP2/Shank3. Domain composition of ProSAP/Shank proteins can be validated on http://www.ncbi.nlm.nih.gov.

ProSAPs/Shanks are large proteins with a molecular mass of more than 180 kDa (Boeckers et al., 1999 a). All three share 63-87% amino acid identity among themselves while SH3, PDZ and SAM domains are conserved the highest. Synamon/Shank1 is only expressed in brain (Yao et al., 1999), ProSAP1/Shank2 also appears in non-neuronal tissue like pancreas, pituitary, lung, liver and testis (Redecker et al., 2001 & 2003) and ProSAP2/Shank3 has been detected in almost every tissue examined (Lim et al., 1999). Within the brain, ProSAPs/Shanks are not limited to neurons, but can also be found in glial cells (Redecker et al., 2001). All three family members are highly expressed in hippocampus and cortex. As far as the cerebellum is concerned, ProSAP1/Shank2 primarily appears in Purkinje cells while ProSAP2/Shank3 is only found in the granular cell layer (Boeckers et al., 1999 a, b). On a subcellular level, ProSAPs/Shanks are not localized directly beneath the postsynaptic membrane, but 25 nm inside the PSD (Naisbitt et al., 1999). Domain composition of ProSAPs/Shanks is regulated by alternative splicing (Boeckers et al., 1999 a; Lim et al., 1999). Shank2E, for example, one of the two

major alternative splice variants of ProSAP1/Shank2 which is only expressed in liver epithelial cells, does indeed have an SH3 domain and N-terminal ankyrin repeats like wildtype ProSAP2/Shank3 and Synamon/Shank1 (McWilliams et al., 2004). Another alternative splice variant of ProSAP1/Shank2 called ProSAP1A misses the ankyrin repeats, but still includes the SH3 domain. Further, there's knowledge of an alternatively spliced Synamon/Shank1 lacking the SAM domain (Sala et al., 2001).

1.6.2.1 Postsynaptic recruitment and assembly of ProSAPs/Shanks

As already described in 1.3, synaptogenesis requires the specific localization of proteins at both sites of the synaptic contact. The postsynaptic recruitment of ProSAP/Shank family members depends on the presence of certain sequences within these molecules called synaptic targeting signals. Synamon/Shank1, for example, only requires an intact PDZ domain for synaptic localization (Sala et al., 2001). In contrast, C-terminal elements of ProSAP1/Shank2 and ProSAP2/Shank3 including the SAM domain, the ppI motif and a serine-rich stretch of about 50 aa representing the minimal binding site for Dynamin-2 (Okamoto et al., 2001; Boeckers et al., 2005) are responsible for dendritic targeting. ProSAP2/Shank3 can additionally be recruited to the PSD via its PDZ domain and Homer binding site (Roussignol et al., 2005). It has further been implied that ProSAP1/Shank2 and ProSAP2/Shank3 already appear in newly formed PSDs being core elements of postsynaptic assembly while Synamon/Shank1 is only recruited during the late process of functional spine morphology regulation. (Sala et al., 2001; Boeckers et al., 2005). This assumption is supported by the fact that transgene expression of ProSAP2/Shank3 is sufficient to induce functional dendritic spines in aspiny cultured cerebellar granule cells while transfection of Synamon/Shank1 doesn't show this effect (Roussignol et al. 2005). A recent study proposes that the SAM domain of ProSAP2/Shank3 is not only essential for postsynaptic targeting, but due to its oligomerization ability also mediates the assembly of large sheets of ProSAPs/Shanks forming the PSP lying at the core of the PSD (Baron et al., 2006).

1.6.2.2 Interaction partners of the ProSAP/Shank family

Interaction partners of the ankyrin repeats and SH3 domain

One interaction partner of the N-terminal ankyrin repeats of ProSAPs/Shanks is α-fodrin which contains spectrin motifs binding to F-actin of dendritic spines (Boeckers et al., 2001; Broderick & Winder, 2002). Moreover, α-fodrin is processed in a calmodulin-dependent manner when intracellular calcium levels are elevated followed by the reorganization of the actin cytoskeleton (Harris & Morrow, 1990). Sharpin is another PSD molecule whose C-terminal half binds to the ankyrin repeats of the ProSAP/Shank family. Due to the fact that it can dimerize through its N-terminal half, it may crosslink ProSAPs/Shanks enhancing their level of multimerization (Lim et al., 2001). Branching of dendritic spines can be induced by Densin-180. This phenomenon disappears as soon as the C-terminal part of Densin-180 binds either to the SH3 domain or to the proline-rich clusters of ProSAP/Shanks (Quitsch et al., 2005). Further, the voltage-gated calcium channel Ca_V 1.3 binds to the SH3 and/or the PDZ domain of ProSAP/Shank family members thus connecting the postsynaptic scaffold to intracellular signaling cascades (Zhang et al., 2005).

Interaction partners of the proline/serine-rich clusters

Linkage of ProSAP/Shank proteins to the actin cytoskeleton of dendritic spines doesn't only happen via its ankyrin repeats and α-fodrin. The ppI motif, a short proline-rich stretch within the C-terminal part of ProSAP1/Shank2 and ProSAP2/Shank3 can interact with the SH3 domain of two proteins that are tightly associated to the cytoskeleton, Cortactin and Actin-binding protein1 (Abp1) (Du et al., 1998; Qualmann et al., 2004). The latter has recently been shown to regulate spine morphology by controlling actin polymerization within spine heads (Haeckel et al., 2008). Small GTPases like cell division cycle 42 (Cdc42) or Ras-related C3 botulinum toxin substrate (Rac) induce the binding of insulin receptor substrate IRSp53 to two more N-terminally positioned consecutive proline-rich clusters of ProSAP2/Shank3. This interaction leads to cytoskeletal reorganization within dendritic spines and thus might be the structural basis for insulin-dependent synaptic remodeling (Bockmann et al., 2002; Soltau et al., 2002). A recent study has characterized a novel interaction partner of these proline-rich clusters of

ProSAP2/Shank3 called Abelson interacting protein 1 (Abi-1) which controls actin assembly and takes part in synapto-nuclear shuttling (Proepper et al., 2007). Binding partner of the proline-rich stretch right next to the serine-rich region of ProSAPs/Shanks is Homer, a protein that clusters mGluRs in the PSD and further interacts with the inositol trisphosphate receptor (IP3R) of the spine apparatus thus establishing optimal conditions for glutamate-dependent calcium signaling (Tu et al., 1999; Sala et al., 2001 & 2005). Moreover, a short serine-rich sequence of the ProSAP/Shank family interacts with the proline-rich region of Dynamin-2, a PSD molecule which participates in membrane turnover and glutamate receptor recycling (Okamoto et al., 2001; Boeckers et al., 2002).

Interaction partners of the PDZ domain

PDZ domains that can be found in several PSD proteins are very important for protein-protein interactions thus contributing to create networks associated to the postsynaptic membrane (Fanning & Anderson, 1996; Niethammer et al., 1996). The abbreviation PDZ derives from the initials of three proteins where this domain has first been described: PSD-95, DlgA and ZO-1 (Garner & Kindler, 1996; Craven & Bredt, 1998; Hata et al., 1998). The architecture of a PDZ domain is predominantly designed for binding to the C-terminus of another protein whose last four amino acids (N-…P-3/P-2/P-1/P-0-C) are crucial for interaction. The amino acid at position P-0, the very end of the C-terminus, should be a hydrophobic one like leucine, isoleucine or valine. Amino acids at positions P-1 and P-3 are less important, but the one at position P-2 forms the basis for the classification of PDZ specificity (Sheng & Sala, 2001). Class I PDZ domains require a serine or threonine at P-2, class II PDZ domains favour a hydrophobic amino acid and class III PDZ domains need a negatively charged amino acid for interaction (Doyle et al., 1996; Songyang et al., 1997). Interestingly, the amino acid at P-2 of almost every PDZ domain binding motif can be phosphorylated which raises the possibilty that PDZ interactions are regulated by phosphorylation (Sheng & Sala, 2001).

The ProSAP/Shank family contains a highly conserved class I PDZ domain that is crucial for the integrity of the PSD because of its various interaction partners. The first to be identified was SAP90/PSD-95-associated protein/guanylate kinase-

associated protein (SAPAP/GKAP) which is a key molecule of the NRC. SAPAP/GKAP namely links members of the Membrane-associated guanylate kinase (MAGuK) family like SAP90/PSD-95 to ProSAP/Shank proteins (Boeckers et al., 1999 b; Naisbitt et al., 1999). Located right beneath the postsynaptic membrane, MAGuKs are primarily involved in recruiting, clustering and signaling of glutamate receptors like the NMDAR & AMPAR (Niethammer et al., 1996; Elias & Nicoll, 2007). The somatostatin receptor (SSTR) which plays a role in neurotransmission and the calcium-independent receptor for α-latrotoxin (CIRL) that may participate in cell adhesion also bind to the PDZ domain of ProSAP/Shanks (Zitzer et al., 1999; Kreienkamp et al., 2000). A further PDZ domain interaction partner of the ProSAP/Shank family is the signal transduction molecule βPIX, a guanine nucleotide exchange factor for the Rac1 and Cdc42 small GTPases that contributes to cytoskeletal reorganization within dendritic spines (Sala et al., 2001; Park et al., 2003). ProSAP interacting protein 2 (ProSAPiP2), the most recently identified protein binding to the PDZ domain of ProSAP2/Shank3 might also be involved in the attachment and modulation of cytoskeletal elements due to actin binding properties (Liebau et al., 2009).

Overall, one can say that the ProSAP/Shank platform is one of the core elements of the PSD predominantly clustering glutamate receptor complexes and stabilizing the actin cytoskeleton of dendritic spines. As the various interactions of ProSAP/Shank proteins are far from being fully understood, our group has focused on the identification and characterization of further interaction partners. Among others, we found a family of 4 homologous proteins: ProSAP interacting protein 1 (ProSAPiP1), Postsynaptic density protein containing leucine-zippers weighing 70 kDa (PSD-Zip70), Nedd4 binding protein 3 (N4BP3) and LAPSER1. These molecules are defined by a conserved Fez1 domain thus being called *“Fezzins”* (Wendholt et al., 2006). ProSAPiP1 and PSD-Zip70 have already been shown to interact with members of the SPAR family, a group of PSD proteins involved in spine morphology regulation (Maruoka et al., 2005; Wendholt et al., 2006; Spilker et al., 2008). Although some aspects and binding partners of *“Fezzin”* family members LAPSER1 and N4BP3 have already been described in non-neuronal cells (Cabeza-Arvelaiz et al., 2001; Murillas et al., 2002; Thyssen et al., 2006; Sudo & Maru, 2007 & 2008), their role in neurons still remains unclear.

From now on, I will only use the term “ProSAP” for members of the ProSAP/Shank family of PSD proteins to avoid confusion and maintain terminological consistency.

1.7 Goals of this work

This work focuses on the characterization of *“Fezzin”* family member LAPSER1 in rat brain.

After computer-based genomic and structural analysis of this protein, the LAPSER1 tissue expression pattern should be evaluated on the mRNA level by Northern Blot analysis and *in situ* hybridization. A polyclonal antibody directed against LAPSER1 should further be generated to evaluate the tissue expression pattern of LAPSER1 on the protein level by Western Blot analysis and immunhistochemistry. Subsequent Western Blot analysis of brain subcellular fractions and PSD preparations as well as immunostaining of neuronal primary cultures should be conducted to confirm the presumed postsynaptic localization of LAPSER1.

Finally, studies of LAPSER1 and its interaction partners should be done to provide insights into the functional role of this protein in brain. First, the interaction between LAPSER1 and ProSAP2 should be confirmed by co-immunoprecipitation and co-transfection experiments of eukaryotic cell lines. Second, the interaction of *“Fezzin”* family members (LAPSER1, ProSAPiP1, PSD-Zip70 & N4BP3) with the postsynaptic spine-modulating protein SPAR1 should be characterized by a yeast-two-hybrid assay. Third and last, the activity-dependent molecular crosstalk between LAPSER1 and its interaction partners SPAR1 and β-Catenin should be investigated by co-transfections of eukaryotic cell lines, co-immunoprecipitations and NMDA-stimulation experiments of primary neuronal cultures.

2. Materials & Methods

2.1 Materials

2.1.1 Tools and machines

Cellculture flasks 250 cm^2	Nunc, Wiesbaden
Cellculture plates 24 well	Nunc, Wiesbaden
Cellculture dishes 94 mm Ø	Nunc, Wiesbaden
Centrifuge Allegra 21R	Beckmann Coulter, Krefeld
Centrifuge Avanti J-25	Beckmann Coulter, Krefeld
Centrifuge Tubes 50 ml	Beckmann Coulter, Krefeld
Chamberslides 76 x 26 mm	Menzel, Braunschweig
Cover glasses 13 mm Ø	Menzel, Braunschweig
Cover glasses 24 x 60 mm	Menzel, Braunschweig
Electroporation cuvettes	BioRad, München
Electroporator 2510	BioRad, München
Eppendorf cups 0,2/0,5,/1,5/2 ml	Eppendorf, Hamburg
Falcon Tubes 15 and 50 ml	Nunc, Wiesbaden
Flasks 100/250/500/1000 ml	Duran, Mainz
Freezer -20 °C	BSH, Giengen
Freezer -86 °C	Forma Scientific, USA
Fridge 4 °C	BSH, Giengen
Heraeus-Multifuge 3 S-R	Heraeus-Kendro, Hanau
Ice Machine	Scotsman, USA
Incubation shaker Certomat H	Braun Biotech, Melsungen
Incubation shaker Innova 4000	New Brunswick Scientific, USA
Incubators 30/37°C	Heraeus-Kendro, Hanau
Magnetic stirring hotplate MR 3001 K	Heidolph, Schwabach
Microscope Axioskop 2 mot plus	Zeiss, Oberkochen
Microscope Axiovert 25	Zeiss, Oberkochen
Microscope Stemi 2000-CS	Zeiss, Oberkochen
Microwave	BSH, Giengen

Neubauer counting chamber	Brand, Wertheim
Nylon cell sieve 125 µm	Falcon, Gräfelfing-Lochham
PCR machine Mastercycler gradient	Eppendorf, Hamburg
Petri dishes 94 mm Ø	Nunc, Wiesbaden
pH meter inoLab Level 1	WTW, Weilheim
Pipetboy	Hirschmann, Eberstadt
Pipette tips 10 µl/200 µl/1 ml	Eppendorf, Hamburg
Pipettes P10, P20, P100, P1000	Eppendorf, Hamburg
Pipettes 5/10/25 ml	Brand, Wertheim
PVDF membrane Hybond	Amersham, UK
SDS-PAGE gel chamber	BioRad, München
SDS-PAGE gel tray	BioRad, München
SDS-PAGE glass plates	BioRad, München
SDS-PAGE power supply	BioRad, München
Sonicator Sonoplus UW 2070	Bandelin electronics, Berlin
Spectrophotometer DU 530	Beckmann Coulter, Krefeld
Sterile bench Laminar flow	Nunc, Wiesbaden
Sterile filters 0,22 µm/0,45 µm	Schleicher & Schuell, Dassel
Tabletop Combispin FVL-2400	Peglab, Erlangen
Tabletop centrifuge Biofuge pico	Heraeus-Kendro, Hanau
Tabletop shaker IKA-vibrax VXR	Janke & Kunkel, Staufen
Tank Blot machinery	Biorad, München
Thermomixer comfort	Eppendorf, Hamburg
Tissue homogenizator Potter S	Braun Biotech, Melsungen
Ultracentrifuge Optima Max-E	Beckmann Coulter, Krefeld
UV cuvettes	Hellma, Mühlheim
UV transilluminator	Life Technologies, USA
Weighing system	Sartorius, USA
Whatman filter papers 70 mm Ø	Schleicher & Schuell, Dassel
X-ray film	Amersham, UK

2.1.2 Chemical substances

2.1.2.1 Antibiotics (stock solutions)

ampicillin 50 mg/ml ampicillin ss to be dissolved in 50% ethanol

→ *Store aliquots at -20 °C and use 100 µg/ml*

kanamycin 25 mg/ml kanamycin ss to be dissolved in 50% ethanol

→ *Store aliquots at -20 °C and use 50 µg/ml*

2.1.2.2 Buffers

All buffers listed are stored at room temperature (RT).

6x loading buffer	5,0%	bromphenole blue
(DNA electrophoresis)	86,0%	glycerol
	→ ad the appropriate volume with deionized water	

10x PBS	80,0 g	NaCl
(pH 7,4)	2,0 g	KCl
	14,4 g	$Na_2HPO_4x2H_2O$
	2,4 g	KH_2PO_4
	→ Add 1 M HCl until pH is 7,4	
	→ ad 1 l with deionized water	

20x SSC	175,3 g	NaCl
	88,2 g	sodium citrate
	→ Add 1 M HCl until pH is 7,0	
	→ ad 1 l with deionized water	

50x TAE	42,0 g	Tris
	57,0 ml	acetic acid
	100,0 ml	EDTA (pH 8)
	→ ad 1 l with deionized water	

10x TBS	24,2 g	Tris
(pH 7,6)	80,0 g	NaCl
	→ Add 1 M HCl until pH is 7,6	
	→ ad 1 l with deionized water	

1M Tris/HCl	121,14 g	Tris
(pH 8,0/8,5)	→ Add 1 M HCl until pH is 8,0 or 8,5 respectively	
	→ ad 1 l with deionized water	

1,5 M Tris/HCl	181,71 g	Tris
(pH 8,0)	→ Add 1 M HCl until pH is 8,0	
	→ ad 1 l with deionized water	

2.1.2.3 Media

All media listed are stored at 4 °C.

LB-medium	20,0 g	tryptone
	5,0 g	yeast extract
	0,5 g	NaCl
	→ ad 1 l with deionized water	
	→ Autoclave solution for 20 min at 121 °C	

SOB-medium	20,0 g	peptone
	5,0 g	yeast extract
	0,5 g	NaCl
	→ ad 1 l with deionized water	
	→ Autoclave solution for 20 min at 121 °C	

2YT-medium	16,0 g	tryptone
	10,0 g	yeast extract
	5,0 g	NaCl
	→ ad 1 l with deionized water	
	→ Autoclave solution for 20 min at 121 °C	

DMEM	10%	FBS
YPD-medium	50,0 g	YPD
	0,1 g	AHS
	→ ad 1 l with deionized water	
	→ Autoclave solution for 15 min at 121 °C	
	→ Add 0,25 ml/l kanamycin	
SD-medium	27,0 g	DOB (or 43,7 g DOBA if agar is needed)
	0,1 g	AHS
	appropriate amount of synthetic dropout supplement:	
	0,74 g	in case of CSM -Trp
	0,69 g	in case of CSM -Leu
	0,64 g	in case of CSM -Leu/-Trp or
	0,62 g	in case of CSM -His/-Leu/-Trp
	→ ad 1 l with deionized water	
	→ Autoclave solution for 15 min at 121 °C	
	→ Add 0,25 ml/l kanamycin	

YPD-medium is used for cultivation of plasmid-free yeast strains.
Selection of transformed yeasts needs cultivation in special minimal media that contain complete supplement mixtures (CSM) of amino acids lacking the ones responsible for selection called synthetic dropout (SD) media:

- CSM -Trp lacking tryptophane for the selection of yeasts containing vectors coding for the GAL4-activation domain (e.g. the pAS2-1 vector)
- CSM -Leu lacking leucine for the selection of yeasts containing vectors coding for the GAL4-binding domain (e.g. the pACT2 vector)
- CSM -Leu/-Trp lacking leucine and tryptophane for the selection of yeasts containing both expression vectors just mentioned
- CSM -His/-Leu/-Trp lacking histidine, leucine and tryptophane for the selection of yeasts containing both expression vectors and their corresponding fusion proteins interacting with each other

2.1.2.4 Stock solutions

10% APS
1,0 g APS
→ ad 10 ml with deionized water
→ Store at 4 °C

500 mM EDTA (pH 8,0)
18,61 g EDTA
→ Add 1 N NaOH until pH is 8,0
→ ad 100 ml with deionized water
→ Store at RT

ethidium bromide
10 mg/ml Store at 4 °C away from light
→ *Use 0,5 µg/ml*

500 mM HEPES (pH 7,4)
5,96 g HEPES
→ Add 1N NaOH until pH is 7,4
→ ad 50 ml with deionized water
→ Store at -20 °C

1 M IPTG
2,0 g IPTG
→ ad 10 ml with deionized water
→ Store at -20 °C

Mowiol
2,4 g Mowiol 4-88
6,0 g glycerol
→ Add 12,0 ml of 0,2 M Tris-HCl pH 8,5
→ ad 20 ml with deionized water and agitate
→ Centrifuge at 13,000 x g for 30 min at RT
→ Store 1 ml aliquots frozen at -20 °C

5 M NaCl
292,0 g NaCl
→ ad 1 l with deionized water
→ Store at RT

1 N NaOH 40,0 g NaOH-pellets
→ ad 1 l with deionized water
→ Store at 4 °C

100 mM NMDA 0,029 g NMDA
→ ad 2 ml with deionized water
→ Store at 4 °C

RNase A 0,2 g RNase A
→ Use 1 µl/ml → ad 10 ml with deionized water

10% SDS 50,0 g SDS
→ ad 500 ml with deionized water
→ Store at RT

2 M sucrose 410,76 g sucrose
→ ad 600 ml with deionized water
→ Store at -20 °C

2% X-Gal 20,0 mg X-Gal
→ ad 1 ml in DMF
→ Store at 4 °C

2.1.3 Kits

name	**used for**	**company**
BCA Protein Assay Kit	protein determination	Pierce, USA
Pierce ECL Western Blotting Substrate	Western Blot detection	Pierce, USA
Polyfect Transfection Reagent	eukaryotic cell transfection	Qiagen, Hilden
QIAquick Gel Extraction Kit	gel extraction	Qiagen, Hilden
QIAquick PCR purification kit	purification of PCR products	Qiagen, Hilden
QIAprep Spin Miniprep Kit	isolation of plasmid DNA	Qiagen, Hilden
TA Cloning Kit	cloning	Invitrogen, Karlsruhe

2.1.4 Biological material

2.1.4.1 Vectors

Prokaryotic vectors

plasmid	used for/as	selection	promoter	company
pCR2.1	cloning	amp/kan	T7	Invitrogen, Karlsruhe
pGEX	GST-fusion vector	amp	Ptac	Amersham, UK

Eukaryotic vectors

plasmid	used for	selection	promoter	company
pACT2	yeast-two-hybrid system	amp	ADH1	Clontech, Heidelberg
pAS2-1	yeast-two-hybrid system	amp	ADH1	Clontech, Heidelberg
pDsRed2	high level expression	kan	CMV	Clontech, Heidelberg
pEGFP	high level expression	kan	CMV	Clontech, Heidelberg

2.1.4.2 cDNA clones

Clones from *Rn*ProSAP2 (Tobias Boeckers), *Rn*LAPSER1, *Rn*N4BP3 (both Angelika Schmitt), *Rn*SPAR1 (Anna Dolnik), *Rn*PSD-Zip70 (AG Sobue, Japan) and *Rn*ProSAPiP1 (Doreen Wendholt) were used in this work.

2.1.4.3 Primers

All Primers were ordered from MWG Biotech, Ebersberg.

primer	sequence	co.
FRnLAPSER1 EcoR1	5'-AAAGAATTCCATGGCCATTGTGCACACT-3'	MWG
B-AS1 LAPSER1Not1	5'-AAAGCGGCCGCCCTGCTGCTCCCTTTCAA-3'	MWG
B-AS2 LAPSER1Not1	5'-AAAGCGGCCGCAGGAGGAAGAGGCTGGCC-3'	MWG
FRnLAPSER1 K-6EcoR1	5'-AAAGAATTCGGGCCAGCCTCTTCCTCCT-3'	MWG
BRnLAPSER1 BamH1	5'-AAAGGATCCCTAGATTTCAGTGGCAGTGAT-3'	MWG
FRnLAPSER1 K-3EcoR1	5'-AAAGAATTCCTTGGGCCACGGCTAGAG-3'	MWG
LAPSER1 in-situ	5'-CAGTGGCAGTGATCTCCTCCAGACAGATGCAAGGGGCCGGC-3'	MWG
Zip70-FEZ No1-s	5'-GTGGAATTCTACAAACTGCGCAAATCC-3'	MWG
Zip70-FEZ No1-as	5'-AAAGGATCCTCAGTTCCGGCCCGAGTC-3'	MWG
Zip70-FEZ No2-s	5'-ATTGAATTCACCCAATGGGAGGTGTGC-3'	MWG
Zip70-FEZ No2-as	5'-AGAGGATCCTCACTGCTGCAGGGCCTT-3'	MWG
SPAR CtNo1-s	5-TGGGAATTCAACTAGACCAAGCCCTGC-3'	MWG
SPAR CtNo1-as	5'-ATACTCGAGTCAGATGTCGGTAAGGGA-3'	MWG
SPAR CtNo2-s	5'-ATTGAATTCTACAGGAGACCCGGAGGC-3'	MWG
SPAR CtNo2-as	5'-AGCCTCGAGTCAAGAGGAGTCCTTACT-3'	MWG
SPAR CCLZNo3-s	5'AGAGAATTCGGCCCACTCTGGCTTCTA-3'	MWG
SPAR CCLZNo3-as	5'-GAACTCGAGTCAGCTCATGTCTATGGT-3'	MWG

2.1.4.4 Primary antibodies

Polyclonal antisera:

pab LAPSER1 from rabbit	Pineda, Berlin
pab ProSAP2 from guinea pig	Pineda, Berlin
pab SPAR1 from goat	Santa Cruz, USA

Monoclonal antisera:

mab β-Catenin (C-term) from mouse	Fitzgerald, USA
mab β-Catenin (N-term) from mouse	Upstate, USA
mab GFP from mouse	Clontech, Heidelberg

2.1.4.5 Secondary antibodies

anti-mouse-IgG, HRP	DakoCytomation, Denmark
anti-mouse-IgG, Alexa Fluor 488	Invitrogen, Karlsruhe
anti-mouse-IgG, Alexa Fluor 647	Invitrogen, Karlsruhe
anti-goat-IgG, HRP	DakoCytomation, Denmark
anti-goat-IgG, Alexa Fluor 647	Invitrogen, Karlsruhe
anti-guinea-pig-IgG, HRP	DakoCytomation, Denmark
anti-guinea-pig-IgG, Alexa Fluor 568	Invitrogen, Karlsruhe
anti-rabbit-IgG, HRP	DakoCytomation, Denmark
anti-rabbit-IgG, Alexa Fluor 488	Invitrogen, Karlsruhe
anti-rabbit-IgG, Alexa Fluor 568	Invitrogen, Karlsruhe

2.1.4.6 Enzymes & enzyme inhibitors

All enzymes and the appropriate buffers used in this work were from Invitrogen, Karlsruhe.

Complete EDTA-free protease inhibitor cocktail tablets from Roche, Mannheim were used as protease inhibitor mix (PIM).

2.1.4.7 Organisms

bacteria	*E. coli* BL21 & *E. coli* DH5α
eukaryotic cell lines	Cos-7, HeLa
yeasts	*S. cerevisiae* Y187 & *S. cerevisiae* AH109

2.1.4.8 Laboratory animals

In this work, adult Wistar rats were sacrificed for tissue extraction while the brains of embryonic Wistar rats were used for hippocampal cell cultures.

2.1.4.9 Markers

1 kb DNA ladder Invitrogen, Karlsruhe

→ 12,216; 11,198; 10,180; 9162; 8144; 7126; 6108; 5090; 4072; 3054; 2036; 1636; 1018; 506; 396; 344; 298 bp

Page Ruler^{TM} Prestained Protein Ladder Fermentas, St. Leon-Rot

→ 170, 130, 100/92, 70, 55, 40, 35, 25, 15, 10 kDa

2.2 Methods of microbiology

2.2.1 Cultivation & storage of *E.coli* bacterial strains

For cultivation, LB-medium was inoculated with bacteria and incubated overnight at 37°C with shaking at 200 rpm. Antibiotic selection had to be ensured when strains containing plasmids were cultivated. Long time storage was guaranteed as glycerol stock culture at -80°C To prepare a new stock, 1 ml of bacterial culture was mixed with 1ml of sterile 50% glycerol and subsequently frozen at -80 °C.

2.2.2 Production & transformation of competent bacteria

2.2.2.1 Production of chemocompetent bacteria

200 ml of LB-medium were inoculated with an overnight culture of the appropriate bacterial strain and grown up to an OD_{600} of approx. 0,3-0,6 at 37 °C with shaking at 200 rpm. After incubation on ice for 15 min, the culture was centrifuged at 750-1000 x g for 15 min at 4 °C. Subsequently, the pellet was resuspended in Chemcomp solution I in 1/3 of the initial volume (~ 67 ml) and incubated on ice for 60-90 min. After another centrifugation at 750-1000 x g for 15 min at 4 °C, the pellet was resuspended in Chemcomp solution II in 1/12.5 of the initial volume (~ 16 ml) and incubated on ice for 15 min. The cells were aliquoted, frozen in liquid nitrogen and permanently stored at -80 °C as 200 µl aliquots.

Chemcomp solution I	**Chemcomp solution II**
100 mM RbCl	10 mM MOPS
50 mM $MnCl_2$	10 mM RbCl
30 mM KAc	75 mM $CaCl_2$
10 mM $CaCl_2$	15% glycerol
→ pH 5,8	→ pH 6,8

Both solutions have to be stored at 4 °C.

2.2.2.2 Transformation of chemocompetent bacteria

After defrosting an aliquot (200µl) of chemocompetent cells on ice, 10-15 µl of ligation or 0,1 µg of plasmid DNA were added and the mixture was incubated on ice for 45 min. Further, these cells were incubated at 37 °C for 3 min, subsequently cooled down at RT for 10 min, mixed with 200 µl of LB-medium and incubated at 37 °C with shaking at 200 rpm for 60-90 min. After resuspension in 100 µl of LB-medium, the cells were plated on the appropriate selection plates which were finally put in an incubator overnight at 37 °C.

2.2.2.3 Production of electrocompetent bacteria

50 ml of 2YT-medium were inoculated with an overnight culture of the appropriate bacterial strain and grown up to an OD_{600} of about 0,3-0,6 at 37 °C with shaking at 200 rpm. The culture was then cooled down on ice for 20 min and centrifuged at 2,000 x g for 10 min at 4 °C. After resuspension in 50 ml of ice-cold deionized water, the cells were centrifuged at 2,000 x g for 10 min at 4 °C again. This washing step was repeated twice until the cells were finally resuspended in 50 ml of ice-cold 10% glycerol. Electrocompetent bacteria were aliquoted, frozen in liquid nitrogen and permanently stored at -80 °C as 50 µl aliquots.

2.2.2.4 Transformation of electrocompetent bacteria

After defrosting an aliquot (50µl) of electrocompetent cells on ice, 0,5-1,5 µl of ligation or 0,1 µg of plasmid DNA were added and the mixture was subsequently electroporated at 1,8 kV in a pre-cooled electroporation cuvette. Washing the bacteria out of the cuvette with 1 ml of SOB-medium was followed by incubation at 37 °C with shaking at 200 rpm for 1 h. Afterwards, the cells were centrifuged at 4,000 x g for 15 min at RT, resuspended in 100 µl of SOB-medium and plated on the appropriate selection plates which were finally put in an incubator overnight at 37 °C.

2.2.3 Cultivation & storage of yeast strains

For storage up to 8 weeks, the *S. cerevisiae* yeast strains used in this work were plated on YPD-plates, incubated at 30 °C for 3-5 days and stored at 4 °C. Long time storage is indefinite in YPD-medium with 50% glycerol at -80°C. Transformed yeast strains should be stored in the appropriate SD-medium to keep selective pressure on the plasmid. To prepare a new glycerol stock culture of yeasts, 1 ml of yeast culture was mixed with 1ml of sterile 50% glycerol.

2.2.4 Production & transformation of competent yeasts

2.2.4.1 Production of electrocompetent yeasts

30-50 ml of YPD-medium or the appropriate SD-medium were inoculated with several colonies or a glycerol stock culture and incubated overnight at 30 °C with shaking at 200 rpm. On the next morning, 5 ml of the overnight culture was transferred into a flask containing 45 ml of YPD- or the appropriate SD-medium (the OD_{600} should be approx. 0,2-0,3) and incubated at 30 °C for 3-5 hours with shaking at 200 rpm until the OD_{600} was approx. 0,4-0,6. The culture was then centrifuged at 2,500 x g for 3 min at 4 °C followed by a resuspension of the pellet in 25 ml of ice-cold aqua deion. This washing step was repeated three times while in the end, 25 ml of ice-cold 1 M sorbitol were used instead of aqua deion. Finally, the pellet was resuspended in 1 M sorbitol. Competent yeasts were stored at 4 °C for 2-3 days.

2.2.4.2 Transformation of electrocompetent yeasts

0,1 µg of plasmid DNA was added to 60 µl of competent yeast cells and the mixture was subsequently electroporated at 2,5 kV in a pre-cooled electroporation cuvette. Washing the yeasts out of the cuvette with 1 ml of YPD-medium was followed by incubation at 30 °C with shaking at 200 rpm for 2 h. Afterwards, the cells were centrifuged at 4,000 x g for 3-5 min at RT, resuspended in 100 µl of YPD-medium and plated on the appropriate selection plates which were finally put in an incubator at 30 °C for 3-7 days.

2.3 Methods of molecular biology

2.3.1 Alkaline mini-prep isolation of plasmid DNA from *E. coli*

This method is based on selective alkaline denaturation of high molecular weight chromosomal DNA while covalently closed circular DNA remains double-stranded. First, cell walls of plasmid-containing bacteria are lysed with SDS and NaOH which also leads to a selective denaturation of chromosomal DNA. Further, the lysate is neutralized by acidic sodium acetate which has the effect that an insoluble network of aggregates is formed by the renatured chromosomal DNA as well as SDS-protein complexes are precipitated. After centrifugation, plasmid DNA can be precipitated with alcohol and later be concentrated.

5 ml of LB-medium containing the appropriate selection antibiotic was inoculated with one single bacterial colony and incubated overnight at 37°C with shaking at 200 rpm. On the next morning, the culture was centrifuged at 13,000 x g for 5 min at RT. Further, the pellet was resuspended in 100 µl of ice-cold solution I (+ RNAse A). Subsequently, 200 µl of freshly prepared solution II were added, mixed gently and incubated for 1 min at RT. Adding 100 µl of ice-cold solution III was followed by incubation on ice for 3-5 min and centrifugation at 13,000 x g for 10 min at RT. After precipitation with 800 µl of 100% ethanol for 30 min at -20 °C, the DNA was centrifuged at 13,000 x g for 5 min at RT. The pellet was then washed with 500 µl of 70% ethanol and centrifuged again at 13,000 x g for 10 min at RT. Finally, the plasmid-DNA was resuspended in 50 µl of aqua deion.

solution I	**solution II**	**solution III**
10 mM EDTA	200 mM NaOH	2M potassium acetate
50 mM glucose	1% SDS	11,5% acetic acid
25 mM Tris/HCl		
→ pH 8,8		

2.3.2 Preparation of plasmid DNA from *E. coli* with anion exchange columns

The *QIAprep Spin Miniprep Kit* from Qiagen was used to obtain a higher degree of DNA purity. Contrary to the alkaline lysis, the purification follows the principle of anion exchange chromatography. The negatively charged DNA binds to a positively charged matrix and is precipitated with isopropyl alcohol after elution.

2.3.3 Calculation of DNA concentration

The general method used for calculation of plasmid DNA concentration is ultraviolet absorption spectroscopy. At a wave length of 260 nm (absorption maximum of DNA), a solution which contains 50 µg/µl of double stranded DNA has an optical density of 1.0. So the following formula was used for calculation:

$[DNA] = OD_{260} \cdot 50\ \mu g/\mu l$

2.3.4 Polymerase chain reaction (PCR)

The polymerase chain reaction (PCR) is an essential method for cloning genes. Two synthetic oligonucleotides which are annealed at both ends of the DNA or RNA sequence to be amplified serve as primers for a thermo-stable polymerase. A defined part of a DNA strand can thus be amplified as long as the primers are well-chosen and the general conditions are appropriate.

The PCR follows 3 steps

1. Denaturation (30-45 sec)
   Double stranded DNA is heated up to 94-95 °C to separate strands.
2. Primer Annealing (60-90 sec)
   Primers are hybridized each on its appropriate separated single strand (temperature optimum depending on the GC-content of the sequence to be amplified, normal range: 52-65 °C)
3. Polymerization
   A polymerase synthesizes the defined part of the DNA
   (temperature optimum depending on the polymerase used)

For performing PCR experiments, the *High Fidelity PCR Supermix* from Invitrogen was used. It contains a *Taq*-polymerase (DNA-polymerase from *Thermus aquaticus*) and a *Pfu*-polymerase (DNA-polymerase from *Pyrococcus furosius*) which are both thermo-stable enzymes. The *Taq*-polymerase adds ATPs to the newly synthesized DNA strand after each amplification and so produces sticky ends while the *Pfu*-polymerase doesn't thus creating blunt ends.

Components per PCR usually were

- 1 µl DNA template
- 1 µl sense primer
- 1 µl antisense primer
- 47 µl *High Fidelity PCR Supermix*

The PCR mix was sometimes also "self-made".
Components of this mix usually were

- 5 µl 10x PCR buffer
- 5 µl 5 M Betain
- 2,5 µl DMSO
- 1 µl 10 mM dNTP
- 0,074 µl *Taq*-polymerase
- 32,5 µl deionized water

1 µl of each primer (sense/antisense) and 1 µl of DNA template were added.

DNA yield could be increased by elongating the polymerization step and by enhancing the number of cycles.

2.3.5 DNA agarose gel electrophoresis

DNA as a negatively charged molecule can be moved through a matrix of agarose by electric current and be separated by size. This is how DNA fragments can easily be analyzed after PCR amplification.

1% agarose was boiled up in 1x TAE buffer and cooled down to 60 °C. After adding ethidiumbromide in a concentration of 0,5 µg/ml, the solution was then poured into a casting tray in which the gel could solidify while a sample comb was added into the gel at one end of the tray to generate sample wells. In the meantime, DNA samples were mixed with 6x loading buffer (sample/loading buffer ratio = 5:1). Later, the sample comb was removed, the casting tray with the gel was put into the electrophoresis chamber and covered with 1x TAE buffer. Subsequently, the samples were pipetted into the sample wells. Current was applied to let the DNA migrate at approx. 8 V/cm until the gel was finally analyzed by UV light photography.

2.3.6 Purification of DNA from agarose gels

For further use, the separated DNA had to be eluted from the agarose gel. In this work, the DNA was cut out of the gel and purified with the *QIAquick Gel Extraction Kit* from Qiagen that follows the principle of anion exchange chromatography.

2.3.7 Restriction enzyme digestion of DNA

Specific restriction endonucleases (class II) recognize a particular DNA recognition sequence and then cut within. In this manner, DNA fragments with terminal cutting sites can be produced that are then used for cloning.

1 µl of 10x restriction endonuclease buffer and 1 U per restriction endonuclease were added to 0,5-1,5 µg of DNA. This mixture was filled up to an end volume of 10 µl with deionized water and was subsequently incubated at the temperature optimum of the restriction endonuclease(s) used (normally at 37 °C) for 60-90 min.

2.3.8 Ligation

Ligation means that linear DNA fragments are joined together with covalent bonds. This kind of reaction is needed when a DNA fragment with the appropriate terminal cutting sites (the insert) has to be cloned into a DNA vector after digestion with restriction enzymes.

Ligation with the T4 DNA Ligase

The T4 DNA Ligase, an ATP-dependent enzyme from the bacteriophage T4, was used for ligation because it catalyzes the formation of a phosphodiester bond between 5'-phosphate and 3'-hydroxyl termini in double-stranded DNA.

50-100 ng of vector DNA was digested with the appropriate restriction endonuclease(s). The DNA insert was then added in a 3:1 up to a 10:1 molar ratio. After addition of 5x ligase buffer (2 µl) and 1 U of T4 DNA Ligase, the mixture was filled up to an end volume of 10 µl with deionized water and either incubated for 2 h at RT or overnight at 14 °C.

TA Cloning

The *TA Cloning Kit* from Invitrogen makes it possible to clone PCR products into the pCR2.1 vector right after purification leaving out the step of restrictive digestion.

2.4 Methods of eukaryotic cell culture

2.4.1 Cultivation, storage & transfection of Cos-7 & HeLa cells

The cells used in this work were stored permanently in liquid nitrogen at -196 °C. However, they could also be temporarily stored at 37 °C & 5% CO_2 as long as they were passaged regularly.

2.4.1.1 Cultivation of Cos-7 & HeLa cells

After being defrosted at 37 °C, the cells were resuspended in 5 ml of culture medium and centrifuged at 600 x g for 5 min at RT. After resuspension in 10 ml of pre-heated (37 °C) culture medium, the cells were transferred into a cell culture flask (surface: 250 cm^2) and could be used for further experiments after 1-2 days at 37 °C.

2.4.1.2 Temporary storage and passaging of Cos-7 & HeLa cells

All media/solutions had to be warmed up to 37 °C before usage and all steps of passaging were done under a laminar flow hood. After the culture medium had been removed, the cells were washed carefully with 1x PBS buffer. They were then covered with 0,25% trypsin and incubated for 1-5 min at 37 °C. Further, the cells were removed from the flask ground by tapping, resuspended in 5 ml of fresh culture medium and finally disseminated:

→ 0,7 x 10^5 cells per 250 cm^2 for temporary storage

→ 0,3 x 10^6 cells per 100 cm^2 for transfection

2.4.1.3 Permanent storage of Cos-7 & HeLa cells

The cells were passaged until resuspension in 5 ml of fresh culture medium as described in 2.4.1.2. After centrifugation at 600 x g for 5 min at RT, the cell pellet was resuspended in 2 ml of FBS and 0,2 ml of DMSO was further added while shaking lightly. The suspension was then cooled down step by step to -70 °C and the cells were stored permanently in liquid nitrogen at -196 °C.

2.4.1.4 Transfection of Cos-7 & HeLa cells

Transfection was performed with *PolyFect Transfection Reagent* from Qiagen while the transfection rate was about 20-30%. After 18-24 hours, the cells were either lysated to produce protein extracts or they were fixed to be analyzed by fluorescent microscopy.

Protein extraction

The cells were lysated with 2x SDS loading buffer and subsequently boiled up for 5 min at 95 °C. Analysis of the protein extract was done by Western Blot as described in 2.5.6.4.

Fixation of cells and fluorescent microscopy

After removal of the culture medium, the cells were washed carefully with 1 x PBS buffer. Subsequently, 0,5 ml of fixation solution was added and the cells were incubated at RT for 10 min. Washing the cells with 1 x PBS buffer 3 times for 5 min each time at RT was followed by incubation with 100 µl of DAPI (1:1000 dilution) for 1-2 min. The cells were then washed again with deionized water for 5-10 min. Finally, a coverslip with cells was each put on a slide covered with one drop of 50 °C hot Mowiol to dry overnight. Analysis of stained or transfected cells was done with the Axioskop 2 mot plus (fluorescent microscope) from Zeiss, Oberkochen.

fixation solution

4,8 ml PFA
6,0 ml 2x PBS
1,2 ml H_2O
15% Sucrose

2.4.2 Preparation of primary hippocampal neurons

Neurons for primary cultures were taken from 18 day old rat embryos (E18).

Sterile cover glasses were placed in 24-well plates, coated with poly-L-lysin, incubated for 1 h at 37 °C and finally washed three times with deionized water.

A pregnant rat (E18) was then sacrificed, the embryos were taken out and subsequently decapitated, while their heads were collected in a petri-dished filled with ice-cold HBSS. The hippocampi were further prepared from the embryos' brains and placed into a falcon tube with 10 ml of ice-cold HBSS.

The following steps were carried out under the laminar flow hood.

After washing the hippocampi three times with 5-10 ml of HBSS, the buffer was finally removed up to a rest volume of 1,8 ml and 200 µl of 2,5% trypsin were added followed by an incubation period of 20 min at 37 °C. The hippocampi were then washed again five times with 5-10 ml of HBSS which was finally removed up

to a rest volume of 1,6 ml. After adding 400 µl of 0,05% DNAse I (final concentration: 0,01%), the hippocampi were pipetted up and down to disperse the cells. The suspension was subsequently applied on a nylon sieve (aperture size: 125 µm) to flow into a falcon tube (50 ml) and 18 ml of DMEM+++ were added. After counting the cells using a Neubauer counting chamber, they were further diluted with DMEM+++ until the appropriate concentration for seeding was reached: for immunostainings 2-3 x 10^4 cells in 500 µl of DMEM+++ per well of a 24-well plate

After 6-12 h, DMEM+++ was removed and the cells were covered with neurobasal medium+++.

Primary cultures cannot be passaged or stored permanently, but they are stable at 37 °C up to 6 weeks.

poly-L-lysin

5 mg poly-L-lysin

→ ad 50 ml with HBSS

DMEM+++

2 mM glutamine

1 ml B27 supplement (50x)

500 µl penicillin/streptomycin (100x)

→ ad 50 ml DMEM

HBSS

16,4 g NaCl

11,9 g HEPES

0,21 g Na_2HPO_4

→ pH 7,05

→ ad 1 l with deionized water

neurobasal medium+++

2 mM glutamine

1 ml B27 supplement (50x)

500 µl penicillin/streptomycin (100x)

→ ad 50 ml neurobasal medium

2.5 Methods of protein biochemistry

2.5.1 Protein overexpression in bacteria

After activation by an external effector, expression vectors make it possible to selectively express a defined protein in an appropriate bacterial strain like *E. coli* BL21. As far as the vector pGEX4T3 is concerned, a molecular mimic of allolactose called IPTG induces protein expression via *lac*Z gene expression. The protein finally expressed is a fusion protein with Glutathione-S-transferase (GST) which makes purification much easier.

5 ml of 2YT-medium were inoculated with one single colony of bacteria containing the appopriate recombinant plasmid and incubated overnight at 37 °C with shaking at 200 rpm. On the next morning, this overnight culture was added to 1000 ml of 2YT-medium which was then incubated for 3 h at 37 °C with shaking at 200 rpm until the OD_{600} was between 0,6 and 0,8. After adding 500 µl of IPTG, the culture was further incubated for 5-6 h at 37 °C with shaking at 200 rpm and finally centrifuged at 12,000 x g for 20 min at 4 °C.

2.5.2 Purification of GST fusion proteins

GST-tagged fusion proteins can be purified very specifically with glutathione affinity chromatography. Bacterial cell lysate is added to a glutathione sepharose column which allows the binding of the GST-part of the fusion protein to the glutathione sepharose while all the other molecules of the solution are washed out. Finally, excess glutathione is used to elute the tagged protein because of its higher binding affinity to glutathione sepharose.

After resuspension of the pellet from the last step described in 2.5.1 in 25 ml of ice-cold 1x PBS buffer, the bacterial cells were lysated with ultrasonics on ice and further centrifuged at 12,000 x g for 20 min at 4 °C resulting in another pellet and a supernatant containing the GST fusion protein. 2,66 ml of glutathione sepharose were added to a column which was subsequently washed three times with 20 ml of ice-cold 1x PBS buffer each time. Further, the supernatant containing the GST fusion protein was applied to the equilibrated column, the flowthrough was collected and once more applied to the column. After washing the column three

times with 20 ml of ice-cold 1x PBS buffer, elution buffer was applied for incubation of 10 min at RT. The purified fusion protein was finally collected in several fractions of 500 µl each.

elution buffer (pH 8)
10 mM reduced glutathione
500 mM Tris/HCl

2.5.3 Methods to guarantee antibody specificity

2.5.3.1 Affinity purification of antibodies

Laboratory animals like rabbits, guinea pigs or mice can be immunizated with a fusion protein for antiserum production. In this work, a GST fusion protein of LAPSER1 was sent to a company (Pineda, Berlin) to be injected in rabbits. As such an antiserum does contain other components that may alter signals in further analytical procedures, the LAPSER1 antiserum was subsequently affinity-purified to guarantee the highest specificity possible.

Affinity purification was performed with a *HiTrap™ NHS-activated HP column* from Amersham, UK. These columns are packed with Sepharose High Performance as base matrix while N-hydroxy-succinimide esters are attached to it. The esters react efficiently with ligands containing amino groups and so give a stable amide linkage. The LAPSER1-GST fusion protein was coupled to the column while the antiserum was later purified against it.

2.5.3.2 Demonstration of antibody specificity by antigen blocking

Antibody specificity can be reached by competing with excess of antigen. A small volume of antibody is first incubated with a grand amount of peptide to neutralize it. Any specific signals should disappear in the analysis which follows.

The LAPSER1 antibody was mixed with the LAPSER1-GST fusion protein in a 1:5 ratio. The mixture was then filled up with the appropriate buffer to a defined end volume, incubated overnight at 4 °C and further centrifuged at 13,000 x g for 15 min at 4 °C. The supernatant was carefully removed and used for analysis.

2.5.5 Methods of tissue extraction

2.5.5.1 General extraction of tissue

Tissue was extracted from adult male & female Wistar rats.

After dissection, tissue was homogenized in 10 ml/g of buffer A + PIM to obtain whole tissue homogenate. To remove cell debris & nuclei, the homogenate was centrifuged at 1,000 x g for 10 min at 4 °C resulting in supernatant S1 and pellet P1. S1 was given into a pre-cooled flask while P1 was further homogenized with 10 ml/g of buffer A and later centrifuged at 1,000 x g for 10 min at 4 °C resulting in supernatant S1' and pellet P1'. Both supernatants S1 & S1' were united and centrifuged at 12,000 x g for 15 min at 4 °C. The pellet P2 was then resuspended in 500 µl of RIPA buffer (+ PIM) and extracted on an overhead shaker for 4-6 h or overnight at 4 °C. After another centrifugation at 12,000 x g for 15 min at 4 °C, the crude membrane fraction could be taken from the supernatant.

RIPA buffer (pH 8)

2 mM EDTA
150 mM NaCl
30 mM sodium pyrophosphate
50 mM Tris/HCl
1% Tritone X-100
0,5% sodium deoxycholate
0,1% SDS

buffer A + PIM

320 mM sucrose
5 mM HEPES
→ pH 7,4
→ Add PIM

2.5.5.2 PSD preparation

Isolation of the PSD fraction from a whole rat brain by a series of centrifugations allows to analyze the enrichment of postsynaptic proteins towards the PSD. It is very important to take samples from each fraction obtained; for further Western Blot analysis see 2.5.6.4.

Three brains from adult rats were homogenized in 10 ml/g of buffer A + PIM (sample: Ho). To remove cell debris & nuclei, the homogenate was centrifuged at 1,000 x g for 10 min at 4 °C resulting in supernatant S1 and pellet P1. S1 was

given into a pre-cooled flask while P1 was further homogenized with 10 ml/g of buffer A + PIM and later centrifuged at 1,000 x g for 10 min at 4 °C resulting in supernatant S1' and pellet P1'. Both supernatants S1 & S1' were united and centrifuged at 12,000 x g for 15 min at 4 °C resulting in supernatant S2 and pellet P2. P2 was further homogenized with 10 ml/g of buffer A + PIM (sample: P2) and centrifuged at 12,000 x g for 10 min at 4 °C resulting in supernatant S2' and pellet P2'. P2' was resuspended in 1,5 ml/g of buffer B and subsequently fractionated on a sucrose gradient (0,85 M - 1,0 M - 1,2 M) at 85,000 x g for 2 h at 4 °C. Myelin (sample: My) could be harvested on top of the gradient, the mitochondria within the pellet on the bottom (sample: Mi) and the synaptosomal fraction (sample: Sy) on the 1,0/1,2 M phase boundary. The latter was extracted with 5 volume units of 1mM Tris/HCl (pH 8,1) for 30 min at 4 °C with stirring and further centrifuged at 33,000 x g for 30 min at 4 °C resulting in supernatant S3 and pellet P3 which contains the synaptosomal membranes. P3 was resuspended in 1,5 ml/g of 5 mM Tris/HCl (pH 8,1) and further fractionated on another sucrose gradient (0,85 M - 1,0 M - 1,2 M) at 85,000 x g for 2 h at 4 °C. The synaptic junctional proteins (sample: Sj) could be harvested at the 1,0/1,2 M phase boundary and were subsequently mixed with 60 ml/g of buffer B and 60 ml/g of buffer C for 15 min at 4 °C with stirring. Finally, this mixture was centrifuged at 33,000 x g for 30 min at 4 °C resulting in supernatant S4 and the first PSD pellet (sample: PSD).

Additional purification of the first PSD pellet was not done for this work.

buffer A + PIM	**buffer B**	**buffer C**
320 mM sucrose	320 mM sucrose	320 mM sucrose
5 mM HEPES	5 mM HEPES	12 mM HEPES
→ pH 7,4	→ pH 8,1	→ pH 8,1
→ Add PIM		→ Add 1% Triton X-100

sucrose gradient solutions

5 mM Tris/HCl (pH 8,1) and…

…0,85 M sucrose	…or 1,0 M sucrose	…or 1,2 M sucrose

2.5.6 Methods of protein analysis

2.5.6.1 Protein determination

For further use, it is essential to know the amount of protein in a lysate because of quantitative analysis. The *BCA Protein Assay Kit* from Pierce was used in this work while spectroscopy at 562 nm helps to determine the concentration of protein in extracts.

After preparing a set of protein standards with BSA concentrations of 0 µg-20 µg, the protein extract was diluted in a 1:10 and 1:50 ratio while the BCA solutions A & B were mixed in a 50:1 ratio. 1 ml of mixed BCA solution was then given to each 50 µl of protein sample (standard as well as extract) for incubation of 30 min at 60 °C. Finally, the samples were measured at 562 nm to determine the protein concentration (µg/µl) with a computer program.

2.5.6.2 SDS polyacrylamide gel electrophoresis (SDS-PAGE)

In SDS-PAGE, proteins are separated according to their size, so the molecular weight can be estimated. Before gel electrophoresis, the proteins to be analyzed are mixed with the anionic detergent SDS to linearize them by denaturing secondary and non-disulfide-linked tertiary structures. Besides, proteins are boiled in the presence of 2-mercaptoethanol which reduces disulfide linkages before they are finally applied to the polyacrylamide gel.

The components for the resolving gel were mixed and subsequently poured between two glass plates especially assembled for SDS-PAGE followed by overlaying isopropanol to ensure a flat surface and to exclude air. After the gel's polymerization for 15-20 min at 60 °C, the isopropanol was washed off. The components for the stacking gel were then mixed and subsequently poured on top of the resolving gel. To form sample slots while the stacking gel polymerizes, a comb was inserted. After the second gel's polymerization, the comb was removed and the gel was inserted into an appropriate gel chamber which was then filled with 1x electrophoresis buffer. The protein samples were further mixed with 2x SDS loading buffer, boiled up for 5 min at 95 °C and layered on the stacking gel. Finally, the electrophoresis was started with 100 V to separate proteins.

4x resolving gel buffer
1,5 M Tris/HCl
0,4% SDS
→ pH 8,8

4x stacking gel buffer
0,5 M Tris/HCl
0,4% SDS
→ pH 6,8

10% resolving gel
1332 µl 30% acrylamide
225 µl 2% bis-acrylamide
1000 µl 4x resolving gel buffer
1420 µl sterile water
3 µl TEMED
20 µl 10% APS

6% stacking gel
400 µl 30% acrylamide
70 µl 2% bis-acrylamide
500 µl 4x stacking gel buffer
1030 µl sterile water
1,5 µl TEMED
10 µl 10% APS

1 x electrophoresis buffer
192 mM glycine
25 mM Tris
0,1% SDS
→ pH 8,3

2x SDS loading buffer
125 mM Tris/HCl
2 mM EDTA
4% SDS
2% glycerol
10% mercaptoethanol
0,05% bromphenole blue

2.5.6.3 Coomassie staining

An SDS gel can be soaked in a blue dye, Coomassie blue – also known as Brilliant Blue – to visualize the bands indicating the protein content of the gel.

After incubation in Coomassie staining solution for 10 min with shaking at RT, the gel was washed with deionized water to remove any dye. Subsequently, the gel was incubated in destaining solution I for 20-30 min with shaking at RT followed by another incubation period of 20-30 min in destaining solution II with shaking at RT.

Coomassie staining solution

21,25 g Coomassie Brilliant Blue R-250
50 ml acetic acid
225 ml methanol
→ ad 500 ml with deionized water & filtrate

destaining solution I	**destaining solution II**
225 ml methanol	25 ml methanol
50 ml acetic acid	25 ml acetic acid
225 ml deionized water	450 ml deionized water

2.5.6.4 Western Blot analysis

After gel electrophoresis, the separated proteins are transferred – or blotted – under the influence of an electrical field onto a membrane which is finally incubated with an antibody specific for the protein to be analyzed. In this work, the technique of tank-electroblotting was used which is mainly based on wetting a sheet of transfer membrane and placing it on the gel to be blotted while blotting takes place in a tank full of transfer buffer.

The SDS gel, 4 Whatman papers and 2 sponge pads were equilibrated in transfer buffer while a PVDF membrane was activated in methanol. Subsequently, the components for blotting were stacked onto the white plastic grid of the tank-blot cassette as follows:

- wet sponge pad
- 2 wet Whatman papers
- PVDF membrane
- SDS gel right after SDS-PAGE
- 2 wet Whatman papers
- wet sponge pad

After closing its black plastic grid, the blot cassette was placed into a tank of transfer buffer containing a cooling jacket. Subsequently, a constant current of about 1 mA/cm^2 was applied for 90 min at 4 °C. The membrane was further incubated for 1-2 h in blocking solution with shaking at RT to block unspecific binding sites until the primary antibody diluted in blocking solution was finally

pipetted on the membrane in the appropriate concentration for overnight incubation at 4 °C. On the next morning, the membrane was washed with TBS + 0,05 % Tween-20 (TBS-T) for 30 min changing the washing buffer every 10 min, followed by incubation with the appropriate HRP-linked secondary antibody for 60-90 min with shaking at RT. The membrane was subsequently washed again with TBS-T for 30 min while changing the washing buffer every 10 min.

The following steps were carried out in a dark room.

The dry membrane was incubated with *Pierce ECL Western Blotting Substrate* and put into an X-ray film cassette followed by exposure to an X-ray film from 30 sec to 30 min depending on the strength of the signal. Finally, the film was put into a developing machine.

transfer buffer	**10x blotting buffer (stock)**
720 ml deionized water	151,5 g Tris
200 ml methanol	720,0 g glycine
80 ml 10x blotting buffer	→ ad 4 l with deionized water

blocking solution

5 g skim milk powder → ad 100 ml with TBS + 0,05 % Tween-20 (TBS-T)

2.6 Analysis of mRNA and protein localization

2.6.1 *In situ* hybridization

This method uses a radioactively labelled complementary cDNA probe to localize a specific mRNA sequence in a tissue section (= *in situ*). Hybridization is performed on 20 µm thick cryosections from unfixed tissue. The probe then hybridizes to the target sequence at elevated temperature while any excess of probe is washed away later.

Radioactive labelling of the cDNA probe

The following components of the hybridization cocktail were mixed:

- 45 µl ^{32}S-labelled dATP
- 1 µl cDNA probe (40 ng/µl)
- 1 µl 10x Terminal Transferase buffer
- 1,5 µl Terminal Transferase
- 2 µl deionized water

After incubation for 4 h at 37 °C, the mix was centrifuged at 2,000 x g for 1 min at RT. 38 µl of deionized water was added and the radioactively labelled cDNA probes were finally purified with Micro Bio-Spin P-30 Tris chromatography columns from ^{32}S-labelled unbound dATP.

In situ hybridization of radioactively labelled probes

10 µl of radioactively labelled cDNA probe were mixed with 60 µl of salmon testes DNA and incubated for 5 min at 37 °C. The mixture was then placed on ice for 3 min and 600 µl of hybridization cocktail as well as 30 µl of tRNA were added. After further application of 60 µl of hybridization solution, the sections were incubated overnight at 42 °C. On the next morning, the sections were washed with 1x SSC for 15 min at RT and subsequently rinsed five times in wash buffer at 50 °C for 15 min each time until they were cooled down in wash buffer for 15 min at RT. Afterwards, the sections were washed three times with 1x SSC at RT for 2 min each time and finally dehydrated at RT:

- 15 sec in 50% ethanol
- 15 sec in 70% ethanol
- 15 sec in 96% ethanol
- 15 sec in 100% ethanol

The following steps were carried out in a dark room.

The dry sections were placed into an X-ray film cassette and subsequently exposed to an X-ray film for 8-24 days until they could finally be developed in a developing machine.

hybridization cocktail

10 ml deionized formamid
4 ml 20x SSC
2 ml 0,2 M PBS
0,2 ml 50x Denhardt's solution
1 ml 20% N-Lauryl-sarcosine
2 g dextransulfate

wash buffer

100 ml 20x SSC
2 ml β-mercaptoethanol
→ ad 2 l with deionized water

2.6.2 Northern Blot analysis

Northern Blot analysis is actually based on the same principles as Western Blot analysis although RNA is separated by gel electrophoresis instead of proteins which requires a complementary cDNA probe for labelling instead of a specific antibody. In this work, the method was done with the *Rat Multiple Tissue Northern Blot* including an *ExpressHyb Solution* from Clontech.

Radioactive labelling of the cDNA probe

The cDNA was diluted to a final concentration of 10 ng in 45 µl of Tris/EDTA buffer. After denaturation for 5 min at 95 °C, the DNA was placed on ice for 5 min. Brief centrifugation at 13,000 x g was followed by adding 5 µl of ^{32}P-labelled dCTP to the denatured DNA. This mixture was further incubated for 10 min at 37 °C until the reaction was stopped by adding 5 µl of 0,2 M EDTA.

Hybridization of radioactively labelled probes

After warming up the *ExpressHyb Solution* to 68 °C, the blot membrane was pre-hybridized in 5 ml of this solution for 30 min with shaking at 68 °C. Subsequently, the radioactively labelled probes were denatured for 2-5 min at 95-100 °C and incubated quickly on ice until being added to 5 ml of fresh *ExpressHyb Solution*. This fresh mixture replaced the *ExpressHyb Solution* on the membrane which was then incubated for 1 h at 68 °C. After washing the membrane several times in wash solution 1 at RT and washing it twice in wash solution 2 at 50 °C, excess wash solution was shaken off and the blot was covered with plastic wrap. Finally, the blot was exposed to X-ray film at -70 °C which could later be developed with a developing machine.

Tris/EDTA buffer	**wash solution I**	**wash solution II**
10 mM Tris/HCl	2x SSC	0,1x SSC
1 mM EDTA	0,05% SDS	0,1% SDS
→ pH 7,4		

2.6.3 Immunhistochemistry

To analyze the expression pattern of LAPSER1 in brain, immunhistochemical stainings were performed using 7 µm thick Bouin's fixed microtome sections from rat brains. LAPSER1 was detected with a polyclonal antibody from rabbit in a 1:1000 dilution using the avidin-biotin-peroxidase-complex technique (ABC-system). In this method, the primary antibody binds to the antigen in the tissue section while the biotin-coupled secondary antibody binds to the primary one. Peroxidase activity of a biotin-peroxidase-streptavidin complex added further is later revealed with diaminobenzidine hydrochlorid (DAB) which stains antigen-antibody sites brown.

For immunhistochemistry, the microtome sections had to be deparaffinated at RT:

- 2 min in xylene
- 2 min in isopropanol
- 2 min in 96% ethanol
- 2 min in 70% ethanol

The deparrafinated sections were washed with 10 mM PBS followed by the application of methanol/H_2O_2 for 10 min at RT to block the endogenous peroxidase. After two further washing steps with 10 mM PBS for 5 min each time, 0,5% Triton in 10 mM PBS was applied for 15 min at RT followed by incubation in 2% BSA in 10 mM PBS for 1 hour at RT. Finally, the primary antibody diluted in 2% BSA in 10 mM PBS in the appropriate concentration was pipetted on the sections for incubation in a wet chamber overnight at 4 °C. On the next morning, the sections were washed with 10 mM PBS twice for 5 min each time and subsequently incubated with the secondary antibody in a 1:500 dilution in 10 mM PBS for 2 h at RT. After two washing steps with 10 mM PBS for 5 min each time, the ABC system was applied for 2 h at RT followed by two further washing steps. Afterwards, DAB was applied for 3-5 min to detect antigen-antibody sites before the sections were washed again with 50 mM Tris/HCl for 5 min and with deionized

water for 5 min. Finally, the sections were dehydrated at RT and mounted permanently with entellane:

- 2 min in 70% ethanol
- 2 min in 96% ethanol
- 2 min in isopropanol
- 2 min in xylene
- Permanent application of entellane

methanol/H_2O_2	**ABC system**	**DAB**
45 ml 10 mM PBS	25 µl solution A	250 µl DAB
5 ml methanol	25 µl solution B	5 ml 50 mM Tris/HCl
50 µl H_2O_2	4 ml 10 mM PBS	2 µl H_2O_2

2.6.4 Immunostaining of cell cultures

In this work, the method of indirect immunofluorescence was used, in which a secondary antibody labelled with fluorochrome is used to recognize the primary antibody. Double or triple immunofluorescence which is principally accomplished the same way as the single techinque, may determine the co-localization of several proteins at the same time.

NMDA-stimulation

Right before immunostaining, cells can be stimulated with certain agents. In this work, hippocampal neurons were stimulated with 100 µM NMDA. After 5 min of NMDA application, the cells were further incubated in conditioned culture medium without NMDA for a certain amount of time.

After discharging the conditioned culture medium, the cells were washed with 1x PBS. Subsequently, 500 µl of ice-cold 4% PFA with 2% sucrose in PBS were added for incubation of 20 min at RT. The cells were then washed three times with 1x PBS for 5 min at RT until they were permeabilized with 1x PBS + 0,05 % Triton X-100 on ice for 5 min. After another incubation with blocking solution for 45 min at RT, the primary antibody diluted in blocking solution in the appropriate concentration was pipetted on the cells for incubation either for 2 h at RT or overnight at 4 °C. The cells were further washed with 1x PBS three times for 5 min

each time at RT and subsequently incubated with the appropriate secondary antibody in blocking solution (1:500-1:1000) for 1 h at RT followed by a further washing step. While putting the cover glass in water for 1 min, Mowiol was heated up to 50 °C and one drop of it was given on each slide. Cells on the cover glass were finally put into the Mowiol to dry overnight. Analysis was done with a fluorescent microsope (Axioskop 2 mot plus from Zeiss, Oberkochen).

4% PFA with 2% sucrose in PBS

8g PFA
→ ad 80 ml with deionized water
8 drops of 1 M NaOH
Agitate at 57 °C until PFA is dissolved
Cool down the solution
→ pH 7,4
4 g sucrose
→ ad 100 ml with 2 x PBS and pool both solutions

blocking solution

0,1% ovalbumin
0,5% Fish gel
0,01% Tween 20

2.7 Analysis of protein-protein interactions

2.7.1 Co-immunoprecipitation (Co-IP)

This common biochemical method of protein-protein-interaction analysis is based on the formation of a labelled immune complex while in this work, the target protein was bound by a specific antibody bound to the Fc region of *µMACS Protein A MicroBeads* from Miltenyi Biotec. The complex can be immobilized magnetically in a column which allows gentle, but efficient washing with the appropriate buffers until the immunoprecipitate is eluted and analyzed by Western Blot.

50 µl of Protein A MicroBeads for magnetic labelling were mixed with 1-2 µg of antibody and incubated on ice for 30 min followed by adding 200 µl of tissue lysate. The sample mixture was then incubated overnight at 4 °C.

On the next morning, the column was placed in the magnetic field of the pre-cooled *μMACS* separator and equilibrated with 200 µl of the buffer from the lysate before applying the sample. The column was then washed 4 times with 200 µl of lysis buffer + PIM and finally once with low salt washing buffer + PIM. Subsequently, 20 µl of pre-heated 95 °C hot elution buffer were applied to the column and incubated for 5 min at RT until the immunoprecipitate could be eluted with 50 µl of pre-heated 95 °C hot elution buffer for further analysis by Western Blot.

lysis buffer	**elution buffer**	**low salt washing buffer**
150 mM NaCl	50 mM Tris/HCl	20 mM Tri/HCl
150 mM Tris/HCl	50 mM DTT	→ pH 7,5
1% Triton-X-100	1% SDS	→ PIM
→ pH 8	0,005% bromphenole	
→ PIM	10% glycerol	
	→ pH 6,8	

2.7.2 The yeast-two-hybrid system

The two-hybrid system is a genetic test in yeasts which allows to study protein-protein interactions *in vivo*. One can use it to test the interaction between two proteins or protein domains which are expected to interact with each other and/or to screen a cDNA library encoding protein sequences in search of potential interaction partners.

The system is based on a protein constitutively expressed in *S. cerevisiae*, the transcription factor GAL4 which is essential for the β-galactose metabolism in yeasts. As many eukaryotic transcription factors, GAL4 consists of two functional domains, an aminoterminal DNA-binding domain (GAL4-BD) and a carboxyterminal transcription-activating domain (GAL4-AD). In the two-hybrid system, the GAL4 domains are separately coded by two different plasmids called “bait” (e.g. pAS2-1) and “prey” (e.g. pACT2) vectors. For analysis, the cDNA of the proteins or protein domains to be tested each has to be cloned into one of those vectors. Further, both constructs are transformed into two different genetically altered yeast strains that are both not able to express native GAL4. Finally, these

transformed strains are cultivated together (mating) so the mated dizygotes contain both two-hybrid plasmids. If there's an interaction between the proteins or protein domains each fused to one of the different GAL4 domains, a functional transcription factor is created and the transcription of specific reporter genes is induced. The corresponding yeasts can easily be detected by growth selection (HIS3 reporter) or by expression of the enzyme β-galactosidase (lacZ reporter) which stains the colonies blue if its substrate X-Gal is in the medium.

The yeast strain Y187 was transformed with the "bait" construct while yeast strain AH109 was transfomed with the "prey" construct. Y187+"bait" was grown on SD -Trp selection plates and AH109+"prey" on SD -Leu selection plates for 3-5 days at 30 °C.

5 ml of SD -Trp medium was inoculated with a colony of Y187+"bait" and 5 ml of SD -Leu medium with a colony of AH109+"prey" which were both incubated overnight at 30 °C with shaking at 200 rpm. On the next morning, the cells were centrifuged at 2,500 x g for 5 min at RT. Subsequently, the Y187+"bait" pellet was resuspended in 5 ml of YPD medium while this suspension was further used to resuspend the AH109+"prey" pellet followed by incubation at 30 °C for 24 hours with smooth shaking at 40 rpm in a flask (mating). On the next day, the cells were centrifuged at 1,000 x g for 10 min at RT and the pellet was resuspended with 2 ml of YPD medium. 100 µl of a 1:10, $1:10^2$ and $1:10^3$ dilution were each plated as control on SD -Leu/-Trp plates and 300 µl on a SD -His/-Leu/-Trp plate while all plates were put in an incubator at 30 °C for 3-5 days.

If the mating was successful, colonies should have grown on the SD -Leu/-Trp plates. Interaction was positive if there were any colonies on the SD -His/-Leu/-Trp plates as well as a filter-lift assay (see below) of the colonies from the SD -Leu/-Trp plates was successful.

Filter-lift assay

As mentioned above, protein-protein interaction in the appropriate yeasts can not only be detected by growth selection, but also by expression of the enzyme β-

galactosidase which stains the colonies blue if its substrate X-Gal is in the medium. The method used for this detection is called filter-lift assay.
After wetting a Whatman filter in a sterile petri dish with 1,5 ml of Z-buffer with X-Gal, another Whatman filter was pressed carefully on the surface of the plate with the yeast colonies to be analyzed. The filter with the colonies on its surface was then dipped into fluid nitrogen for 5 sec and layed with the colonies upwards on the pre-wet filter in the petri dish which was finally put in an incubator at 30 °C.

The dish had to be inspected throughout a period of 4 hours because if the interaction was positive, the colonies should become blue within this time frame.

Z-buffer

60 mM Na_2HPO_4
40 mM NaH_2PO_4
10 mM KCl
1 mM $MgSO_4$
→ pH 7,0

3. Results

3.1 Genomic and protein structure of LAPSER1

3.1.1 Genomic structure

Database analysis reveals that the LAPSER1 gene is localized on rat chromosome 1q54 while its genomic locus of approximately 11 kilobases (kb) consists of 5 exons and 4 introns with an open reading frame (ORF) of 2013 base pairs (bp) (NCBI acc. no.: DQ176638.2). The homologous mouse gene of approx. 12 kb is localized on mouse chromosome 19C3 and also consists of 5 exons and 4 introns with an ORF of 2016 bp (NCBI acc. no.: BC014695.1). Human chromosome 10q24 contains the human LAPSER1 gene whose genomic length is approx. 11 kb. Similar to mouse and rat, it has an ORF of 2010 bp, and consists of 5 exons and 4 introns (NCBI acc. no.: NM_032429). Among all three species, the start codon is localized on exon 2, the stop codon on exon 5. Genomic data are summarized in Table 1 while the exon-intron-structure is presented in Figure 3.

Table 1 Genomic alignment of LAPSER1 in rat, mouse and human

Data derive from the NCBI database (http://www.ncbi.nlm.nih.gov)

(acc. no. = accession number, ORF = open reading frame, kb = kilobases, bp = base pairs).

species	chromosome	length of gene	exons	ORF	acc. no.
Rattus norvegicus	1q54	~ 11 kb	5	2013 bp	DQ176638.2
Mus musculus	19C3	~ 12 kb	5	2016 bp	BC014695.1
Homo sapiens	10q24	~ 11 kb	5	2010 bp	NM_032429

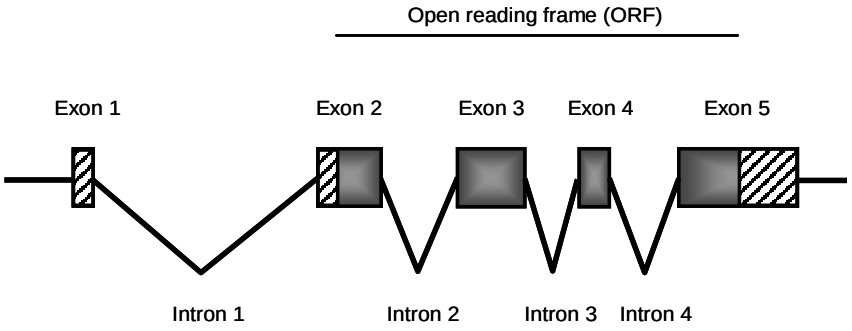

Figure 3 Exon-intron-structure of the LAPSER1 gene

Exons are shown as boxes filled with grey color, untranslated parts are hatched within those boxes.

3.1.2 Protein structure

The *Rattus norvegicus* LAPSER1 protein consists of 670 amino acids (aa) and has a calculated molecular mass of approx. 72 kilodalton (kDa). It has two putative start methionines (aa 1 & 26), a cryptic myristoylation motif (aa 16-20) and contains a central coiled-coil domain (aa 377-540) with two internal leucine zipper motifs (aa 391-419, aa 458-486). Furthermore, LAPSER1 contains a C-terminal Fez1 domain (aa 440-626) and a PDZ domain binding motif at the very C-terminus (aa 667-670). Additionally, a nuclear export signal (NES) can be found right after the C-terminal end of the Fez1 domain (aa 632-641) (Figure 4).

A

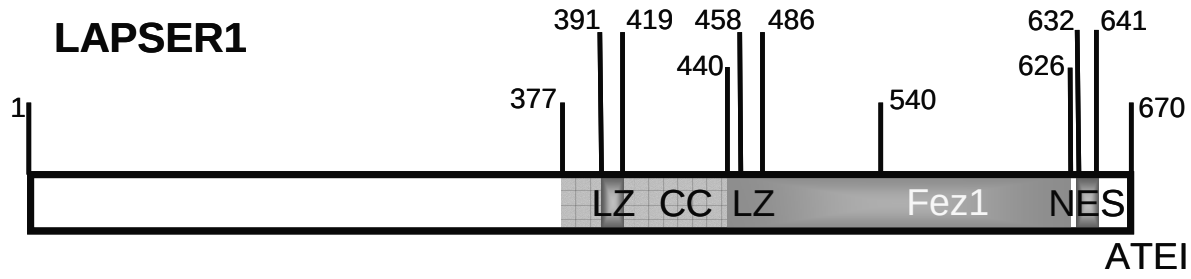

B

MAIVHTLPVPLEPARETATAPQTPAMGSVSSLISGRPCPGGPAPQRHHGVPGPTFFRQQDGLLRGGYEAQEPLCPAVPPRKTVPGNSFTY 90
VNEDFRTESPPSPSSDVEDPREHQAHNAHLRGPPPKLIPVSGRLEKNMEKILIRPTAFKPVLPKPRGAPSLPGFLGPRAAGLSGSQGSLT 180
QLFGGPASSSSSSSSSAADKPLALSGWASGCPSGTLSDSGRNSLSSLPTYSTGGAEPTANSPGGHLPSHGPGRGPLPGPARGVPTGPSH 270
SDSGRSSSSKSTGSLGARVAGGLLGSGARASPGSSSGGDRSPPPPPLPPPSDEALLHCVLEGKLRDREAELQQLRDSVDESEAAVCQAFG 360
ARQRRWPGEREDCASHAQQATQRVQRAQQLLQLQVFQLQQEKRQLQDDFAQLLQEREQLERRCATFEREQQELGPRLEETKWEVCQKSGE 450
ISLLKQQLKESQAELVQKGSELVALRVALREARAALRVSEGRARGLQEAARARELELEACSQELQRYRQEAEQLREKARHLDAEAAGLRE 540
PPVPPATTDPFLLAESDEAKVQRAAAGTGGSLRAQVERLRQELQREQRRGDEQRNSFEGERLAWQAEKEQVIRYQKQLQHNYVQMYRRNR 630
QLEQELQQLSLELEARELADLGLSEPAPCICLEEITATEI 670

Figure 4 Structural organization of the LAPSER1 protein

Schematic overview (**A**) and amino acid sequence (**B**) of LAPSER1. (**A**) The first and last amino acids of the whole protein and of each domain marked within the schematical presentation are indicated above (CC = coiled-coil domain, LZ = leucine zipper, Fez1 = Fez1 domain, NES = nuclear export signal, ATEI = PDZ domain binding motif). (**B**) The 2 putative start methionines are in *boldface letters & underlined*, the cryptic myristoylation site is *underlined* only. The coiled-coil domain is *boxed*, but not marked. The leucine zipper motifs are indicated in *boldface* and marked in *grey*. The Fez1 domain is *italicized*, printed in *white letters* and marked in *dark grey*. The nuclear export signal is in *boldface* and marked in *light grey* while the PDZ domain binding motif (ATEI) is *boxed* and also marked in *light grey*. The sequence derives from the NCBI database (http://www.ncbi.nlm.nih.gov – accession number: ABA06435.2).

3.2 LAPSER1 belongs to the *"Fezzin"* protein family

A C-terminal Fez1 domain (F37/esophageal cancer-related gene coding leucine zipper motif 1) homologous to the one in LAPSER1 can be found in three other molecules: ProSAPiP1 (ProSAP interacting protein 1), PSD-Zip70 (Postsynaptic density protein containing leucine-zippers weighing 70 kDa) and N4BP3 (Nedd4 binding protein 3). ProSAPiP1, PSD-Zip70 and LAPSER1 have a molecular weight between 70 and 75 kDa, harbor a central coiled-coil-domain with an internal leucine zipper while the very carboxyterminal part of all three proteins also contains a PDZ domain interaction motif. N4BP3 is smaller (approx. 54 kDa) and does not have a PDZ domain binding motif at its very C-terminus (Figure 5).

```
LAPSER1          SPPPPPPPPPSDEALLHCVLEGKLRDREAELQQLRDSVDESEAAVCQAFGARQRRWPGER 370
ProSAPiP1        PFAACSPPSPS---ALIQELEERLWEKEQEVAALRRSQEQSEAAVAQVLEERQKAWEREL 394
PSD-Zip70        ------SPLSTDECTIQ-ELEQKLLQRETALQKLQRSFDEKEFASGQTFEERPRRTRDEL 306
N4BP3            -------PPPPYEFSCPTTEEVAVLPDTCEELKRDLGDQDVSNPFTQVLEERQRLWLSEL 290

LAPSER1          E----DCASHAQQATQRVQRAQQLLQLQVFQLQQEKRQLQDDFAQLLQEREQLERRCATF 426
ProSAPiP1        AELRQGCSGKLQQVARRAQRAQQGLQLQVLRLQQDKKQLQEEAAQLIRQREELEDKVAAC 454
PSD-Zip70        ECL--EPKSKLKPASQKSQRTQQVLQLQVLQLQQEKRQLRQELESLMKEQDLLETKLRSY 364
N4BP3            KRL---YVDRLHEVAQKAERSERNLQLQLFMAQQEQRRLRKELRAQQGLAPEPRTSGPPM 347

LAPSER1          EREQQELGPRLEETKWEVCQKSGEISLLKQQLKESQAELVQKGSELVALRVALREARAALL 486
ProSAPiP1        QKEQADFLPRMEETKWEVCQKAGEISLLKQQLKDSQADVSQKLSEIVGLRSQLREGRASL 514
PSD-Zip70        EREKTNFAPALEETQWEVCQKSGEISLLKQQLKESQMEVNAKASEILSLKAQLKDTRGKL 424
N4BP3            EADPN--ARPEEEARWEVCQKTAEISLLKQQLREAQAELAQKLAEIFSLKTQLRGSRAQA 405

LAPSER1          RVSEGHARGLQEAARARELELEACSQELQ-------RYRQEAEQLREKARHLDAEAAGLR 539
ProSAPiP1        REKEEQLLSLRDSFGSKQASLELSEGELPPACLKPALTPVDLVEPQEALASCESDEAKMR 574
PSD-Zip70        EGMELKTQDLESALRTKGLELEVCENELQ-------RKKNEAELLREKVNLLEQELLELR 477
N4BP3            QAQDAELARLREAVRS----------------------LQEQAPREEAPGSCETDDCKSR 443

LAPSER1          EPPVPPATTDPFLLAESDEAKVQRAAAGTGGSLRAQVERLRQELQREQRRGDEQRNSFEG 599
ProSAPiP1        RQAGVAAAASLVSVDG----EVDAGGEGGTRALRREVGRLQAELAAERRARERQGASFAE 630
PSD-Zip70        AQAALHRDAAPLGPPG-----IGLTFSEDIPALQRELDRLRAELKEERQGHDQMSSGFQH 532
N4BP3            ----------------------GLLGEAGGNEAREGAEQLRAELLQERLRGQEQALRFEQ 481

LAPSER1          ERLAWQAEKEQVIRYQKQLQHNYVQMYRRNRQLEQELQQLSLELEARELADLGLSEP--A 657
ProSAPiP1        ERRVWLEEKEKVIEYQKQLQLSYVEMYQRNQQLERRLRERGAAGGSRTPTPQHGEEEKAW 690
PSD-Zip70        ERLVWKEEKEKVIQYQKQLQQSYLAMYQRNQRLEKALQQLARGDIAGEPFEIDLEG---- 588
N4BP3            ERQTWQEEKERVLRYQREIQGSYMDMYRRNQALEQELRVLREP----------------- 524

LAPSER1          PCICLEEITATEI 670
ProSAPiP1        TPSRLERIESTEI 703
PSD-Zip70        ADIPYEDIIATEI 601
N4BP3            PTSWSPRLESSKI 537
```

Figure 5 Alignment of the amino acid sequences of *"Fezzin"* C-termini

Coiled-coil domains are *boxed*, leucine zipper motifs are in *boldface letters* and marked *grey*, the Fez1 domains are *italicized*, printed in *white letters* and marked in *dark grey* while the PDZ domain binding motifs are *boxed* and marked in *light grey*. All sequences derive from the NCBI database (http://www.ncbi.nlm.nih.gov).

3.3 Localization of LAPSER1 mRNA

3.3.1 Multiple tissue distribution

Northern Blot analysis with a *Rat Multiple Tissue Northern Blot* (Clontech) and a radioactively labelled cDNA-probe which recognizes a C-terminal sequence of the LAPSER1 mRNA (bp 1157-end) revealed expression at its highest level in brain where a dense band at approx. 4.2 kb could be identified. In addition, there was also a clear signal in heart, lung, kidney and testis at 4.2 kb while the other tissues tested did not show mRNA expression (Figure 6).

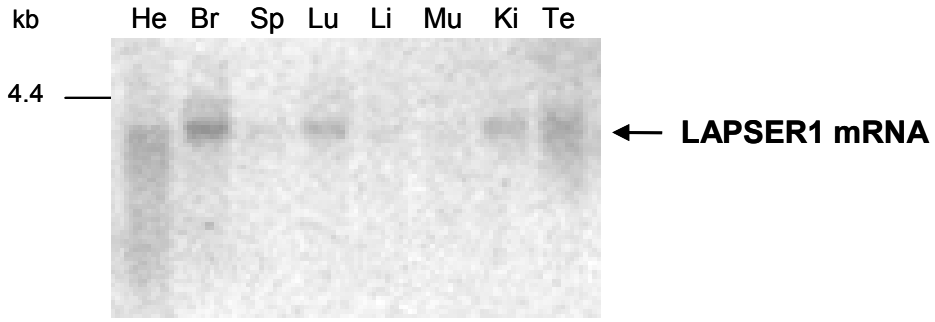

Figure 6 Multiple tissue distribution of LAPSER1 mRNA

Hybridization of a *Rat Multiple Tissue Northern Blot* (Clontech) with a radioactive-labelled LAPSER1 cDNA probe (kb = kilobases, He = heart, Br = brain, Sp = spleen, Lu = lung, Li = liver, Mu = skeletal muscle, Ki = kidney, Te = testis).

3.3.2 Regional distribution in brain

A different radioactively labelled cDNA-probe recognizing the C-terminal part of the LAPSER1 mRNA (bp 1965-end) was used for *in situ* hybridization of horizontal and sagittal rat brain sections at defined stages of brain development to show the regional distribution of the transcript. From postnatal day 16, LAPSER1 mRNA was highly abundant in the cerebellum while slight expression started in the hippocampus and the cortex. In the adult rat brain, transcription of LAPSER1 was mainly concentrated in the cerebellum, but could also be found in the cerebral cortex. In the hippocampus, LAPSER1 transcripts were clearly detected in the dentate gyrus and both CA1 and CA3 regions. Interestingly, commissury fibres of the corpus callosum also seemed to be positive for LAPSER1 mRNA expression from postnatal day 21 onwards (Figure 7).

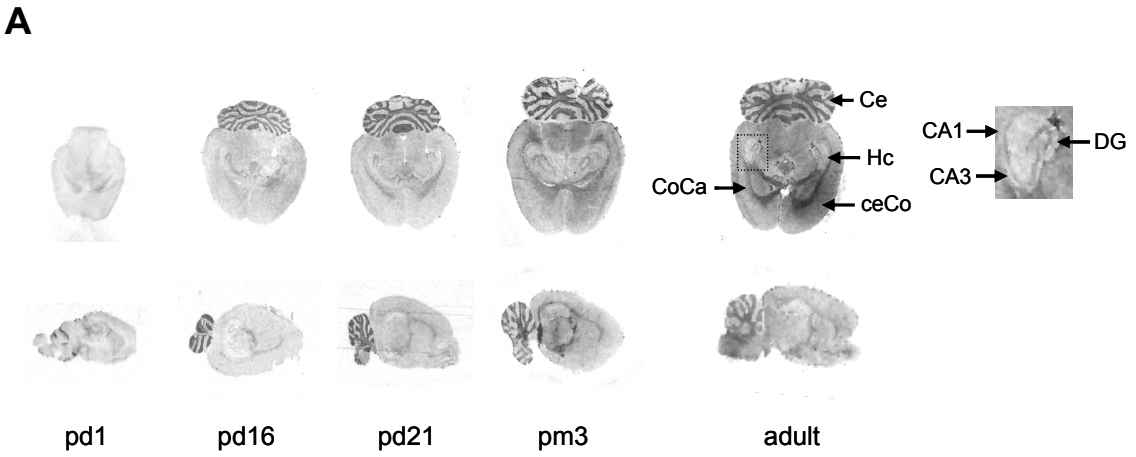

Figure 7 Regional distribution of LAPSER1 mRNA in brain

In situ hybridizations of horizontal and sagittal whole rat brain sections with a radioactive-labelled LAPSER1 cDNA probe during postnatal brain development including a 5-fold magnification of the hippocampal formation from the adult horizontal section (pd = postnatal day, pm = postnatal month, Ce = cerebellum, Hc = Hippocampus, ceCo = cerebral cortex, CoCa = corpus callosum, CA1 & CA3 = Cornu ammonis regions 1 & 3, DG = dentate gyrus).

3.4 Localization of the LAPSER1 protein

3.4.1 Generation and characterization of the LAPSER1 antibody

For antibody production, a defined part of the LAPSER1 cDNA (bp 1-1346 = aa 1-448) was subcloned into the expression vector pGEX4T3 to generate a GST-LAPSER1 fusion protein expressed in the *E. coli* strain BL21. This approx. 70 kDA recombinant fusion protein was then purified from the bacterial lysate with a glutathione sepharose column and subsequently used for the immunization of rabbits (Pineda, Berlin) (Figure 8A). To guarantee highest specificity possible, the later obtained antiserum was purified against the original fusion protein and further analyzed by Western Blot using lysates of GFP-LAPSER1-transfected Cos-7 cells and untransfected Cos-7 cells. In the lysate of the GFP-LAPSER1-transfected Cos-7 cells, the purified polyclonal LAPSER1 antibody detected a protein of approx. 100 kDa which corresponds to the calculated molecular weight of LAPSER1 (72 kDa) plus the GFP-tag (27 kDa) (Figure 7, lane 1). This GFP-LAPSER1 fusion protein was also detected by a monoclonal GFP-antibody (Figure 7, lane 3) at 100 kDa. There was no signal in the lysate of the untransfected Cos-7 cells (Figure 7, lane 2). For additional specificity testing, the purified LAPSER1

antibody was pre-incubated with an excess of the original antigen (LAPSER1-GST fusion protein) in a 1:5 ratio to neutralize the LAPSER1 antibody. This treatment made the 100 kDa LAPSER1 band (Figure 8, lane 4) disappear (Figure 8, lane 5).

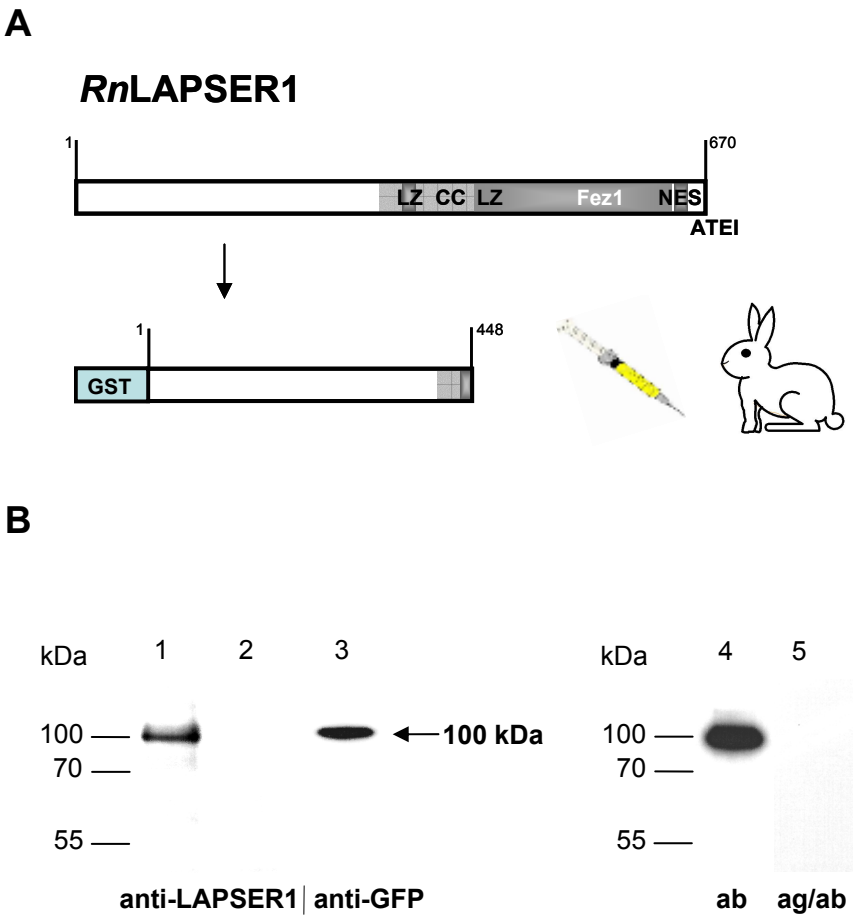

Figure 8 Generation and characterization of the polyclonal LAPSER1 antibody

(**A**) The aminoterminal part of the *Rattus norvegicus* LAPSER1 (*Rn*LAPSER1) protein (aa 1-448) was expressed as LAPSER1-GST fusion protein for the immunization of rabbits (CC = coiled-coil domain, LZ = leucine zipper, Fez1 = Fez1 domain, NES = nuclear export signal, ATEI = PDZ domain binding motif) (**B**) SDS-PAGE: 1, 3, 4, 5 = lysate of GFP-LAPSER1-transfected Cos-7 cells, 2 = lysate of untransfected Cos-7 cells; Western Blot: 1, 2: LAPSER1 affinity-purified antibody 1:500, 3: GFP-antibody 1:2000, 4: LAPSER1-affinity purified antibody (ab) 1:500, 5: LAPSER1 affinity-purified antibody 1:500 pre-incubated with excess of the LAPSER1-GST fusion protein (ag/ab). (GST = Glutathione-S-transferase, GFP = green fluorescent protein, kDa = kilodalton).

3.4.2 Multiple tissue distribution of LAPSER1

After preparation of lysates from different tissues of adult rats, the specific LAPSER1 antibody was used to analyze the multiple tissue distribution of the protein by Western Blot with identical protein amounts of 15 µg per lane (Figure 9). LAPSER1 was highly abundant in testis whereas heart and kidney showed weaker, but very clear bands at a molecular weight of approx. 70 kDa. In brain, two signals appeared at approx. 70 and 85 kDa, respectively.

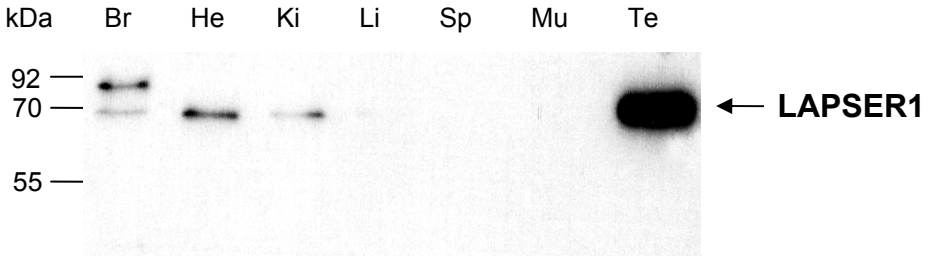

Figure 9 Multiple tissue distribution of the LAPSER1 protein

SDS-PAGE: protein lysates from the following tissues from rat: brain (Br), heart (He), kidney (Ki), liver (Li), spleen (Sp), skeletal muscle (Mu), testis (Te); Western Blot: LAPSER1 antibody 1:500 (kDa = kilodalton)

3.4.3 Regional distribution of LAPSER1 in brain

Lysates from adult rat cortex and cerebellum were separately analyzed by Western Blot with identical protein amounts of 20 µg per lane. There was a stronger signal of the 70 kDa LAPSER1 isoform in the cerebellum while the 85 kDa LAPSER1 isoform only appeared in cortex (Figure 10A). Sagittal sections from Bouin's fixed whole rat brains at different stages of brain development were incubated with the polyclonal LAPSER1 antibody to study the regional distribution of the protein in brain. From postnatal day one, there was a clear specific staining of the cerebellar purkinje cells and the principal neurons in the hippocampus and the cerebral cortex (Figure 10B-E). LAPSER1 expression concentrated on the cerebellum from postnatal month 3 (Figure 10B) – especially within its granular layer (Figure 10D). In the hippocampus, the LAPSER1 protein was detected on a moderate level in the dentate gyrus and in the CA1 and CA3 regions (Figure 10C).

A

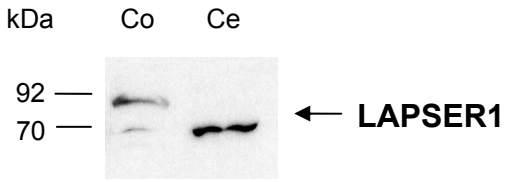
kDa
Co
Ce
92
70
LAPSER1

B

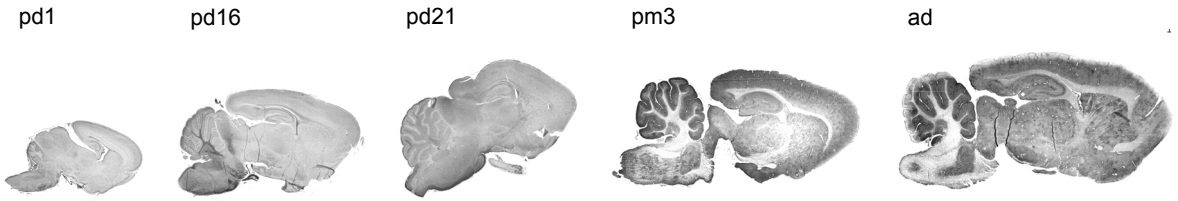
pd1
pd16
pd21
pm3
ad

C

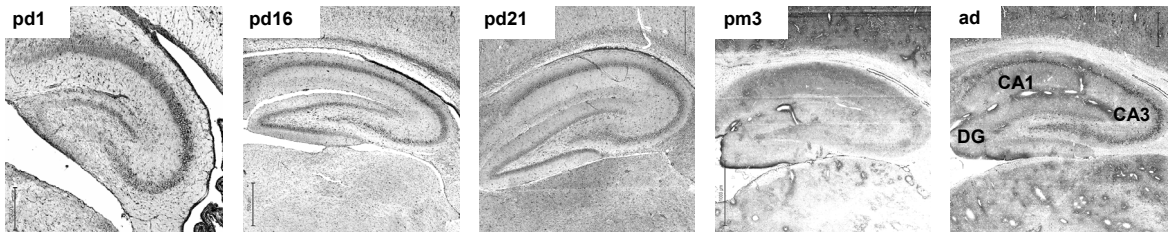
pd1
pd16
pd21
pm3
ad
CA1
CA3
DG

D

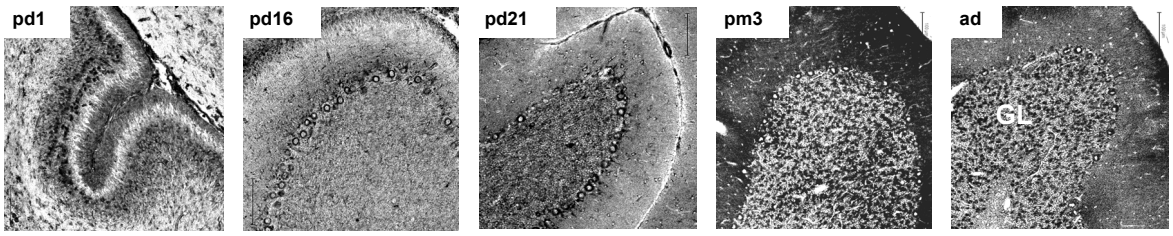
pd1
pd16
pd21
pm3
ad
GL

E

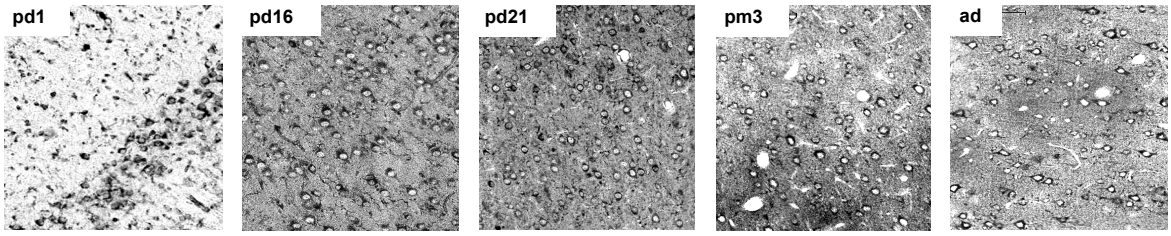
pd1
pd16
pd21
pm3
ad

Figure 10 Regional distribution of the LAPSER1 protein in brain

(**A**) SDS-PAGE: lysates of the rat cortex (Co) and the rat cerebellum (Ce); Western Blot: LAPSER1 antibody 1:500 (kDa = kilodalton). (**B-E**) Sagittal sections from Bouin's fixed rat brains at defined stages of development (pd1/16/21 = postnatal day 1/16/21; pm3 = postnatal month 3; ad = adult) incubated with the LAPSER1 antibody 1:1000. Whole brain overviews at 2x magnification (**B**), the hippocampus at 20x magnification (**C**), layers of the cerebellar cortex (**D**) and cerebral cortex (**E**) at 40x magnification (GL = granular layer of the cerebellum, CA1 & CA3 = Cornu ammonis regions 1 & 3, DG = dentate gyrus).

3.4.4 Synaptic localization of LAPSER1

Subcellular fractionation and PSD preparation of whole adult rat brains by centrifugation and subsequent Western Blot analysis with equal protein amounts of 20 µg per lane allowed to study the synaptic localization of the LAPSER1 protein which showed high enrichment within the PSD fraction. Quality control of the PSD preparation was done by analysis of the same fractions with a ProSAP2 antibody (Figure 11A). To receive a better resolution of the LAPSER1 signal within the PSD fraction, exposition time was reduced from 30 sec to 5 sec when developing the film. Thus, two clear bands at 70 kDa and 85 kDa could be identified (Figure 11B). To further confirm the postsynaptic localization of LAPSER1, double immunostainings of hippocampal neurons at 21 days in vitro (DIV) with the polyclonal LAPSER1 antibody from rabbit and a polyclonal ProSAP2 antibody from guinea pig were performed resulting in a clear match of LAPSER1 (Figure 11C-1/C-1a) and postsynaptic marker protein ProSAP2 (Figure 11C-2/C-2a) in dendritic spines (Figure 11C-3/C-3a) while LAPSER1 could also be found in the dendritic shaft (Figure 11C-1/C-1a).

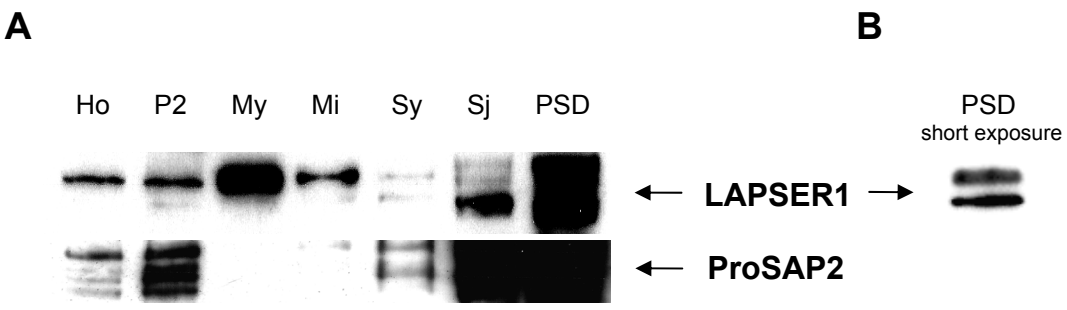

C

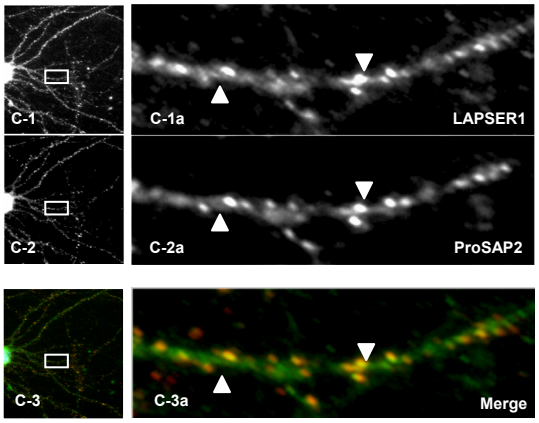

Figure 11 Subcellular distribution and synaptic localization of LAPSER1

(**A**) SDS-PAGE: whole brain homogenate (Ho), P2 fraction containing predominantly membrane-associated proteins (P2), myelin fraction (My), mitochondrial fraction (Mi), synaptosomal fraction (Sy), fraction containing synaptic junctions (Sj), postsynaptic density fraction (PSD); Western Blot: LAPSER1 antibody 1:500, ProSAP2 antibody 1:2000. (**B**) SDS-PAGE: postsynaptic density fraction (PSD); Western Blot: LAPSER1 antibody 1:500. (**C**) Hippocampal neurons fixed at 21 DIV stained with antibodies directed against LAPSER1 1:400 (Alexa Fluor 488: green) (**C-1/C-1a**) and ProSAP2 1:600 (Alexa Fluor 568: red) (**C-2/C-2a**). Merge of pictures C1/C-1a & C-2/C-2a (**C-3/C-3a**). Arrowheads point out LAPSER1/ProSAP2 positive puncta at postsynaptic densities (DIV = days in vitro).

3.5 Studies of LAPSER1 and its interaction partners

3.5.1 LAPSER1 interacts with ProSAP2

When P2 fraction from rat brain predominantly containing membrane-associated proteins was immunoprecipitated with the polyclonal LAPSER1 antibody from rabbit, the classical endogenous ProSAP2 multiple band pattern could be detected in the immunoprecipitate with a polyclonal ProSAP2 antibody from guinea pig (Figure 12A).

Single transfections with GFP-/RFP-LAPSER1 and GFP-/RFP-ProSAP2 constructs showed characteristic expression patterns of the corresponding fusion proteins in Cos-7 cells: cluster-like in the case of full length GFP-ProSAP2 (Figure 12B-1), punctate in the case of full length GFP-/RFP-LAPSER1 (Figure 12B-3/4) as well as RFP-LAPSER1 ΔC-term (Figure 12B-5) while RFP-ProSAP2 PDZ was distributed homogenously (Figure 12B-2). When co-transfected, the full length constructs of RFP-LAPSER1 and GFP-ProSAP2 co-localized in the same dot-like aggregates within the cytoplasm (Figure 12C, 1-3) while the RFP-LAPSER1 ΔC-term construct missing aa 421-670 including the PDZ domain binding motif did not co-cluster with GFP-ProSAP2 (Figure 12C, 4-6). Heterologous expression of RFP-ProSAP2 PDZ domain and GFP-LAPSER1 full length fusion proteins completely altered the expression pattern of GFP-LAPSER1 which seemed to be recruited to the ProSAP2 PDZ domain-containing aggregates (Figure 12C, 7-9).

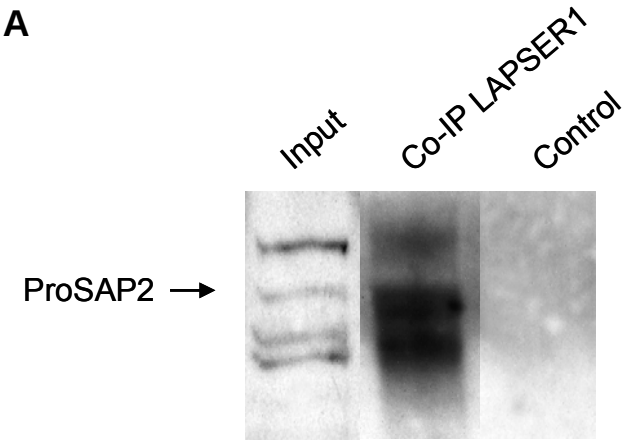

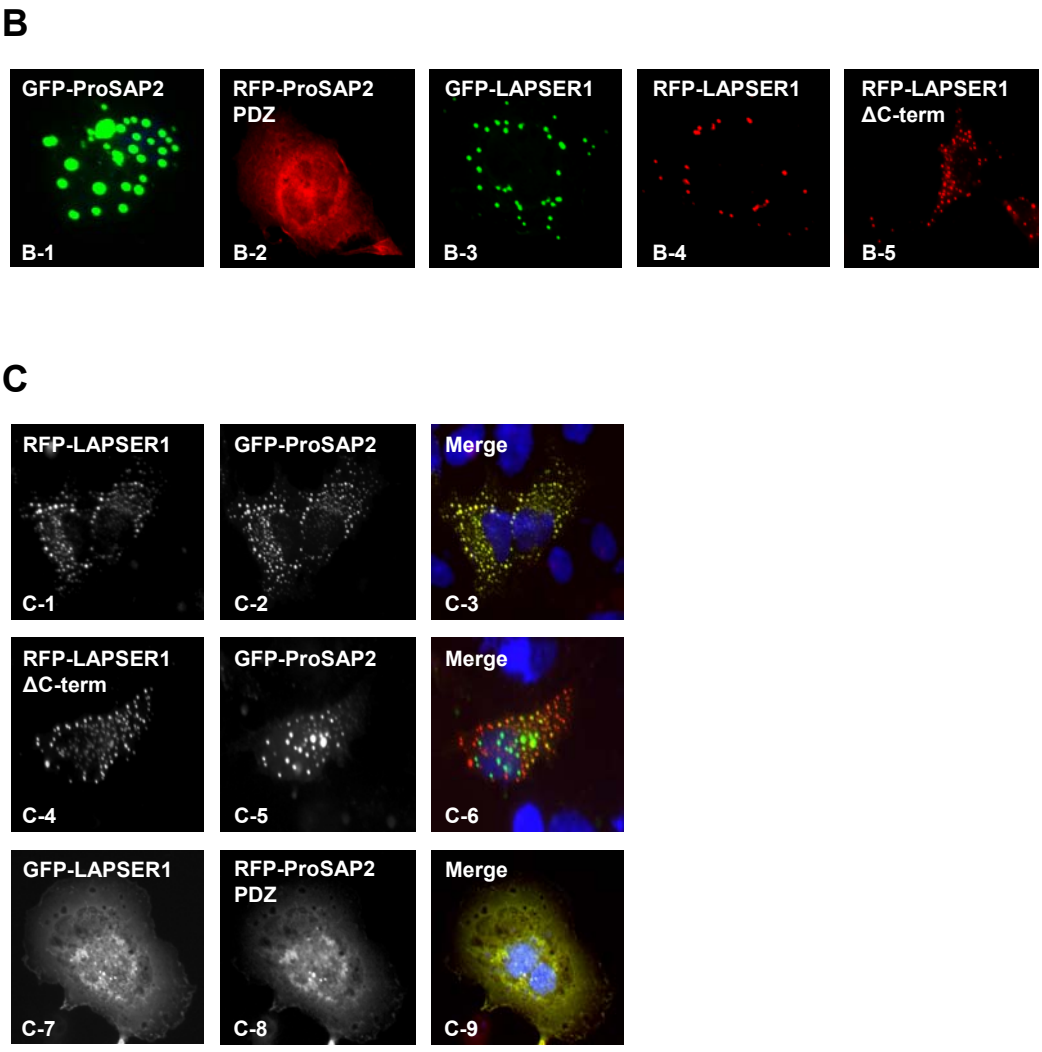

Figure 12 Interaction of LAPSER1 and ProSAP2

(**A**) Co-immunoprecipitation: Input = P2 fraction containing membrane-associated proteins from rat brain, Co-IP LAPSER1 = immunoprecipitation of P2 fraction with the LAPSER1 antibody coupled to Protein A beads, Control = beads & lysate without the LAPSER1 antibody; Western Blot: ProSAP2 antibody 1:2000. (**B-C**) Transfections of Cos-7 cells. (**B**) Single transfections of the following constructs: GFP-ProSAP2 (**B-1**), RFP-ProSAP2 PDZ (**B-2**), GFP-LAPSER1 (**B-3**), RFP-LAPSER1 (**B-4**) and RFP-LAPSER1 ΔC-term (**B-5**). (**C, 1-3**) Co-transfection of the RFP-LAPSER1 and the GFP-ProSAP2 constructs. (**C, 4-6**) Co-transfection of the RFP-LAPSER1 ΔC-term and the GFP-ProSAP2 constructs. (**C, 7-9**) Co-transfection of the GFP-LAPSER1 and the RFP-ProSAP2 PDZ constructs. Single channels in (**C**) are shown in b/w, merged pictures in color while the latter also include DAPI staining of cell nuclei (GFP = green fluorescent protein, RFP = red fluorescent protein, DAPI = 4,6-di-amidino-2-phenylindol).

3.5.2 LAPSER1 and other *"Fezzins"* interact with SPAR1

In a yeast-two-hybrid screen with the Fez1 domain as bait, members of the SPAR family of PSD-proteins could be identified as interaction partners (data by Tobias Boeckers). Double immunostainings of hippocampal neurons at 21 DIV with the polyclonal LAPSER1 antibody from rabbit and a polyclonal SPAR1 antibody from goat resulted in a co-localization of both molecules at postsynaptic sites (Figure 13). Based on the fact that the C-terminal Fez1 domain of all *"Fezzin"* family members is highly conserved (Figure 14), the cDNA of this domain in LAPSER1 (bp 1317-1878), PSD-Zip70 (bp 1132-1713) and N4BP3 (bp 1075-1557) was each cloned into the bait-vector pAS2-1. Every bait construct was then used for a mini-mating with the same prey construct from the screen mentioned above containing the C-terminal part of SPAR1 (bp 4597-5469 = SPAR1 C-term). This two-hybrid assay resulted in a positive interaction of the Fez1 domains of LAPSER1 and PSD-Zip70 with the C-terminal part of SPAR1 while the Fez1 domain of N4BP3 showed only weak interaction (Figure 15A). Additionally, the cDNA of a defined N-terminal part of PSD-Zip70 (bp 67-531) which had once been described as another putative Fez1 domain according to the NCBI database (acc. no. BAC16535) was also cloned into the bait-vector pAS2-1 and used for a mini-mating with the same prey construct. This second putative Fez1 domain of PSD-Zip70 showed no interaction with SPAR1 at all (Figure 15A). The cDNA of the previously mentioned SPAR1 prey construct (SPAR1 C-term) was further subdivided into three segments that were each cloned into the prey vector pACT2 (bp 4867-5016 = SPAR1 C-t-1, bp 5017-5255 = SPAR1 C-t-2, bp 5256-5469 = SPAR1 C-t-3) because of their putative leucine element binding sites shown in Figure 15B. Thus, these prey constructs were then each used for a mini-mating with the LAPSER1 Fez1 domain as bait resulting in an overall positive interaction. (Figure 15B).



Figure 13 Co-localization of SPAR1 and LAPSER1 in hippocampal neurons

Hippocampal neurons fixed at 21 DIV stained with antibodies directed against SPAR1 1:250 (Alexa Fluor 647: dark red) (**A**) and LAPSER1 1:400 (Alexa Fluor 488: green) (**B**). Merge of pictures A/B (**C**). Arrowheads point out SPAR1/LAPSER1 positive puncta at postsynaptic densities (DIV = days in vitro).

```
RnLAPSER1          TKWEVCQKSGEISLLKQQLKESQAELVQKGSELVALRVALREARAALRVSEGRARGLQEA  60
RnProSAPiP1        TKWEVCQKAGEISLLKQQLKDSQADVSQKLSEIVGLRSQLREGRASLREKEEQLLSLRDS  60
RnPSD-Zip70(1)     TQWEVCQKSGEISLLKQQLKESQMEVNAKASEILSLKAQLKDTRGKLEGMELKTQDLESA  60
RnN4BP3            ARWEVCQKTAEISLLKQQLREAQAELAQKLAEIFSLKTQLRGSRAQAQAQDAELARLREA  60

RnPSD-Zip70(2)     --------------YKLRKSSHLKKLNRYSDGLLRFGFSQDSGRGKSSSKMGKSEDFFYI  46

RnLAPSER1          ARARELELEACSQELQR-------YRQEAEQLREKARHLDAEAAGLREPPVPPATTDPFL 113
RnProSAPiP1        FGSKQASLELSEGELPPACLKPALTPVDLVEPQEALASCESDEAKMRR----QAGVAAAA 116
RnPSD-Zip70(1)     LRTKGLELEVCENELQR-------KKNEAELLREKVNLLEQELLELRA----QAALHRDA 109
RnN4BP3            VRSLQEQAPR----------------------EEAPGSCETDDCKSRG----LLG-----  89

RnPSD-Zip70(2)     KVSQKARGSH------------------------RPDYTALSSGDMGG----QTGVDFDP  78

RnLAPSER1          LAESDEAKVQRAAAGTGGSLRAQVERLRQELQREQRRGDEQRNSFEGERLAWQAEKEQVI 173
RnProSAPiP1        SLVSVDGEVDAGGEGGTRALRREVGRLQAELAAERRARERQGASFAEERRVWLEEKEKVI 176
RnPSD-Zip70(1)     APLGPPG-IGLTFSEDIPALQRELDRLRAELKEERQGHDQMSSGFQHERLVWKEEKEKVI 168
RnN4BP3            ---------EAGGN----EAREGAEQL AELLQERLRGQEQALRFEQERQTWQEEKERVL 136

RnPSD-Zip70(2)     ATPPKLMPFSSQLEMSSDKAAVRPTAFKPVLPRSGAILHSSPESTNHQLHPMPPDKPKEQ 138

RnLAPSER1          RYQKQLQHNYVQMY------------- 187
RnProSAPiP1        EYQKQLQLSYVEMYQR-N--------- 193
RnPSD-Zip70(1)     QYQKQLQQSYLAMYQR-NQRLEKALQQ 194
RnN4BP3            RYQREIQGSYMDMYRR-NQALEQELR- 161

RnPSD-Zip70(2)     ELKPGLCSGALSDSGR-N--------- 155
```

Figure 14 Fez1 domain alignment of all 4 *"Fezzins"*

Identical and homologous amino acid residues among the Fez1-domains of all 4 *"Fezzins"* in *Rattus norvegicus (Rn)* are highlighted in *black* (identical ones) and *grey* (homologous ones), respectively. The second putative Fez1 domain of PSD-Zip70 (*Rn*PSD-Zip70 (2)) is pointed out by a break within the alignment. All sequences derive from the NCBI database (http://www.ncbi.nlm.nih.gov).

A

YTH-Assay



bait: Fez1 domain of…	prey: SPAR1 C-term	no.
…ProSAPiP1	+++	not shown
…PSD-Zip70(1)	+++	1
…PSD-Zip70(2)	-	2
…LAPSER1	+++	3
…N4BP3	+	4

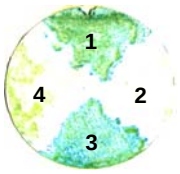

B

YTH-Assay

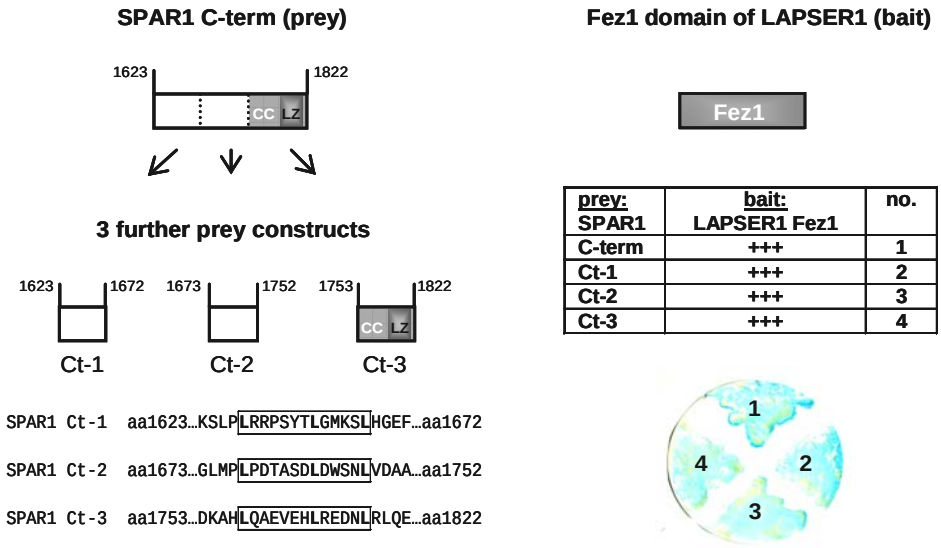

prey: SPAR1	bait: LAPSER1 Fez1	no.
C-term	+++	1
Ct-1	+++	2
Ct-2	+++	3
Ct-3	+++	4

Figure 15 Interaction of *"Fezzin"* family members with SPAR1 via Fez1 domains

(**A**) Yeast-two-hybrid-(YTH)-Assay: schematic overview, semi-quantitative analysis and filter lift assay of 4 mini-matings each with the same prey construct (SPAR1 C-term), but different bait constructs (Fez1 domains) from the following *"Fezzin"* family members: PSD-Zip70(1) (no. 1), PSD-Zip70(2) (no. 2), LAPSER1 (no. 3) and N4BP3 (no. 4). The mini-mating of the ProSAPiP1 Fez1 domain and the SPAR1 C-term construct is not shown on the filter. (**B**) Yeast-two-hybrid-(YTH)-Assay: schematic overview, semi-quantitative analysis and filter lift assay of 4 mini-matings each with the same bait construct (LAPSER1 Fez1), but different prey constructs (SPAR1 C-term (no. 1), Ct-1 (no. 2), Ct-2 (no. 3), Ct-3 (no. 4)). The putative leucine-element binding sites marked within the amino acid alignment of the SPAR1 segments Ct-1, Ct-2 and Ct-3 are in *boldface letters* and *boxed*. In (**A**) and (**B**), blue-stained colonies on the filter indicate positive interaction between bait and prey while the following symbols refer to color intensity that in turn represents binding affinity: +++ = strong interaction, + = weak interaction, - = no interaction (CC = coiled-coil domain, LZ = leucine zipper, Ct = C-term, no. = number).

3.5.3 LAPSER1, SPAR1 and Wnt pathway member β-Catenin are members of a protein complex in brain

Western Blot analysis of subcellular fractions and PSD preparations from rat brain with identical protein amounts of 20 µg per lane were performed with monoclonal antibodies directed against the C- or N-terminus of β-Catenin and with a polyclonal SPAR1 antibody showing high abundancy of these proteins in the PSD (Figure 16A). These biochemical studies were followed by heterologous expression of GFP-SPAR1 and RFP-LAPSER1 fusion proteins in HeLa cells while endogenous β-Catenin was stained at the same time with the monoclonal antibody recognizing its C-terminus. This experiment resulted in a co-localization of all three proteins in the same punctate aggregates throughout the cytoplasm (Figure 16B) while endogenous β-Catenin was also detected in the nucleus (Figure 16B-3). The following co-immunoprecipitations with the polyconal LAPSER1 antibody from rabbit, the polyclonal SPAR1 antibody from goat and both monoclonal β-Catenin antibodies from mouse using P2 fractions from rat brain containing membrane-associated proteins as input revealed the existence of a protein complex in brain harboring all three molecules interacting directly or indirectly with each other. (The ~ 85 kDa LAPSER1 band was detected in the precipitates) (Figure 16C).

A

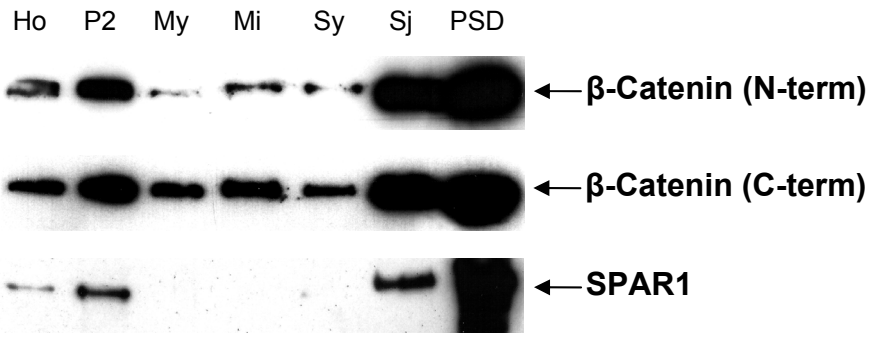

B

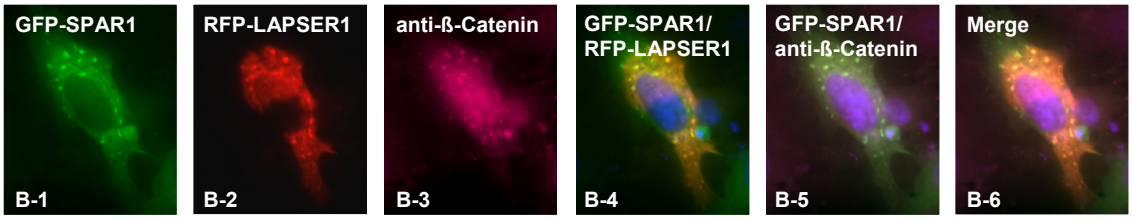

C

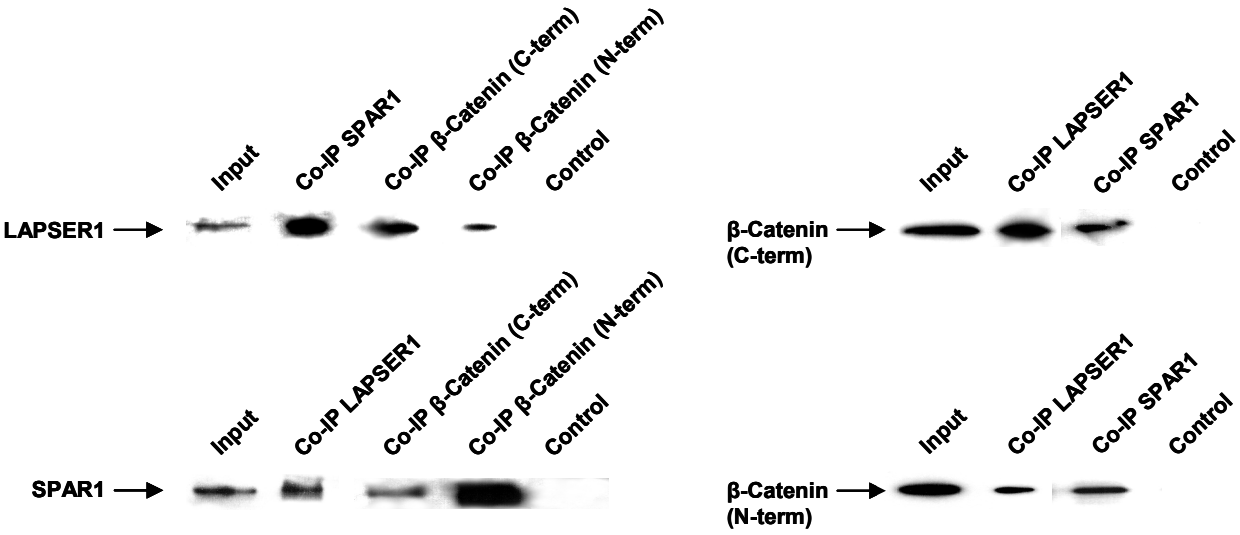

Figure 16 A protein complex in brain contains LAPSER1, SPAR1 and β-Catenin

(**A**) SDS-PAGE: whole brain homogenate (Ho), P2 fraction containing membrane-associated proteins (P2), myelin (My), mitochondrial (Mi) and synaptosomal (Sy) fractions, fraction containing synaptic junctions (Sj), postsynaptic density fraction (PSD); Western Blots: β-Catenin antibodies (C-term/N-term) 1:1000, SPAR1 antibody (1:800). (**B**) Transfection/immunostaining of HeLa cells. Co-transfection of GFP-SPAR1 (single channel: **B-1**) and RFP-LAPSER1 (single channel: **B-2**). Immunostaining with the β-Catenin C-term antibody 1:400 (Alexa Fluor 647: dark red) (single channel: **B-3**). Merge of pictures B-1/B-2 (**B-4**), B-1/B-3 (**B-5**) and of B-1/B-2/B-3 (**B-6**). DAPI staining of nuclei in B-4/B-5/B-6 (GFP = green fluorescent protein, RFP = red fluorescent protein, DAPI = 4,6-di-amidino-2-phenylindol). (**C**) Co-immunoprecipitations: Input = P2 fraction from rat brain, Co-IP SPAR1, Co-IP LAPSER1, Co-IP β-Catenin (C-term/N-term) = immunoprecipitations of P2 fraction with either SPAR1, LAPSER1 or β-Catenin antibodies coupled to Protein A beads, Control = beads & lysate only; Western Blots: antibodies directed against LAPSER1 (1:500), SPAR1 (1:800) or β-Catenin (C-term/N-term, 1:1000).

3.5.5 NMDA stimulation leads to nuclear accumulation of LAPSER1 and β-Catenin in hippocampal neurons

Triple immunostainings of hippocampal neurons at 14 DIV with the monoclonal β-Catenin antibody (C-term) from mouse, the polyclonal LAPSER1 antibody from rabbit and the polyclonal SPAR1 antibody from goat resulted in a colocalization of all three proteins in dendrites and dendritic spines (Figure 17A-1a, 17A-2a & 17A-3a). β-Catenin and LAPSER1 also seemed to be present throughout the whole cell body including the nuclear compartment (Figure 17A-1, 17A-2 & 17A-4) while SPAR1 only showed a dendritic localization (Figure 17A-3). Treatment of neurons

with 100 µm NMDA for 5 min without altering any other condition resulted in a clear nuclear accumulation and cytoplasmic as well as dendritic decrease of β-Catenin and LAPSER1 (Figure 17B-1/B-1a/B-1b & 17B-2/B-2a/B-2b) after 30 min while SPAR1 showed no change in subcellular distribution, but could still be found enriched in dendritic spines (Figure 15B-3/B-3a/B-3b).

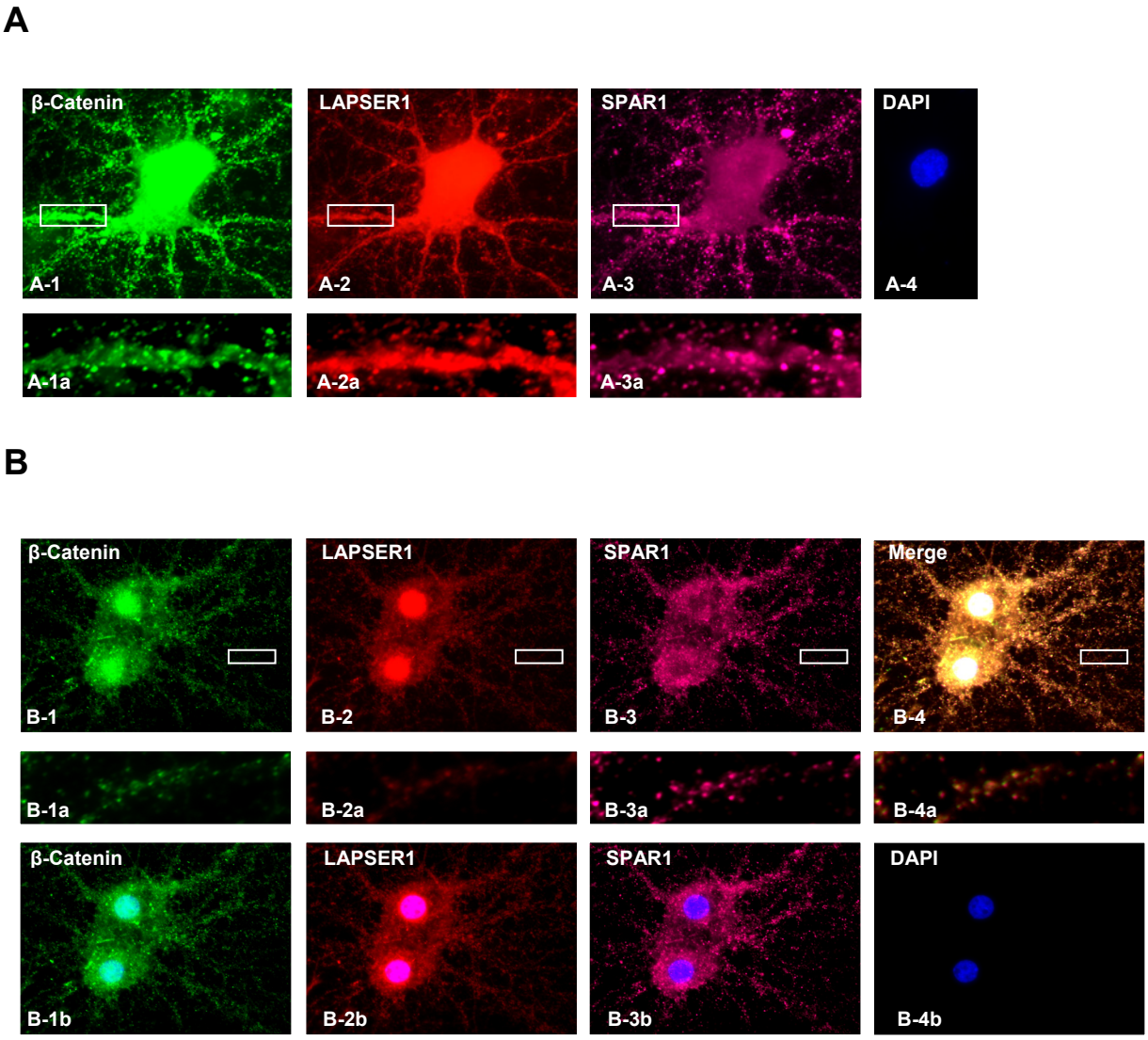

Figure 17 Molecular crosstalk between LAPSER1, SPAR1 and β-Catenin

(**A**) Hippocampal neurons fixed at 14 DIV stained with antibodies directed against β-Catenin (C-term) (Alexa Fluor 488: green) (**A-1/A-1a**), LAPSER1 (Alexa Fluor 568: red) (**A-2/A-2a**) and SPAR1 (Alexa Fluor 647: dark red) (**A-3/A-3a**). DAPI staining of the nucleus (**A-4**). (**B**) Hippocampal neurons treated with 100 µmol NMDA for 5 min at 14 DIV and fixed 30 min later stained with antibodies directed against β-Catenin (C-term) (Alexa Fluor 488: green) (**B-1/B-1a**), LAPSER1 (Alexa Fluor 568: red) (**B-2/B-2a**) and SPAR1 (Alexa Fluor 647: dark red) (**B-3/B-3a**). Merge of pictures (**B-4/B-4a**). DAPI staining of cell nuclei in B-1b/B-2b/B-3b/B-4b (DIV = days in vitro, DAPI = 4,6-di-amidino-2-phenylindol).

4. Discussion

4.1 LAPSER1 and other *"Fezzins"* contain conserved sequences mediating protein-protein interactions.

The human LAPSER1 gene has first been described as a putative tumor suppressor gene due to its location on human chromosome 10q24.3, a subregion known to be deleted in various cancers (Cabeza-Arvelaiz et al., 2001). The name LAPSER derives from the protein's high content of the amino acids leucine (L), alanine (A), proline (P), serine (S), glutamatic acid (E) and arginine (R). Transfection of LAPSER1 cDNA into prostate and other cancer cells significantly decreased their growth rate indicating the protein's involvement in cell growth regulation (Cabeza-Arvelaiz et al., 2001). Among *Homo sapiens*, *Rattus norvegicus* and *Mus musculus*, the LAPSER1 gene shows a conserved genomic organization of 5 exons and 4 introns with an open reading frame of approximately 2013 base pairs (Table 1 & Figure 3).

LAPSER1 (Figure 4) and closely related proteins ProSAPiP1, PSD-Zip70 and N4BP3 all contain a C-terminally positioned Fez1 domain that was named after a putative tumor suppressor gene (F37/esophageal cancer-related gene-coding leucine-zipper motif 1) (Ishii et al., 1999). This protein-protein interaction domain with high content of hydrophobic amino acids shows a homology of 56-58 % among all four molecules while its own 5'- and 3'-ends are conserved the most (Wendholt et al., 2006 & Figure 14). Therefore, LAPSER1, ProSAPiP1, PSD-Zip70 and N4BP3 are founding a novel protein family, the so-called *"Fezzins"*. Except for N4BP3, *"Fezzin"* family members additionally share a long central coiled-coil domain and leucine zipper motifs (Figure 5). A coiled-coil domain is known to mediate protein-protein interactions, especially with other proteins containing coiled-coil domains (Burkhard et al., 2001). There are long coiled-coil domains of several hundred amino acids and short coiled-coil domains of six or seven heptad repeats, also called leucine zippers (Rose & Meier, 2004). The latter are common dimerization domains found in proteins involved in gene regulation (Landschulz et al., 1988). Several PSD proteins like Sharpin, Homer1c or βPIX are known to form multimers via coiled-coil domains and/or leucine zippers (Tadokoro et al., 1999;

Lim et al., 2001; Park et al., 2003). As already shown for the *"Fezzin"* ProSAPiP1 (Wendholt et al., 2006), expression of GFP- or RFP-LAPSER1 fusion proteins in Cos-7 cells led to the formation of punctate aggregates throughout the cytoplasm indicating the formation of homo-oligomers (Figure 12B-3/4). Based on the fact that ProSAPiP1 and PSD-Zip70 have already been shown to form hetero-oligomers via their coiled-coil domains which are both very homologous to the one in LAPSER1 (Wendholt et al., 2006), we assume that all *"Fezzin"* family members can form hetero-oligomers. The PDZ domain binding motif of LAPSER1 and PSD-Zip70 (A-T-E-I) differs from the one of ProSAPiP1 at position P-3 which harbors a serine instead of an alanine (S-T-E-I) (Figures 4 & 5). However, all three motifs contain a threonine at position P-2 (Figure 5) which is the prerequisite to interact with class I PDZ domains like the ones of the ProSAP family (Doyle et al., 1996; Boeckers et al., 2002).

4.2 LAPSER1 is a novel PSD protein which shows a wide distribution in rat brain.

Identification of LAPSER1 as a homologue to the recently characterized PSD protein ProSAPiP1 (Wendholt et al., 2006) let us question its role in postmitotic cells like neurons. After generation and characterization of a specific LAPSER1 antibody (Figure 8), expression of LAPSER1 mRNA in rat brain as well as heart, kidney and testis could be confirmed on the protein level (Figures 6 & 9). Within the brain, LAPSER1 mRNA was found in cortex and hippocampus, but from early developmental stages onwards, expression predominantly appeared in the cerebellum (Figure 7). These findings were confirmed on the protein level by immunhistochemical stainings of sagittal rat brain sections (Figure 10B-E) and semi-quantitative Western Blot analysis of region-specific rat brain lysates (Figure 10A). As nerve sheaths of the corpus callosum were not stained for the LAPSER1 protein in immunhistochemistry (Figure 10B), we assume that the positive signal for LAPSER1 mRNA found in these fibres (Figure 7) may either be due to unspecific background staining or derive from untranslated mRNA. Clear enrichment of LAPSER1 immunoreactivity in the PSD fraction after subcellular fractionation of whole rat brain lysate and detection of endogenous LAPSER1 in dendrites and dendritic spines of hippocampal neurons at 21 DIV finally revealed the postsynaptic localization of this protein in brain (Figure 11A-C). Interestingly,

two LAPSER1 isoforms seem to exist exclusively in brain. According to Western Blot analysis of protein lysates from whole rat brain (Figure 9) and cerebral cortex (Figure 10A) and of synaptosomes, synaptic junctions and the PSD fraction (Figure 11A/B), one can separate two different bands at approximately 70 kDa and 85 kDa, respectively, while the ~ 85 kDa band could not be detected in the cerebellum (Figure 10A). Although alternative splicing of the human LAPSER1 gene has been indicated for human testis and prostate (Cabeza-Arvelaiz et al., 2001), we could not verify any LAPSER1 splice variants in brain by Northern Blot analysis (Figure 6). This makes it more likely that the two isoforms derive from posttranslational modification that may differ regionally within the brain. The LAPSER1 homologue PSD-Zip70 has been shown to be N-terminally myristoylated, thereby providing a possible anchor to the postsynaptic membrane (Konno et al., 2002). As an identical myristoylation motif is also present within the N-terminal parts of ProSAPiP1 and LAPSER1 (Wendholt et al., 2006 & Figure 4B), it needs to be clarified if myristoylated and nonmyristoylated isoforms of these proteins are synthesized using alternative in-frame start codons. Furthermore, putative phosphorylation sites have been predicted for the amino acid sequences of LAPSER1 and homologues (Ishii et al., 1999, Cabeza-Arvelaiz et al., 2001, Teufel et al., 2005). Due to the fact that serine phosphorylation of PSD-Zip70 homologue FEZ1/LZTS1 resulted in differently migrating protein bands on SDS-PAGE (Ishii et al., 2001), it should further be investigated if the LAPSER1 doublet in brain represents phosphorylated and dephosphorylated isoforms.

4.3 *"Fezzin"* family members interact with ProSAP molecules of the PSD.

The class I PDZ domain binding motifs of *"Fezzins"* ProSAPiP1, PSD-Zip70 and LAPSER1 have the potential to mediate interaction with PDZ domain-containing molecules of the PSD (Boeckers et al., 2002). ProSAPiP1 is already known to interact with the PDZ domain of ProSAP2 (Wendholt et al., 2006) while in this study, LAPSER1 was shown to be another interaction partner of ProSAP2 by co-immunoprecipitation of rat brain lysate with ProSAP2 and LAPSER1 antibodies (Figure 12A) and co-localization of GFP-ProSAP2 and RFP-LAPSER1 fusion proteins in Cos-7 cells (Figure 12C1-3). In this context, a truncated form of LAPSER1 termed RFP-LAPSER1 ΔC-term missing aa 421-670 of LAPSER1

including the PDZ domain binding motif did not co-cluster with GFP-ProSAP2 any more (Figure 12C4-6). Moreover, GFP-LAPSER1 completely changed its subcellular distribution pattern being recruited to aggregates of the RFP-tagged ProSAP2 PDZ domain when both constructs were co-transfected (Figure 12C7-9). These results strongly support the fact that LAPSER1 is tightly associated to the PDZ domain of ProSAP2. Noteworthy in this regard, PSD-Zip70 also has the potential to interact with the PDZ domain of ProSAP2 *in vitro*, but with a much weaker affinity (Wendholt et al., 2006). Due to the fact that the PDZ domain binding motifs of PSD-Zip70 and LAPSER1 are identical, but likely show different binding affinities to ProSAP2, presumably more than the last four amino acids of a binding partner's C-terminus are necessary for PDZ interaction. It has already been shown that up to 8 C-terminal amino acids of a protein can support its interaction with a PDZ domain, although only 3 amino acids fit into the binding pocket (Songyang et al., 1997). Comparing *in vivo* expression patterns, ProSAP2, ProSAPiP1 and LAPSER1, but not PSD-Zip70, are found in the same cellular and subcellular structures in brain. For example, ProSAP2 (Boeckers et al., 1999 b), ProSAPiP1 (Wendholt et al., 2006) and LAPSER1 (Figure 10D) are highly expressed in the granular cell layer of the cerebellum while PSD-Zip70 is not expressed in the cerebellum at all (Konno et al., 2002).

4.4 The *"Fezzin"* family of PSD proteins serves as binding scaffold for SPARs.

RapGTPases belong to the Ras superfamily of small GTP-binding proteins regulating various cellular processes by coupling extracellular signals to intracellular responses (Takai et al., 2001). Recent studies showed that RapGTPases Rap1 and Rap2 are involved in dendritic development and spine morphology thus requiring spatial and temporal regulation which is mediated by Rap GTPase activating proteins (RapGAPs) (Pak et al., 2001; Chen et al., 2005; Fu et al., 2007; Spilker et al., 2008). The first neuronal RapGAP to be identified was Spine-associated RapGAP (SPAR or SPAR1), a PSD protein which interacts with SAP90/PSD-95 and is capable of enlarging dendritic spines (Pak et al., 2001). Novel RapGAPs closely related to SPAR1 have recently been characterized and named SPAR2 and SPAR3, respectively (Dolnik, 2008; Spilker et al., 2008).

It could be shown that SPAR1, SPAR2 and SPAR3 each bind to *"Fezzin"* family member ProSAPiP1 via their C-terminal coiled-coil domains (Wendholt et al., 2006; Dolnik, 2008; Spilker et al., 2008). The central coiled-coil domain which is conserved among *"Fezzin"* family members has so far been identified as the corresponding SPAR1 binding domain in ProSAPiP1 and PSD-Zip70 (Wendholt et al., 2006). By performing a yeast-two-hybrid screen with the Fez1 domain as bait, we could identify the Fez1 domain as second binding motif within *"Fezzin"* proteins interacting with the C-terminal part of the SPAR family. Yeast-two-hybrid assays confirmed this interaction for the Fez1 domains of ProSAPiP1, PSD-Zip70 and LAPSER1, while N4BP3 did not bind to SPAR1 as effective as the others (Figure 15A). This may result from N4BP3's lesser homology to the other three *"Fezzins"* including a shorter Fez1 domain missing several amino acids within (Figure 14). The Fez1 interaction motif in SPAR1 doesn't seem to be limited to the coiled-coil domain, but covers a larger, leucine-rich stretch of the SPAR1 C-terminus (Figure 15B), i.e. parts of its guanylate kinase binding domain (GKBD) as it has already been shown for PSD-Zip70 (Maruoka et al., 2005). Taken together, these findings strongly support the proposed scaffolding function of *"Fezzins"* within the PSD and their ability to cross-link SPARs to ProSAP platforms. Although a *"Fezzin"* like LAPSER1 seems to interact with various SPAR family members like SPAR1 (Figures 13 & 15) or SPAR3 (Dolnik, 2008), binding preferences may exist due to overlapping *in vivo* distribution patterns. SPAR1, for example, is predominantly expressed in the cerebral cortex and the hippocampus whereas cerebellar expression is low (Spilker et al., 2008). This matches the distribution pattern of its interaction partner PSD-Zip70 which is highly expressed in the same brain areas (Konno et al., 2002). SPAR2 and SPAR3, however, show intense expression in the cerebellum, just like SPAR2-interaction partner ProSAPiP1 or SPAR3-interaction partner LAPSER1 (Dolnik, 2008, Spilker et al., 2008). The exact role of *"Fezzins"* and their Fez1 domains as "docking station" for members of the SPAR family at PSDs of excitatory synapses should more intensely be focused on in further studies exploring how *"Fezzin"* family members contribute to Rap-GAP-associated cytoskeletal reorganization within dendritic spines.

4.5 LAPSER1 is linked to the Wnt signaling pathway.

Wnt signaling plays a very important role during early life. The name Wnt is a combination of Wingless and Int, two homologous genes whose encoded proteins are morphogenic ligands establishing a pattern of development in multicellular organisms (Rijsewijk et al., 1987). Recent studies have revealed the roles of Wnts in the CNS which include differentiation of synaptic specializations, synaptic protein organization and the modulation of synaptic efficacy (Ciani & Salinas, 2005; Li et al., 2005; Davis et al., 2008). Identification of neurons secreting Wnts and those containing the molecular components downstream of the Wnt receptor apparatus suggest that Wnt ligands are indeed important for signaling events within the mammalian brain (Speese & Budnik, 2007).

Wnts signal through a receptor complex that includes Frizzled (Fz) seven transmembrane receptors, low density lipoprotein receptor-related proteins 5/6 (LRP-5/6) and tyrosine kinase-related receptor RYK (Yoshikawa et al., 2003). Wnt binding subsequently activates Dishevelled (DVL), a cytosolic protein bringing together signaling components for efficient transduction (Tamai et al., 2000; Wehrli et al., 2000; Wharton, 2003). Downstream of DVL, the Wnt pathway diverges into three main branches: the canonical or Wnt/β-Catenin pathway on the one hand and the non-canonical planar cell polarity (PCP) and Wnt/calcium pathways on the other hand (Ciani & Salinas, 2005). As the Wnt/β-Catenin pathway leads into the nuclear compartment, it is involved in the regulation of neuronal cell fate and synaptogenesis (Hall et al., 2000; Lie et al., 2005). Key event of the canonical pathway is the DVL-mediated disruption of a so-called “destruction complex” containing Glycogen synthase kinase-3β (GSK-3β), Axin and Adenomatous polyposis coli (APC) finally resulting in the cytoplasmic stabilization and activation of β-Catenin followed by its nuclear accumulation where it regulates gene expression. In the absence of Wnt signaling, the “destruction complex” constitutively phosphorylates β-Catenin, leading to its proteasomal degradation (Wodarz & Nusse, 1998).

In our study, we could confirm the postsynaptic localization of β-Catenin which co-localizes with postsynaptic marker proteins in PSDs of hippocampal neurons and is significantly enriched in the PSD fraction after subcellular fractionation of rat

brain lysate (data by Andreas Grabrucker included in Schmeisser et al., 2009 & Figure 16A). The detection of other Wnt signaling members like LRP 5/6, GSK 3β or CK1ε in the same PSD fraction and their co-localization with ProSAP1 in dendritic spines of hippocampal neurons (data by Andreas Grabrucker included in Schmeisser et al., 2009) support the previously indicated fact that postsynaptic specializations of excitatory synapses in the mammalian CNS are equipped with all crucial molecular components of Wnt signaling (Tang, 2007). Interestingly, LAPSER1 has recently been shown to interact with the armadillo repeats of β-Catenin. Due to the existence of a functional nuclear export signal (NES) within its C-terminal part, LAPSER1 regulates the subcellular localization of β-Catenin in tumor cells by enhancing its nuclear export and thus repressing β-Catenin-mediated transcription (Thyssen et al., 2006). Co-immunoprecipitation experiments with P2 fractions from rat brain containing membrane-associated proteins (Figure 16C) and co-localization studies in hippocampal cultures (Figure 17A) revealed that LAPSER1 and β-Catenin can be found within the same complex also in neurons. In addition, overexpression of GFP-LAPSER1 in hippocampal neurons led to the recruitment of endogenous β-Catenin into LAPSER1-positive clusters at postsynaptic sites (data by Andreas Grabrucker included in Schmeisser et al., 2009). LAPSER1 therefore may be connected to neuronal Wnt signaling by having a regulatory effect on β-Catenin. In this context, it should be noted that apart from its crucial role in the canoncial Wnt pathway, β-Catenin further interacts with the axodendritical adhesion molecule N-Cadherin (Miskevich et al., 1998; Perego et al., 2000) and the actin-binding protein α-Catenin which links cadherin-coupled β-Catenin to the cytoskeleton (Drees et al., 2005). Synaptic β-Catenin has also been shown to bind synaptic scaffolding molecule (S-SCAM) that is associated to the NMDA receptor complex (NRC) either indirectly via SAP90/PSD-95 or directly via the NMDA receptor (NMDAR) subunit NR2A (Nishimura et al., 2002; Al-Hallaq et al., 2007). Both functions of β-Catenin are known to be executed by separate protein pools, the free cytoplasmic pool and the membrane-bound pool which are in equilibrium with each other (Bienz & Clevers, 2000). It would be very interesting to further clarify which role LAPSER1 plays in the regulation of those pools – especially within the PSD of excitatory synapses.

4.6 LAPSER1 and its interaction partner β-Catenin take part in activity-dependent synapse-to-nucleus shuttling.

The neurobiological core elements of learning and memory are believed to be changes in gene expression and protein synthesis during L-LTP leading to alterations in spine morphology (Kelleher RJ 3rd et al., 2004 a & b; Costa-Mattioli M et al., 2005; Wu et al., 2007). These complex neuronal processes require the transport of signals generated at the synapse to the nucleus and their conversion into the transcription of certain genes. This activity-dependent synapse-to-nucleus signaling is known to be mediated by nucleocytoplasmic shuttling of transcription factors and/or their regulatory proteins (West et al., 2002; Deisseroth et al., 2003; Alberini, 2009). In the hippocampus, for example, activation of the NMDAR followed by Ca^{2+} entry leads to the nuclear import of calmodulin, protein kinase A (PKA) and mitogen-activated protein kinase (MAPK) resulting in phosphorylation-dependent regulation of nuclear cAMP-response element-binding protein (CREB), a transcription factor responsible for learning and memory formation (Kandel, 2001; Waltereit & Weller, 2003). CREB-mediated gene transcription subsequently alters the protein composition within the neuron and therefore lays the foundation for long-term memory storage on a molecular level (Carlezon et al., 2005).

Interestingly, recent studies have demonstrated that certain proteins enriched in PSDs of excitatory synapses accumulate in the nucleus in response to synaptic activity. Some of those proteins were shown to be specific NMDAR dependent messengers such as Abi-1, AIDA-1, and Jacob (Jordan & Kreutz, 2009). After treatment of hippocampal neurons with NMDA, Abi-1, which organizes dendrite formation during synaptogenesis, translocates into the nucleus in a phosphorylation-dependent manner and binds to the Myc/Max complex of transcription factors (Proepper et al., 2007). AIDA-1 shuttles to the nucleus upon NMDA stimulation inducing an increase in nucleolar numbers thus influencing global translational capacities of the neuron (Jordan et al., 2007). After being recruited to neuronal nuclei upon NMDAR activation, Jacob is involved in signaling events resulting in stripping of synaptic contacts and the alteration of dendritic morphology (Dieterich et al., 2008). In untreated neurons, LAPSER1 and its interaction partner β-Catenin were not only found at synaptic sites, but also being observed in the nucleus on a moderate level (Figure 17A-1/2) supporting the fact

that both proteins are distributed in various subcellular compartments of neuronal cells *in vivo*. We could further show that NMDAR activation in hippocampal neurons induces the nuclear translocation of LAPSER1 and its interaction partner β-Catenin (Figure 17B). Under these conditions, LAPSER1-interaction partner SPAR1 – which is found within the same protein complex as LAPSER1 and β-Catenin (Figures 16A-C, 17A) – stays in dendritic spines (Figure 17B). As nuclear shuttling of LAPSER1/β-Catenin could not be elicited upon membrane depolarization alone or AMPA receptor activation (data by Andreas Grabrucker included in Schmeisser et al., 2009), it seems that activity-dependent LAPSER1/β-Catenin-signaling is coupled only to the NMDAR. Even more interesting is the observation that application of commercially available Wnt ligands 5a, 7a and 3a of which the latter has already been linked to NMDAR dependent nuclear accumulation of β-Catenin in neurons (Chen et al., 2006), did not show any effect on the nuclear translocation of LAPSER1/β-Catenin (data by Andreas Grabrucker included in Schmeisser et al., 2009). As the presence of Wnts is usually essential to rescue β-Catenin from the destruction complex (see 4.5), our experiments indicate that either Wnt ligands we were not able to identify might be co-released from presynaptic compartments upon NMDAR activation or that neuronal cells have developed a different mechanism to stabilize β-Catenin possibly involving LAPSER1. Recent data support the latter hypothesis as cleaved β-Catenin was already shown to shuttle from synapse-to-nucleus upon NMDAR activation without a specific Wnt signal (Abe & Takeichi, 2007).

4.7 LAPSER1 regulates the nuclear localization of β-Catenin in hippocampal neurons

Downregulation of LAPSER1 by RNAi in primary hippocampal neurons and the following application of NMDA to the cell cultures didn’t disrupt the nuclear import of β-Catenin. However, β-Catenin could still be found in the nuclear compartment 4 h after application of NMDA in the LAPSER1-RNAi transfected neurons – an observation substantially different from control cells where β-Catenin was mainly redistributed into the cytoplasm, dendrites and dendritic spines at this point of time (data by Andreas Grabrucker included in Schmeisser et al., 2009). As the expression of β-Catenin target genes was significantly prolonged in LAPSER1-depleted neurons, our findings strongly support the fact that LAPSER1 not only

has a regulatory effect on β-Catenin-mediated gene transcription in mitotic cells (Thyssen et al., 2006), but also in neurons. Taken together, our functional studies of LAPSER1 in hippocampal neurons point towards a self-limiting function of the LAPSER1/β-Catenin complex in neuronal nuclei in response to synaptic activation.

4.8 Conclusion

The fact, that *"Fezzin"* family member LAPSER1 could be characterized as a novel PSD component interacting directly with the PDZ domain of ProSAP2 adds important information to a better understanding of the molecular machinery within postsynaptic specializations and again highlights the function of ProSAPs as master scaffolding molecules of the PSD. Furthermore, identifiying the Fez1 domain of all four *"Fezzins"* as interacting module for members of the SPAR family shows that *"Fezzins"* essentially contribute to cross-link SPARs to ProSAPs thus possibly having an influence on the regulation of dendritic spine morphology. The most exciting finding of this work, however, is the association of LAPSER1 and β-Catenin in hippocampal neurons. Upon NMDA receptor activation, both molecules that are found within the same complex at synaptic sites, shuttle to the nucleus while LAPSER1 regulates β-Catenin-mediated gene expression. All the above mentioned findings are visualized in Figure 18 below.

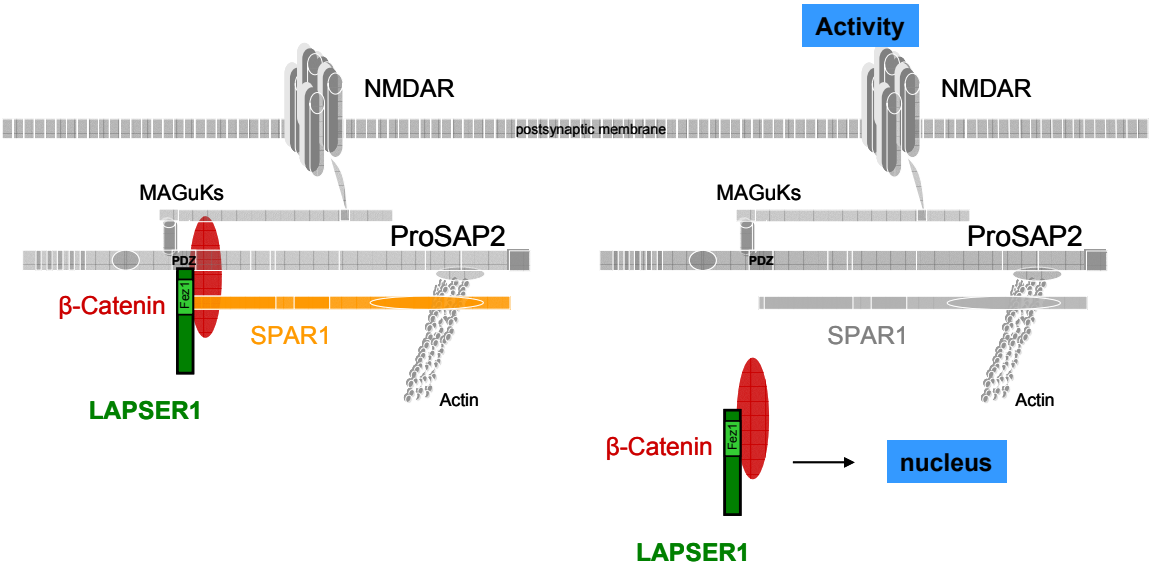

Figure 18 LAPSER1 & the postsynaptic density – a schematic overview

LAPSER1 is presented in *green*, β-Catenin in *red* and SPAR1 in *orange* on the left side (NMDAR = NMDA receptor). For the theoretical background of this figure, please see the text above (4.8).

5. Summary

Neuronal communication is essential for learning and memory. On the cellular level, this communciation happens via synapses – complex cell-cell contacts between neurons. As memory formation has been shown to depend upon long lasting plastic changes of the molecular composition within the synapse, synaptic proteins being responsible for these changes are of special interest. Analysis of those molecules helps to encode more and more of the complex molecular machinery of so-called ‘synaptic plasticity’.

This work was focused on the characterization of a newly identified postsynaptic protein called LAPSER1 that belongs to the *“Fezzin”* family of synaptic proteins. The LAPSER1 protein whose gene consists of 5 exons and 4 introns that are conserved among human, rat and mouse, contains several protein-protein interaction domains. It is highly expressed in brain and localizes to the postsynaptic compartment interacting directly with the major postsynaptic scaffolding molecule ProSAP2. It also cross-links spine morphology regulator SPAR1 to the ProSAP platform via its conserved C-terminal Fez1 domain that could further be characterized as an interaction module for all members of the SPAR family. In addition, LAPSER1 interacts with Wnt pathway member β-Catenin at postsynaptic densities. Upon NMDA (N-methyl-D-aspartate) receptor activation, LAPSER1 rapidly shuttles to the nucleus in a complex with β-Catenin and tightly regulates the nuclear localization of the latter by enhancing its nuclear export thus repressing β-Catenin-mediated transcription.

As activity-dependent changes in gene expression and protein synthesis are believed to be the core elements of neuronal circuit formation, the characterization of LAPSER1 and the description of its potential role in neurons add important knowledge which further helps to understand the molecular processes of postsynaptic plasticity and memory formation.

List of literature

1. Abe K, Takeichi M:
   NMDA receptor activation induces calpain-mediated β-Catenin cleavages for triggering gene expression.
   Neuron 53: 387-397 (2007)

2. Al-Hallaq RA, Conrads TP, Veenstra TD, Wenthold RJ:
   NMDA di-heteromeric receptor populations and associated proteins in rat hippocampus.
   J Neurosci 27: 8334-8343 (2007)

3. Alberini CM:
   Transcription factors in long-term memory and synaptic plasticity.
   Physiol Rev 89: 121-145 (2009)

4. Alvarez-Maubecin V, Garcia-Hernandez F, Williams JT, Van Bockstaele EJ:
   Functional coupling between neurons and glia.
   J Neurosci 20: 4091-4098 (2000)

5. Aravamudan B, Fergestad T, Davis WS, Rodesch CK, Broadie K:
   Drosophila UNC-13 is essential for synaptic transmission.
   Nat Neurosci 2: 965-971 (1999)

6. Augustin I, Rosenmund C, Südhof TC, Brose N:
   Munc13-1 is essential for fusion competence of glutamatergic synaptic vesicles.
   Nature 400: 457-461 (1999)

7. Baron MK, Boeckers TM, Vaida B, Faham S, Gingery M, Sawaya MR, Salyer D, Gundelfinger ED, Bowie JU:
   An architectural framework that may lie at the core of the postsynaptic density.
   Science 311: 531-535 (2006)

8. Bennett MV, Zukin RS:
   Electrical coupling and neuronal synchronization in the mammalian brain.
   Neuron 41: 495-511 (2004)

9. Bienz M, Clevers H:
   Linking colorectal cancer to Wnt signaling.
   Cell 103: 311-320 (2000)

10. Bliss TV, Lomo T:
    Long-lasting potentiation of synaptic transmission in the dentate area of the anaesthetized rabbit following stimulation of the perforant path.
    J Physiol 232: 331-356 (1973)

11. Bockmann J, Kreutz MR, Gundelfinger ED, Boeckers TM:
ProSAP/Shank postsynaptic density proteins interact with insulin receptor tyrosine kinase substrate IRSp53.
J Neurochem 83: 1013-1017 (2002)

12. Boeckers TM, Kreutz MR, Winter C, Zuschratter W, Smalla KH, Sanmarti-Vila L, Wex H, Langnaese K, Bockmann J, Garner CC, Gundelfinger ED:
Proline-rich synapse-associated protein-1/cortactin binding protein 1 (ProSAP1/CortBP1) is a PDZ-domain protein highly enriched in the postsynaptic density.
J Neurosci 19: 6506-6518 (1999 a)

13. Boeckers TM, Winter C, Smalla KH, Kreutz MR, Bockmann J, Seidenbecher C, Garner CC, Gundelfinger ED:
Proline-rich synapse-associated proteins ProSAP1 and ProSAP2 interact with synaptic proteins of the SAPAP/GKAP family.
Biochem Biophys Res Commun 264: 247-252 (1999 b)

14. Boeckers TM, Mameza MG, Kreutz MR, Bockmann J, Weise C, Buck F, Richter D, Gundelfinger ED, Kreienkamp HJ:
Synaptic scaffolding proteins in rat brain. Ankyrin repeats of the multidomain Shank protein family interact with the cytoskeletal protein alpha-fodrin.
J Biol Chem 276: 40104-40112 (2001)

15. Boeckers TM, Bockmann J, Kreutz MR, Gundelfinger ED:
ProSAP/Shank proteins – a family of higher order organizing molecules of the postsynaptic density with an emerging role in human neurological disease.
J Neurochem 81: 903-910 (2002)

16. Boeckers TM, Liedtke T, Spilker C, Dresbach T, Bockmann J, Kreutz MR, Gundelfinger ED:
C-terminal synaptic targeting elements for postsynaptic density proteins ProSAP1/Shank2 and ProSAP2/Shank3.
J Neurochem 92: 519-524 (2005)

17. Boeckers TM:
The postsynaptic density.
Cell Tissue Res 326: 409-422 (2006)

18. Bresler T, Shapira M, Boeckers T, Dresbach T, Futter M, Garner CC, Rosenblum K, Gundelfinger ED, Ziv NE:
Postsynaptic density assembly is fundamentally different from presynaptic active zone assembly.
J Neurosci 24: 1507-1520 (2004)

19. Broderick MJ, Winder SJ:
Towards a complete atomic structure of spectrin family proteins.
J Struct Biol 137: 184-193 (2002)

20. Burkhard P, Stetefeld J, Strelkov SV:
Coiled coils: a highly versatile protein folding motif.
Trends Cell Biol 11: 82-88 (2001)

21. Cabeza-Arvelaiz Y, Thompson TC, Sepulveda JL, Chinault AC:
LAPSER1: a novel candidate tumor suppressor gene from 10q24.3.
Oncogene 46: 6707-6717 (2001)

22. Calakos N, Schoch S, Südhof TC, Malenka RC:
Multiple roles for the active zone protein RIM1alpha in late stages of neurotransmitter release.
Neuron 42: 889-896 (2004)

23. Carlezon WA Jr, Duman RS, Nestler EJ:
The many faces of CREB
Trends Neurosci 28: 436-445 (2005)

24. Chen J, Park CS, Tang SJ:
Activity-dependent synaptic Wnt release regulates hippocampal long term potentiation
J Biol Chem 281: 11910-11916 (2006)

25. Chen Y, Wang PY, Ghosh A:
Regulation of cortical dendrite development by Rap1 signaling.
Mol Cell Neurosci 28: 215-228 (2005)

26. Cheng D, Hoogenraad CC, Rush J, Ramm E, Schlager MA, Duong DM, Xu P, Wijayawardana SR, Hanfelt J, Nakagawa T, Sheng M, Peng J:
Relative and absolute quantification of postsynaptic density proteome isolated from rat forebrain and cerebellum.
Mol Cell Proteomics 5: 1158-1170 (2006)

27. Ciani L, Salinas PC:
Wnts in the vertebrate nervous system: from patterning to neuronal connectivity.
Nat Rev Neurosci 6: 351-362 (2005)

28. Collins MO, Husi H, Yu L, Brandon JM, Anderson CN, Blackstock WP, Choudhary JS, Grant SG:
Molecular characterization and comparison of the components and multiprotein complexes in the postsynaptic proteome.
J Neurochem 97: 16-23 (2006)

29. Costa-Mattioli M, Gobert D, Harding H, Herdy B, Azzi M, Bruno M, Bidinosti M, Ben Mamou C, Marcinkiewicz E, Yoshida M, Imataka H, Cuello AC, Seidah N, Sossin W, Lacaille JC, Ron D, Nader K, Sonenberg N:
Translational control of hippocampal synaptic plasticity and memory by the eIF2alpha kinase GCN2.
Nature 436: 1166-1173 (2005)

30. Craig AM, Graf ER, Linhoff MW:
How to build a central synapse: clues from cell culture.
Trends Neurosci 29: 8-20 (2006)

31. Craven SE, Bredt DS:
PDZ proteins organize synaptic signaling pathways.
Cell 93: 495-498 (1998)

32. Davis EK, Zou Y, Ghosh A:
Wnts acting through canonical and noncanonical signaling pathways exert opposite effects on hippocampal synapse formation.
Neural Dev 3: 32 (2008)

33. Dean C, Dresbach T:
Neuroligins and neurexins: linking cell adhesion, synapse formation and cognitive function.
Trends Neurosci 29: 21-29 (2006)

34. Deisseroth K, Mermelstein PG, Xia H, Tsien RW:
Signaling from synapse to nucleus: the logic behind the mechanisms.
Curr Opin Neurobiol 13: 354-365 (2003)

35. Dieterich DC, Karpova A, Mikhaylova M, Zdobnova I, König I, Landwehr M, Kreutz M, Smalla KH, Richter K, Landgraf P, Reissner C, Boeckers TM, Zuschratter W, Spilker C, Seidenbecher CI, Garner CC, Gundelfinger ED, Kreutz MR:
Caldendrin-Jacob: a protein liaison that couples NMDA receptor signaling to the nucleus.
PLoS Biology 6: 286-306 (2008)

36. Dolnik A:
Spar3, a novel protein of the postsynaptic density.
PhD thesis, Faculty for Medicine, Ulm University (2008)

37. Douglas RM, Goddard GV:
Long term potentiation of the perforant path-granule cell synapse in the rat hippocampus.
Brain Res 86: 205-215 (1975)

38. Doyle DA, Lee A, Lewis J, Kim E, Sheng M, MacKinnon R:
Crystal structures of a complexed and peptide-free membrane protein-binding domain: molecular basis of peptide recognition by PDZ.
Cell 85: 1067-1076 (1996)

39. Drees F, Pokutta S, Yamada S, Nelson WJ, Weis WI:
α-Catenin is a molecular switch that binds E-cadherin-β-Catenin and regulates actin-filament-assembly.
Cell 123: 903-915 (2005)

40. Dresbach T, Qualmann B, Kessels M, Garner CC, Gundelfinger ED:
The presynaptic cytomatrix of brain synapses.
Cell Mol Life Sci 58: 94-116 (2001)

41. Dresbach T, Hempelmann A, Spilker C, tom Dieck S, Altrock WD, Zuschratter W, Garner CC, Gundelfinger ED:
Functional regions of the presynaptic cytomatrix protein bassoon: significance for synaptic targeting and cytomatrix anchoring.
Mol Cell Neurosci 23: 279-291 (2003)

42. Dresbach T, Torres V, Wittenmayer N, Altrock WD, Zamorano P, Zuschratter W, Nawrotzki R, Ziv NE, Garner CC, Gundelfinger ED:
Assembly of active zone precursor vesicles: obligatory trafficking of presynaptic cytomatrix proteins Bassoon and Piccolo via a trans-Golgi compartment.
J Biol Chem 281: 6038-6047 (2006)

43. Du Y, Weed SA, Xiong WC, Marshall TD, Parsons JT:
Identification of a novel cortactin SH3 domain-binding protein and its localization to growth cones of cultured neurons.
Mol Cell Biol 18: 5838-5851 (1998)

44. Elias GM, Nicoll RA:
Synaptic trafficking of glutamate receptors by MAGUK scaffolding proteins.
Trends Cell Biol 17: 343-352 (2007)

45. Ethell IM, Pasquale EB:
Molecular mechanisms of dendritic spine development and remodeling.
Prog Neurobiol 75: 161-205 (2005)

46. Fanning AS, Anderson JM:
Protein-protein interactions: PDZ domain networks.
Curr Biol 6: 1385-1388 (1996)

47. Fejtová A, Gundelfinger ED:
Molecular organization and assembly of the presynaptic active zone of neurotransmitter release.
Results Probl Cell Differ 43: 49-68 (2006)

48. Fenster SD, Chung WJ, Zhai R, Cases-Langhoff C, Voss B, Garner AM, Kaempf U, Kindler S, Gundelfinger ED, Garner CC:
Piccolo, a presynaptic zinc finger protein structurally related to Bassoon.
Neuron 25: 203-214 (2000)

49. Fenster SD, Kessels MM, Qualmann B, Chung WJ, Nash J, Gundelfinger ED, Garner CC:
Interactions between Piccolo and the actin/dynamin-binding protein Abp1 link vesicle endocytosis to presynaptic active zones.
J Biol Chem 278: 20268-20277 (2003)

50. Fiala JC, Feinberg M, Popov V, Harris KM:
Synaptogenesis via dendritic filopodia in developing hippocampal area CA1.
J Neurosci 18: 8900-8911 (1998)

51. Friedman HV, Bresler T, Garner CC, Ziv NE:
Assembly of new individual excitatory synapses: time course and temporal order of synaptic molecule recruitment.
Neuron 27: 57-69 (2000)

52. Furshpan EJ, Potter DD:
Transmission at the giant motor synapses of the crayfish.
J Physiol 145: 289-325 (1959)

53. Fu Z, Lee SH, Simonetta A, Hansen J, Sheng M, Pak DT:
Differential roles of Rap1 and Rap2 small GTPases in neurite retraction and synapse elimination in hippocampal spiny neurons.
J Neurochem 100: 118-131 (2007)

54. Garner CC, Kindler S:
Synaptic proteins and the assembly of synaptic junctions.
Trends Cell Biol 6: 429-433 (1996)

55. Garner CC, Waites CL, Ziv NE:
Synapse development: still looking for the forest, still lost in the trees.
Cell Tissue Res 326: 249-262 (2006)

56. Genoux D, Montgomery JM:
Glutamate receptor plasticity at excitatory synapses in the brain.
Clin Exp Pharmacol Physiol 34: 1058-1063 (2007)

57. Gerrow K, Romorini S, Nabi SM, Colicos MA, Sala C, El-Husseini A:
A preformed complex of postsynaptic proteins is involved in excitatory synapse development.
Neuron 49: 547-562 (2006)

58. Gibson JR, Beierlein M, Connors BW:
Functional properties of electrical synapses between inhibitory interneurons of neocortical layer 4.
J Neurophysiol 93: 467-480 (2005)

59. Goda Y, Davis GW:
Mechanisms of synapse assembly and disassembly.
Neuron 40: 243-264 (2003)

60. Gray EG:
Electron microscopy of synaptic contacts on dendritic spines of the cerebral cortex.
Nature 183: 1592-1593 (1959)

61. Gundelfinger ED, tom Dieck S:
Molecular organization of excitatory chemical synapses in the mammalian brain.
Naturwissenschaften 87: 513-523 (2000)

62. Haeckel A, Ahuja R, Gundelfinger ED, Qualmann B, Kessels MM::
The actin-binding protein Abp1 controls dendritic spine morphology and is important for spine head and synapse formation.
J Neurosci 28: 10031-10044 (2008)

63. Hall AC, Lucas FR, Salinas PC:
Axonal remodeling and synaptic differentiation in the cerebellum is regulated by Wnt-7a signaling.
Cell 100: 525-535 (2000)

64. Harris AS, Morrow JS:
Calmodulin and calcium-dependent protease I coordinately regulate the interaction of fodrin with actin.
Proc Natl Acad Sci USA 87: 3009-3013 (1990)

65. Hata Y, Nakanishi H, Takai Y:
Synaptic PDZ domain-containing proteins.
Neurosci Res 32: 1-7 (1998)

66. Hebb D:
The Organization of Behaviour: A Neuropsychological Theory.
Wiley-Interscience, New York, p. 62 (1949)

67. Hjorth J, Blackwell KT, Kotaleski JH:
Gap junctions between striatal fast-spiking interneurons regulate spiking activity and synchronization as a function of cortical activity.
J Neurosci 29: 5276-5286 (2009)

68. Hollmann M, Heinemann S:
Cloned glutamate receptors.
Annu Rev Neurosci 17: 31-108 (1994)

69. Hormuzdi SG, Filippov MA, Mitropoulou G, Monyer H, Bruzzone R:
Electrical synapses: a dynamic signaling system that shapes the activity of neuronal networks.
Biochim Biophys Acta 1662: 113-137 (2004)

70. Ishii H, Baffa R, Murakumo Y, Rattan S, Inoue H, Mori M, Fidanza V, Alder H, Croce CM:
The *FEZ1* gene at chromosome 8p22 encodes a leucine-zipper protein, and its expression is altered in multiple human tumors.
Proc Natl Acad Sci USA 96: 3928-3933 (1999)

71. Ishii H, Vecchione A, Murakumo Y, Baldassarre G, Numata S, Trapasso F, Alder H, Baffa R, Croce CM:
FEZ1/LZTS1 gene at 8p22 suppresses cancer cell growth and regulates mitosis.
Proc Natl Acad Sci USA 98: 10374-10379 (2001)

72. Jontes JD, Smith SJ:
Filopodia, spines and the generation of synaptic diversity.
Neuron 27: 11-14 (2000)

73. Jordan BA, Fernholz BD, Khatri L, Ziff EB:
Activity-dependent AIDA-1 nuclear signaling regulates nucleolar numbers and protein synthesis in neurons.
Nat Neurosci 10: 427-435 (2007)

74. Jordan BA, Kreutz MR:
Nucleocytoplasmic protein shuttling: the direct route in synapse-to-nucleus signaling.
Trends Neurosci 32: 392-401 (2009)

75. Kandel ER:
Nerve Cells and Behavior.
In: Kandel ER, Schwartz JH, Jessell TM (Editors):
Principles of Neural Science, Third Edition.
Appleton & Lange, East Norwalk, p. 18-19 (1991)

76. Kandel ER:
The molecular biology of memory storage: a dialogue between genes and synapses.
Science 294: 1030-1038 (2001)

77. Kelleher RJ 3rd, Govindarajan A, Jung HY, Kang H, Tonegawa S:
Translational control by MAPK signaling in long-term synaptic plasticity and memory.
Cell 116: 467-479 (2004 a)

78. Kelleher RJ 3rd, Govindarajan A, Tonegawa S:
Translational regulatory mechanisms in persistent forms of synaptic plasticity.
Neuron 44: 59-73 (2004 b)

79. Kim DY, Kim SH, Choi HB, Min C, Gwag BJ:
High abundance of GluR1 mRNA and reduced Q/R editing of GluR2 mRNA in individual NADPH-diaphorase neurons.
Mol Cell Neurosci 17: 1025-1033 (2001)

80. Kim E, Sheng M:
PDZ domain proteins of synapses.
Nat Rev Neurosci 5: 771-781 (2004)

81. Kirsch J:
Glycinergic transmission.
Cell Tissue Res 326: 535-540 (2006)

82. Konno D, Ko JA, Usui S, Hori K, Maruoka H, Inui M, Fujikado T, Tano Y, Suzuki T, Tohyama K, Sobue K:
The postsynaptic density and dendritic raft localization of PSD-Zip70, which contains an N-myristoylation sequence and leucine-zipper motifs.
J Cell Sci. 115: 4695-4706 (2002)

83. Kreienkamp HJ, Zitzer H, Gundelfinger ED, Richter D, Boeckers TM:
The calcium-independent receptor for alpha-latrotoxin from human and rodent brains interacts with members of the ProSAP/SSTRIP/Shank family of multidomain proteins.
J Biol Chem 275: 32387-32390 (2000)

84. Kuno M:
The Synapse: Function, Plasticity and Neurotrophism.
Oxford University Press, Oxford New York, p. 3 (1995)

85. Kunze A, Congreso MR, Hartmann C, Wallraff-Beck A, Hüttmann K, Bedner P, Requardt R, Seifert G, Redecker C, Willecke K, Hofmann A, Pfeifer A, Theis M, Steinhäuser C:
Connexin expression by radial glia-like cells is required for neurogenesis in the adult dentate gyrus.
Proc Natl Acad Sci USA 106: 11336-11341 (2009)

86. Landschulz WH, Johnson PF, McKnight SL:
The leucine zipper: a hypothetical structure common to a new class of DNA binding proteins.
Science 240: 1759-1764 (1988)

87. Li F, Chong ZZ, Maiese K:
Vital elements of the Wnt-Frizzled signaling pathway in the nervous system.
Curr Neurovasc Res 2: 331-340 (2005)

88. Lie DC, Colamarino SA, Song HJ, Désiré L, Mira H, Consiglio A, Lein ES, Jessberger S, Lansford H, Dearie AR, Gage FH:
Wnt signalling regulates adult hippocampal neurogenesis.
Nature 437: 1370-1375 (2005)

89. Liebau S, Proepper C, Schmidt T, Schoen M, Bockmann J, Boeckers TM:
ProSAPiP2, a novel postsynaptic density protein that interacts with ProSAP2/Shank3.
Biochem Biophys Res Commun 385: 460-465 (2009)

90. Lim S, Naisbitt S, Yoon J, Hwang JI, Suh PG, Sheng M, Kim E:
Characterization of the Shank family of synaptic proteins.
J Biol Chem 274: 29510-29518 (1999)

91. Lim S, Sala C, Yoon J, Park S, Kuroda S, Sheng M, Kim E:
Sharpin, a novel postsynaptic density protein that directly interacts with the Shank family of proteins.
Mol Cell Neurosci 17: 385-397 (2001)

92. Liu XB, Murray KD, Jones EG:
Switching of NMDA receptor 2A and 2B subunits at thalamic and cortical synapses during early postnatal development.
J Neurosci 24: 8885-8895 (2004)

93. Lynch MA:
Long-term potentiation and memory.
Physiol Rev 84: 87-136 (2004)

94. Malinow R:
AMPA receptor trafficking and long-term potentiation.
Philos Trans R Soc Lond B Biol Sci 358: 707-714 (2003)

95. Maruoka H, Konno D, Hori K, Sobue K:
Collaboration of PSD-Zip70 with its binding partner, SPAR, in dendritic spine maturity.
J Neurosci 25: 1421-1430 (2005)

96. Massey PV, Bashir ZI:
Long-term depression: multiple forms and implications for brain function.
Trends Neurosci 30: 176-184 (2007)

97. McWilliams RR, Gidey E, Fouassier L, Weed SA, Doctor RB:
Characterization of an ankyrin repeat-containing Shank2 isoform (Shank2E) in liver epithelial cells.
Biochem J 380: 181-191 (2004)

98. Miskevich F, Zhu Y, Ranscht B, Sanes JR:
Expression of multiple cadherins and catenins in the chick optic tectum.
Mol Cell Neurosci 12: 240-255 (1998)

99. Murillas R, Simms KS, Hatakeyama S, Weissman AM, Kuehn MR:
Identification of developmentally expressed proteins that functionally interact with Nedd4 ubiquitin ligase.
J Biol Chem 277: 2897-2907 (2002)

100. Naisbitt S, Kim E, Tu JC, Xiao B, Sala C, Valtschanoff J, Weinberg RJ, Worley PF, Sheng M:
Shank, a novel family of postsynaptic density proteins that binds to the NMDA receptor/PSD-95/GKAP complex and cortactin.
Neuron 23: 569-582 (1999)

101. Nishimura W, Yao I, Iida J, Tanaka N, Hata Y:
Interaction of synaptic scaffolding molecule and beta-Catenin.
J Neurosci 22: 757-765 (2002)

102. Niethammer M, Kim E, Sheng M:
Interaction between the C terminus of NMDA receptor subunits and multiple members of the PSD-95 family of membrane-associated guanylate kinases.
J Neurosci 16: 2157-2163 (1996)

103. Ohtsuka T, Takao-Rikitsu E, Inoue E, Inoue M, Takeuchi M, Matsubara K, Deguchi-Tawarada M, Satoh K, Morimoto K, Nakanishi H, Takai Y:
Cast: a novel protein of the cytomatrix at the active zone of synapses that forms a ternary complex with RIM1 and Munc13-1.
J Cell Biol 158: 577-590 (2002)

104. Okamoto PM, Gamby C, Wells D, Fallon J, Vallee RB:
Dynamin isoform-specific interaction with the shank/ProSAP scaffolding proteins of the postsynaptic density and actin cytoskeleton.
J Biol Chem 276: 48458-48465 (2001)

105. Pak DT, Yang S, Rudolph-Correia S, Kim E, Sheng M:
Regulation of dendritic spine morphology by SPAR, a PSD-95-associated RapGAP.
Neuron 31: 289-303 (2001)

106. Perego C, Vanoni C, Massari S, Longhi R, Pietrini G:
Mammalian LIN-7 PDZ proteins associate with beta-Catenin at the cell-cell junctions of epithelia and neurons.
EMBO J 19: 3978-3989 (2000)

107. Park E, Na M, Choi J, Kim S, Lee JR, Yoon J, Park D, Sheng M, Kim E:
The Shank family of postsynaptic density proteins interacts with and promotes synaptic accumulation of the beta PIX guanine nucleotide exchange factor for Rac1 and Cdc42.
J Biol Chem 278: 19220-19229 (2003)

108. Proepper C, Johannsen S, Liebau S, Dahl J, Vaida B, Bockmann J, Kreutz MR, Gundelfinger ED, Boeckers TM:
Abelson interacting protein 1 (Abi-1) is essential for dendrite morphogenesis and synapse formation.
EMBO J 26: 1397-1409 (2007)

109. Qualmann B, Boeckers TM, Jeromin M, Gundelfinger ED, Kessels MM:
Linkage of the actin cytoskeleton to the postsynaptic density via direct interactions of Abp1 with the ProSAP/Shank family.
J Neurosci 24: 2481-2495 (2004)

110. Quitsch A, Berhörster K, Liew CW, Richter D, Kreienkamp HJ:
Postsynaptic Shank antagonizes dendrite branching induced by the leucine-rich repeat protein Densin-180.
J Neurosci 25: 479-487 (2005)

111. Racca C, Stephenson FA, Streit P, Roberts JD, Somogyi P:
NMDA receptor content of synapses in stratum radiatum of the hippocampal CA1 area.
J Neurosci 20: 2512-2522 (2000)

112. Redecker P, Gundelfinger ED, Boeckers TM:
The Cortactin-binding postsynaptic density protein ProSAP1 in non-neuronal cells.
J Histochem Cytochem 49: 639-648 (2001)

113. Redecker P, Kreutz MR, Bockmann J, Gundelfinger ED, Boeckers TM:
Brain synaptic junctional proteins at the acrosome of rat testicular germ cells.
J Histochem Cytochem 51: 809-819 (2003)

114. Revel JP, Karnovsky MJ:
Hexagonal array of subunits in intercellular junctions of the mouse heart and liver.
J Cell Biol 33: C7-C12 (1967)

115. Rijsewijk F, Schuermann M, Wagenaar E, Parren P, Weigel D, Nusse R:
The Drosophila homolog of the mouse mammary oncogene int-1 is identical to the segment polarity gene wingless.
Cell 50: 649-657(1987)

116. Rose A, Meier I:
Scaffolds, levers, rods and springs: diverse cellular functions of long coiled-coil proteins.
Cell Mol Life Sci 61: 1996-2009 (2004)

117. Roussignol G, Ango F, Romorini S, Tu JC, Sala C, Worley PF, Bockaert J, Fagni L:
Shank expression is sufficient to induce functional dendritic spine synapses in aspiny neurons.
J Neurosci 25: 3560-3570 (2005)

118. Sala C, Piëch V, Wilson NR, Passafaro M, Liu G, Sheng M:
Regulation of dendritic spine morphology and synaptic function by Shank and Homer.
Neuron 31: 115-130 (2001)

119. Sala C, Roussignol G, Meldolesi J, Fagni L:
Key role of the postsynaptic density scaffold proteins Shank and Homer in the functional architechture of Ca2+ homeostasis at dendritic spines in hippocampal neurons.
J Neurosci 25: 4587-4592 (2005)

120. Schmeisser MJ, Grabrucker AM, Bockmann J, Boeckers TM:
Synaptic crosstalk betweeen NMDA receptors and LAPSER1/β-Catenin at excitatory synapses.
J Biol Chem 284: 29146-29157 (2009)

121. Schoch S, Gundelfinger ED:
Molecular organization of the presynaptic active zone.
Cell Tissue Res 326: 379-391 (2006)

122. Schulz DJ:
Plasticity and stability in neuronal output via changes in intrinsic excitability: it's what's inside that counts.
J Exp Biol 209: 4821-4827 (2006)

123. Shapira M, Zhai RG, Dresbach T, Bresler T, Torres VI, Gundelfinger ED, Ziv NE, Garner CC:
Unitary assembly of presynaptic active zones from Piccolo-Bassoon transport vesicles.
Neuron 38: 237-252 (2003)

124. Sheng M, Sala C:
PDZ domains and the organization of supramolecular complexes.
Annu Rev Neurosci 24: 1-29 (2001)

125. Sheng M, Hoogenraad CC:
The postsynaptic architechture of excitatory synapses: a more quantitative view.
Annu Rev Biochem 76: 823-847 (2007)

126. Siksou L, Rostaing P, Lechaire JP, Boudier T, Ohtsuka T, Fejtová A, Kao HT, Greengard P, Gundelfinger ED, Triller A, Marty S:
Three-dimensional architecture of presynaptic terminal cytomatrix.
J Neurosci 27: 6868-6877 (2007)

127. Siksou L, Varoqueaux F, Pascual O, Triller A, Brose N, Marty S:
A common molecular basis for membrane docking and functional priming of synaptic vesicles.
Eur J Neurosci 30: 49-56 (2009)

128. Skeberdis VA, Lan J, Opitz T, Zheng X, Bennett MV, Zukin RS:
mGluR1-mediated potentiation of NMDA receptors involves a rise in intracellular calcium and activation of protein kinase C.
Neuropharmacology 40: 856-865 (2001)

129. Soltau M, Richter D, Kreienkamp HJ:
The insulin receptor substrate IRSp53 links postsynaptic Shank1 to the small G-protein Cdc42.
Mol Cell Neurosci 21: 575-583 (2002)

130. Song I, Huganir RL:
Regulation of AMPA receptors during synaptic plasticity.
Trends Neurosci 25: 578-588 (2002)

131. Songyang Z, Fanning AS, Fu C, Xu J, Marfatia SM, Chishti AH, Crompton A, Chan AC, Anderson JM, Chantley LC:
Recognition of unique carboxy-terminal motifs by distinct PDZ domains.
Science 275: 73-77 (1997)

132. Spacek J, Harris KM:
Three-dimensional organization of smooth endoplasmic reticulum in hippocampal CA1 dendrites and dendritic spines of the immature and mature rat.
J Neurosci 17: 190-203 (1997)

133. Spacek J, Harris KM:
Three-dimensional organization of cell adhesion junctions at synapses and dendritic spines in area CA1 of the rat hippocampus.
J Comp Neurol 393: 58-68 (1998)

134. Speese SD, Budnik V:
Wnts: up-and-coming at the synapse.
Trends Neurosci 30: 268-275 (2007)

135. Spilker C, Acuña Sanhueza GA, Boeckers TM, Kreutz MR, Gundelfinger ED:
SPAR2, a novel SPAR-related protein with GAP activity for Rap1 and Rap2.
J Neurochem 104: 187-201 (2008)

136. Spires TL, Molnár Z, Kind PC, Cordery PM, Upton AL, Blakemore C, Hannan AJ:
Activity-dependent regulation of synapse and dendritic spine morphology in developing barrel cortex requires phospholipase C-beta1 signalling.
Cereb Cortex 15: 385-393 (2005)

137. Stephenson FA:
Structure and trafficking of NMDA and $GABA_A$ receptors.
Biochem Soc Trans 34: 877-881 (2006)

138. Sudo H, Maru Y:
LAPSER1 is a putative cytokinetic tumor suppressor that shows the same centrosome and midbody subcellular localization pattern as p80 katanin.
FASEB J 21: 2086-2100 (2007)

139. Sudo H, Maru Y:
LAPSER1/LZTS2, a pluripotent tumor suppressor linked to the inhibition of katanin-mediated microtubule severing.
Hum Mol Genet 17: 2524-2540 (2008)

140. Sweatt JD:
Toward a molecular explanation for long-term potentiation.
Learn Mem 6: 399-416 (1999)

141. Tadokoro S, Tachibana T, Imanaka T, Nishida W, Sobue K:
Involvement of unique leucine-zipper motif of PSD-Zip45 (Homer 1c/vesl-1L) in group 1 metabotropic glutamate receptor clustering.
Proc Natl Acad Sci USA 96: 13801-13806 (1999)

142. Takai Y, Sasaki T, Matozaki T:
Small GTP-binding proteins.
Physiol Rev 81: 153-208 (2001)

143. Takeichi M, Abe K:
Synaptic contact dynamics controlled by cadherin and catenins.
Trends Cell Biol 15: 216-221 (2005)

144. Tamai K, Semenov M, Kato Y, Spokony R, Liu C, Katsuyama Y, Hess F, Saint-Jeannet JP, He X:
LDL-receptor-related proteins in Wnt signal transduction.
Nature 407: 530-535 (2000)

145. Tang SJ:
The synaptic Wnt signaling hypothesis.
Synapse 61: 866-868 (2007)

146. Teufel A, Weinmann A, Galle PR, Lohse AW
In silico characterization of LZTS3, a potential tumor suppressor.
Oncol Rep 14: 547-551 (2005)

147. Thyssen G, Li TH, Lehmann L, Zhuo M, Sharma M, Sun Z:
LZTS2 is a novel β-Catenin-interacting protein and regulates the nuclear export of β-Catenin.
Mol Cell Biol 26: 8857-8867 (2006)

148. tom Dieck S, Sanmartí-Vila L, Langnaese K, Richter K, Kindler S, Soyke A, Wex H, Smalla KH, Kämpf U, Fränzer JT, Stumm M, Garner CC, Gundelfinger ED:
Bassoon, a novel zinc-finger CAG/glutamine-repeat protein selectively localized at the active zone of presynaptic nerve terminals.
J Cell Biol 142: 499-509 (1998)

149. Tu JC, Xiao B, Naisbitt S, Yuan JP, Petralia RS, Brakeman P, Doan A, Aakalu VK, Lanahan AA, Sheng M, Worley PF:
Coupling of mGluR/Homer and PSD-95 complexes by the Shank family of postsynaptic density proteins.
Neuron 23: 583-592 (1999)

150. Waltereit R, Weller M:
Signaling from cAMP/PKA to MAPK and synaptic plasticity.
Mol Neurobiol 27: 99-106 (2003)

151. Waites CL, Craig AM, Garner CC:
Mechanisms of vertebrate synaptogenesis.
Annu Rev Neurosci 28: 251-274 (2005)

152. Wehrli M, Dougan ST, Caldwell K, O'Keefe L, Schwartz S, Vaizel-Ohayon D, Schejter E, Tomlinson A, DiNardo S:
Arrow encodes an LDL-receptor-related protein essential for Wingless signaling.
Nature 407: 527-530 (2000)

153. Wendholt D, Spilker C, Schmitt A, Dolnik A, Smalla KH, Proepper C, Bockmann J, Sobue K, Gundelfinger ED, Kreutz MR, Boeckers TM:
ProSAP-interacting protein 1 (ProSAPiP1), a novel protein of the postsynaptic density that links the Spine-associated Rap-Gap (SPAR) to the scaffolding protein ProSAP2/Shank3.
J Biol Chem 281: 13805-13816 (2006)

154. West AE, Griffith EC, Greenberg ME:
Regulation of transcription factors by neuronal activity.
Nat Rev Neurosci 3: 921-931 (2002)

155. Wharton KA Jr.:
Runnin' with the Dvl: proteins that associate with Dsh/Dvl and their significance to Wnt signal transduction.
Dev Biol 253: 1-17 (2003)

156. Willecke K, Eiberger J, Degen J, Eckardt D, Romualdi A, Gueldenagel M, Deutsch U, Soehl G:
Structural and functional diversity of connexin genes in the mouse and human genome.
Biol Chem 383: 725-737 (2002)

157. Wodarz A, Nusse R:
Mechanisms of Wnt signaling in development.
Annu Rev Cell Dev Biol 14: 59-88 (1998)

158. Wu H, Zhou Y, Xiong ZQ:
Transducer of regulated CREB and late phase long-term synaptic potentiation.
FEBS J 274: 3218-3223 (2007)

159. Yao I, Hata Y, Hirao K, Deguchi M, Ide N, Takeuchi M, Takai Y:
Synamon, a novel neuronal protein interacting with synapse-associated protein 90/postsynaptic density-95-associated protein.
J Biol Chem 274: 27463-27466 (1999)

160. Yoshikawa S, McKinnon RD, Kokel M, Thomas JB:
Wnt-mediated axon guidance via the Drosophila Derailed receptor.
Nature 422: 583-588 (2003)

161. Yuste R, Bonhoeffer T:
Morphological changes in dendritic spines associated with long-term synaptic plasticity.
Annu Rev Neurosci 24: 1071-1089 (2001)

162. Zhai RG, Olias G, Chung WJ, Lester RA, tom Dieck S, Langnaese K, Kreutz MR, Kindler S, Gundelfinger ED, Garner CC:
Temporal appearance of the presynaptic cytomatrix protein Bassoon during synaptogenesis.
Mol Cell Neurosci 15: 417-428 (2000)

163. Zhang H, Maximov A, Fu Y, Xu F, Tang TS, Tkatch T, Surmeier DJ, Bezprozvanny I:
Association of $Ca_V1.3$ L-type calcium channels with Shank.
J Neurosci 25: 1037-1049 (2005)

164. Zitzer H, Hönck HH, Bächner D, Richter D, Kreienkamp HJ:
Somatostatin receptor interacting protein defines a novel family of multidomain proteins present in human and rodent brain.
J Biol Chem 274: 32997-33001(1999)

165. Ziv NE, Smith SJ:
Evidence for a role of dendritic filopodia in synaptogenesis and spine formation.
Neuron 17: 91-102 (1996)

166. Ziv NE, Garner CC:
Cellular and molecular mechanisms of presynaptic assembly.
Nat Rev Neurosci 5: 385-399 (2004)

167. Zürner M, Schoch S:
The mouse and human Liprin-alpha family of scaffolding proteins: genomic organization, expression profiling and regulation by alternative splicing.
Genomics 93: 243-253 (2009)

Figures & Tables

Fig. 1	"Scaffolding" within PSDs of glutamatergic synapses of the CNS	9
Fig. 2	The ProSAP/Shank family of PSD proteins in brain	10
Fig. 3	Exon-intron-structure of the LAPSER1 gene	54
Fig. 4	Structural organization of the LAPSER1 protein	55
Fig. 5	Alignment of the amino acid sequences of *"Fezzin"* C-termini	56
Fig. 6	Multiple tissue distribution of LAPSER1 mRNA	57
Fig. 7	Regional distribution of LAPSER1 mRNA in brain	58
Fig. 8	Generation and characterization of the polyclonal LAPSER1 antibody	59
Fig. 9	Multiple tissue distribution of the LAPSER1 protein	60
Fig. 10	Regional distribution of the LAPSER1 protein in brain	61/62
Fig. 11	Subcellular distribution and synaptic localization of LAPSER1	62/63
Fig. 12	Interaction of LAPSER1 and ProSAP2	64/65
Fig. 13	Co-localization of SPAR1 and LAPSER1 in hippocampal neurons	66
Fig. 14	Fez1 domain alignment of all 4 *"Fezzins"*	67
Fig. 15	Interaction of *"Fezzin"* family members with SPAR1 via Fez1 domains	67/68
Fig. 16	A protein complex in brain contains LAPSER1, SPAR1 and β-Catenin	69/70
Fig. 17	Molecular crosstalk between LAPSER1, SPAR1 and β-Catenin	71
Fig. 18	LAPSER1 & the postsynaptic density – a schematic overview	81

Table 1	Genomic alignment of LAPSER1 in rat, mouse and human	54

Danksagung

Diese Arbeit wurde im Institut für Anatomie und Zellbiologie der Universität Ulm unter der Betreuung von Prof. Dr. med. Tobias M. Böckers angefertigt, dem ich allen voran für seine konstante Unterstützung und Hilfe danken möchte.

Tobias, ein herzliches Dankeschön für deine stets so außergewöhnlich frische und motivierende Art, mit der du wissenschaftliches Denken und Arbeiten vermittelst und damit auch in mir die Leidenschaft zur Forschung wecken konntest.

Mein besonderer Dank gilt auch meinem Kollegen Andreas Grabrucker, dessen Studien über den Wnt pathway in Neuronen auf einmal die Wege meines Moleküls kreuzten und wir somit den Grundstein für eine erste fruchtbare Kooperation legen konnten, die sicherlich nicht unsere letzte sein wird. Des weiteren möchte ich mich bei meinen Kollegen Angelika Schmitt, Christian Pröpper, Anna Dolnik, Jürgen Bockmann, Michael Schön, Ursula Pika-Hartlaub, Sibylle Etter und Natalie Damm bedanken, für ihre Hilfe und Geduld beim Erlernen der Methodik im Labor und die immer offenen Ohren bei all' meinen praktischen und theoretischen Fragen. Allen anderen Mitarbeiten des Instituts für Anatomie und Zellbiologie sei an dieser Stelle für Ihre Anregungen, Unterstützung und stete Diskussionsbereitschaft gedankt.

Nicht zuletzt danken möchte ich auch Prof. Dr. med. Hayrettin Tumani für die Übernahme der Zweitkorrektur sowie Prof. Dr. rer. nat. Thomas Wirth und dem Promotionsprogramm für Experimentelle Medizin der Unversität Ulm für die finanzielle Unterstützung meiner Arbeit und die interessanten Seminare, welche mir einen Einblick in unterschiedliche Forschungsbereiche gewährt und somit den wissenschaftlichen Austausch mit anderen Doktoranden gefördert haben.

Herzlichen Dank auch an meine Freundin Stephanie für Ihr Verständnis und Ihre Geduld, so dass ich meine freien Stunden am Abend oder am Wochenende oft im Labor verbringen konnte. Insbesondere gilt mein Dank jedoch meinen Eltern und meiner Familie, die schon immer meine Interessen ausnahmslos unterstützt und gefördert und somit meiner Neugier und meinem Entdeckergeist freien Lauf gelassen haben.

Lebenslauf

Name:	Michael Joachim Schmeißer
Geburtsdatum:	02.06.1983
Geburtsort:	Kempten, Allgäu

Ausbildung

1989-2002	Schule	
2002	Abitur am Carl-von-Linde-Gymnasium, Kempten	
2002-2009	Studium der Humanmedizin, Universität Ulm	
08/2004	1. Ärztliche Prüfung (Physikum)	
2008	Praktisches Jahr	
	Innere Medizin	Tufts University, Boston
	Neurologie	Universität Ulm
	Allgemeinchirurgie	University of Glasgow
	Neurochirurgie	Universität Basel
05/2009	2. Ärztliche Prüfung und Approbation	
Seit 06/2009	Wissenschaftlicher Mitarbeiter im Institut für Anatomie und Zellbiologie, Universität Ulm	
Seit 10/2009	Aufbaustudium innerhalb der International Graduate School in Molecular Medicine Ulm zum Erwerb des PhD bzw. Dr. rer. nat.	

Stipendien/Auszeichnungen

2003	Certificate of Excellence Kursus der mikroskopischen Anatomie, Universität Ulm
2004	Certificate of Excellence Kursus der physiologischen Chemie, Universität Ulm
2005	9-monatiges Forschungsstipendium „Experimentelle Medizin“, Universität Ulm
2008	4-monatiges DAAD-Auslandsstipendium PJ-Tertial Innere Medizin, Tufts University, Boston
2008	Stethosglobe-Reisestipendium Allianz Private Krankenversicherung AG PJ-Tertial Chirurgie, Universitäten Glasgow/Basel
2008	GlaxoSmithKline Reisestipendium 38th annual meeting of the SfN, Washington, DC

Lehrtätigkeit

2005-2008	Kursus der mikroskopischen Anatomie Kursus der makroskopischen Anatomie Anatomie im Bild (Kursorganisation)
2007-2008	Kurs „Problemorientiertes Lernen“ (POL) Allgemeine Pharmakologie & Toxikologie

Wissenschaftliche Tätigkeit

seit 2005 Promotion im Institut für Anatomie und Zellbiologie
AG Prof. Dr. med. Tobias M. Böckers

seit 2007 Mitglied der Society for Neuroscience (SfN)

seit 2009 Mitglied des Sonderforschungsbereichs (SFB) 497
„Signale und Signalverarbeitung bei der zellulären Differenzierung“

Abstracts:

Schmeisser MJ, Schmitt A, Boeckers TM:
Cloning and characterization of LAPSER1, a member of the *“Fezzin”* family of PSD proteins.
23. Arbeitstagung der Anatomischen Gesellschaft, Würzburg 2006.

Grabrucker AM, Thomas U, **Schmeisser MJ**, Gundelfinger ED, Boeckers TM:
Possible connection of ProSAP/Shank family proteins to the Wnt signaling pathway in mammals and drosophila.
24. Arbeitstagung der Anatomischen Gesellschaft, Würzburg 2007.

Schmeisser MJ, Grabrucker AM, Boeckers TM:
LAPSER1 interacts with SPAR1 via its C-terminal Fez1-domain.
24. Arbeitstagung der Anatomischen Gesellschaft, Würzburg 2007.

Dolnik A, Bockmann J, **Schmeisser MJ**, Boeckers TM:
Characterization of SPAR3, a novel Rap-Gap domain containing protein of the postsynaptic density (PSD) that interacts with *“Fezzin”* family members.
37th annual meeting of the Society for Neuroscience (SfN), San Diego, CA 2007.

Schmeisser MJ, Grabrucker AM, Boeckers TM:
PSD proteins of the *"Fezzin"* family interact with SPAR1 via conserved Fez1 domains.
37th annual meeting of the Society for Neuroscience (SfN), San Diego, CA 2007.

Grabrucker AM, **Schmeisser MJ**, Thomas U, Gundelfinger ED, Boeckers TM:
Cross-activation of the Wnt-signaling pathway at excitatory synapses through NMDA-stimulation.
25. Arbeitstagung der Anatomischen Gesellschaft, Würzburg 2008.

Schmeisser MJ, Grabrucker AM, Boeckers TM:
"Fezzin" family member LAPSER1 takes part in synapto-nuclear translocation in hippocampal neurons.
38th annual meeting of the Society for Neuroscience (SfN), Washington, DC 2008.

Schmeisser MJ, Unrath A, Otto M, Tumani H, Abler B:
Moyamoya disease precipitating Sydenham's chorea.
82. Kongress der Deutschen Gesellschaft für Neurologie (DGN), Nürnberg 2009

Schmeisser MJ, Grabrucker AM, Bockmann J, Boeckers TM:
Upon NMDA-receptor activation, the PSD protein LAPSER1 regulates nuclear localization of β-catenin in hippocampal neurons.
26. Arbeitstagung der Anatomischen Gesellschaft, Würzburg 2009

Schmeisser MJ, Grabrucker AM, Bockmann J, Boeckers TM:
The PSD protein LAPSER1 regulates nuclear localization of beta-catenin in neurons.
39th annual meeting of the Society for Neuroscience (SfN), Chicago, IL 2009.

Original-Veröffentlichungen:

Schmeisser MJ, Unrath A, Otto M, Tumani H, Abler B:
Moyamoya disease precipitating Sydenham's chorea in a 19-year old Caucasian woman.
Mov Disord 24: 1401-1403 (2009)

Schmeisser MJ, Grabrucker AM, Bockmann J, Boeckers TM:
Synaptic crosstalk between NMDA receptors and LAPSER1/β-catenin at excitatory synapses.
J Biol Chem 284: 29146-29157 (2009)

Übersichtsartikel:

Schmeisser MJ, Boeckers TM:
The Fezzin family of synaptic proteins – novel candidates within the postsynaptic pathways of autism spectrum disorders?
In preparation